SURFACE FUNCTIONALIZED AND MOLECULARLY IMPRINTED POLYMERS FOR PHOSPHATE REMOVAL IN PATIENTS WITH END STAGE RENAL DISEASE

By

ANIKA ASSATA ODUKALE EDWARDS

A DISSERTATION PRESENTED TO THE GRADUATE SCHOOL
OF THE UNIVERSITY OF FLORIDA IN PARTIAL FULFILLMENT
OF THE REQUIREMENTS FOR THE DEGREE OF
DOCTOR OF PHILOSOPHY

UNIVERSITY OF FLORIDA

2008

To those who kept me along the way.

ACKNOWLEDGMENTS

Realizing that no one makes this journey alone is one of the greatest gifts that I have been given. Recognizing those who will never know how much of an impact that they have had on me academically, and more-so personally, is the best way in which I can express my lifelong gratitude.

I thank my advisor, Dr. Christopher Batich, for the opportunity to work on a project that has allowed me to learn how to creatively analyze science based problems from a unique and nontraditional point of view. My greatest gratitude goes to my committee: Dr. E. Goldberg, Dr. H. El-Shall, Dr. L. S. Holliday, and Dr. W. Sigmund, for their patience and understanding.

I am extremely thankful to Dr. Hassan El-Shall, Dr. Eugene Goldberg, and Dr. Anne Donnelly for their support and open doors. They will probably never know how much their advice and encouragement has meant to me.

I am appreciative to the Batich group, especially Tara Washington, Jompo, Taili, and to members of the Goldberg group. Very special thanks to Jennifer Wrighton for always making sure that all of the i's were dotted and t's crossed. I would like to acknowledge the facility directors and trainers at MAIC and the ERC for use of their equipment and expertise.

I am grateful for the support from Martha, Doris, and Jennifer, in our Graduate Office. You have always shared in my success…we did it! And to Joni Nattiel, for always making sure that I received a paycheck. I would also like to express gratitude to the Department Chairman, Dr. Kevin Jones, who allowed me the opportunity to TA many different classes in an effort to provide various experiences that would support my goal of teaching.

I would like to thank my family, who have been my always cheerleaders. My mother, Jabari, always told me that I could do anything growing up, and even ventured on the internet to learn about polymers, so that she could tell everyone what her daughter studied. To my brothers

Kao, whose humor could shed light on the bright side of anything, “Go Vikes!”, Baba, J-Rock, and Femi, for being proud of their “Sis.”

My greatest appreciation goes to my husband, best friend and confidant, laughing partner, motivator, reality checker and constant companion, Jesse. I simply could not have done this without him. He will never know how much I adore him, or how grateful I am for everything that he has done for me. In the immortal words of Piglet; “We’ll be friends forever, won’t we, Pooh” asked Piglet. “Even longer,” Pooh answered. I give thanks to you for my precious son Akil, and for beloved my step-son and “Little Buddy” Tyler, and for the blessed family that we are.

I would like to acknowledge and dedicate this to Eddie Lloyd, Jr., Constance Fabunmi, Mark Maykoski, and Brenda Smith, who are all greatly missed.

TABLE OF CONTENTS

page

ACKNOWLEDGMENTS 4

LIST OF TABLES 10

LIST OF FIGURES 11

LIST OF ABBREVIATIONS 15

ABSTRACT 16

CHAPTER

1 INTRODUCTION 18

Rationale 18
Specific Aims 19
Specific Aim 1: Develop and Characterize Surface Functionalized Polymers for Phosphate Removal in Aqueous Systems. 19
Specific Aim 2: Develop and Characterize Molecularly Imprinted Polymers for Phosphate Removal in Aqueous Systems. 20
Specific Aim 3: Determine the Efficacy of Phosphate Uptake with these Functionalized Polymers *In-Vitro*. 21

2 BACKGROUND 22

Introduction 22
Emulsions 22
Phosphate Poisoning and Chronic Renal Failure 23
Surface Functionalization of Polymeric Microparticles 25
Molecular Imprinting 25
Covalent vs. Noncovalent Synthesis 27
Radiation Polymerization 29
Previous Related Work 30

3 RENAGEL CHARACTERISTICS 33

Understanding Renagel® 33
Structural Properties of Renagel® 33
Renagel® Swelling Behavioral Studies 34
Experimental Methods 34
Effect of pH on Phosphate Uptake 35
Phosphate Binding Mechanism 37
Molecular Dynamics 39
Vacuum system 39

Solvated System 39
Monte Carlo 40
Determining the Shell Volume 40
Generating Random Numbers 41
Determining the Ratio 41
Determining the Volume of the Molecule 41
Results 42
Conclusions 47

4 POLYMERIZATION PARAMETERS 50

Experimental Design and Material Selection 50
Synthesis Parameters 51
Template Molecule 51
Functional Monomer 53
Initiator 56
Crosslinking Agent 57
Genipin crosslinked microspheres 58
Glutaraldehyde crosslinked microspheres 59
Dextran 60
D,L-glyceraldehyde 61
Porogen 63
Determine the Efficacy of Phosphate Uptake with the Polymers *in-vitro* 64
Assessment of the Reaction Parameters 64
Recovery 64
In-Vitro Analysis of Phosphate Uptake in the Functionalized Polymer 64
Instrumentation 65
ICP 65
UV/VIS 65
Phosphate meter 65
Characterization of bulk polymer 66
Scanning Electron Microscopy (SEM) 66
Infrared (IR) 66

5 GELATIN MICROSPHERES VIA EMULSIFICATION 67

Water in Oil Emulsions 67
Crosslinked Gelatin Microspheres 69
Synthesis of Gelatin Microspheres 69
Crosslinking Gelatin Microspheres with Genipin 70
Crosslinking Gelatin Microspheres with Glutaraldehyde 70
Crosslinking Gelatin Microspheres with additional agents 71
Dextran 71
Glyceraldehyde 72

Gelatin Microsphere Processing 72
Removal of the Template 72
Base Wash Extractions 72
Acid Wash Extractions 73
Results 74
Gelatin Inverse Emulsions 74
Genipin Crosslinked Gelatin Polymerization 79
Glutaraldehyde Crosslinked Gelatin 81
Dextran Crosslinked Gelatin 82
Glyceraldehyde Crosslinked Gelatin 83
Conclusions 83

6 MOLECULARLY IMPRINTED POLYMERS 86

Microwave Fabricated Gelatin Microspheres as Phosphate Binding Agents 86
Crosslinked Gelatin Microspheres via Microwave Radiation 86
Microwave Treatment 87
Results 87
Gelatin Emulsion Microspheres 87
Genipin and Glutaraldehyde Crosslinked Microspheres 88
Conclusions 92

7 GUANYLATED POLYMERS 94

Functionalized Gelatin Microspheres via Guanylation 95
Imprinted Gelatin Microspheres 96
Room Temperature Guanylation 96
Heat Assisted Guanylation 97
Surface Guanylated Gelatin Microspheres 97
Results 97
Imprinted Polymers 97
Glutaraldehyde 99
Surface Modified Crosslinked Polymers 101
Genipin 101
Glutaraldehyde 101
Glyceraldehyde 103
Conclusions 104

8 DISCUSSION 107

Synopsis 107
Conclusions 112
Future Work 115
Crosslinking Agent 115
Substrate Imprinting 116
Instrumentation 116

Polymer Binding....116
Enzyme Studies....117

APPENDIX CALIBRATION OF A PHOSPHATE MEASURING APPARATUS....118

Experimental Methods....118
Conclusions....121

LIST OF REFERENCES....122

BIOGRAPHICAL SKETCH....129

LIST OF TABLES

Table page

3-1 Interatomic distance values (mean, standard deviation, high, and low) for the NVT ensemble simulation in vacuum for four phosphate system with dielectric 1 debye.....47

3-2 Interatomic distance values (mean, standard deviation, high, and low) for the NVT ensemble with dielectric 78 debye to mimic a solvated system (H2O).....48

5-1 Phosphate uptake in gelatin crosslinked microspheres that have been either acid or base washed prior to trials.....84

6-1 Phosphate uptake in microwave irradiated gelatin crosslinked microspheres that have been either acid or base washed prior to trials.....92

7-1 Phosphate uptake in surface functionalized and molecularly imprinted gelatin crosslinked microspheres prepared by either emulsion or microwave irradiated.....105

A-1 Phosphate calibration values using the Hannah HI 93717 meter. 119

A-2 Phosphate readings from the Hannah HI 93717 meter compared to those obtained from the Shimadzu UV/Vis. 120

LIST OF FIGURES

Figure		page
1-1	Surface functionalized crosslinked gelatin microsphere interacting with phosphate molecules	20
1-2	Formation of imprinted cavities for phosphate molecules in gelatin microsphere used to bind phosphate molecules	20
2-1	Hormonal control loop for calcium metabolism	25
2-2	Concept of molecular imprinting of polymers	27
2-3	Simplified schematics of covalent and noncovalent imprinting procedures	28
2-4	Depiction of an HPLC column packed with a MIP stationary phase used for chiral separations	31
2-5	Nucleation of calcite at the polymer surface	31
3-1	Chemical structure of sevelamer hydrochloride	34
3-2	Phosphate (P) uptake in Renagel®..	37
3-4	Observed swelling of dry particles	38
3-5	Van der Waals representation of the space filled model system with four phosphate ions bound to the polymer	43
3-6	Interatomic distance between Nitrogen (126) and Phosphorous (237) in the model system Renagel® and four triphosphate ions, with an N-P separation adjustment of the system at about 480 ps.	44
3-7	Interatomic distance between Nitrogen (204) and Phosphorous (237) in the model system Renagel® and four triphosphate ions	45
3-8	The change of interatomic distance between N(89) and P(237).	45
3-9	The P(237)-P(216) interatomic separations versus simulation time..	46
4-1	Common polyprotic molecular structures of the phosphate ion.	52
4-2	Titration curve for phosphoric acid	52
4- 3	Relative fractions of the various forms of phosphate at different pH levels.	53
4-4	Molecular structures of common amino acids found *in-vivo*	55

4-5 Structure of Gelatin....56

4-6 The molecular structure of Genipin and Geniposide. 59

4-7 Crosslinked structures of genipin crosslinked gelatin microspheres 60

4-8 The molecular structure of glutaraldehyde. 60

4-9 Crosslinked structures of glutaraldehyde crosslinked gelatin microspheres 61

4-10 Molecular structure of dextran.....62

4-11 Preparation of gelatine hydrogels crosslinked with partially oxidized dextrans. 62

4-12 Molecular structure of D,L-glyceraldehyde.....63

5-1 An inverse emulsion system. 67

5-2 Interfacial tension and emulsion variations versus formulation (as HLD) at near unit water-to-oil-ratio. 69

5- 3 Template removal from the active binding site. 73

5-4 SEM and corresponding EDS analysis of raw Type B (bovine) gelatin.....74

5-5 SEM and corresponding EDS analysis of gelatin microspheres prepared via water in oil emulsion.....75

5-8 FTIR spectrum of unprocessed Type B (bovine) gelatin.....77

5-9 FTIR spectrum of gelatin microspheres via water-in-oil emulsion. 78

5-10 FTIR spectrum of gelatin microspheres containing phosphate via water-in-oil emulsion.....79

5-11 Gelatin microspheres crosslinked with 15% genipin without phosphate: before and after phosphate testing, and with phosphate: before and after phosphate testing. 80

5-12 FTIR spectrum of genipin crosslinked gelatin microspheres. 81

5-13 FTIR spectrum of genipin crosslinked gelatin microspheres containing phosphate. 81

5-14 FTIR spectrum of glutaraldehyde crosslinked gelatin without phosphate, and with phosphate. 82

6-1 SEM of gelatin crosslinked microspheres via microwave processing without phosphate : before and after phosphate testing, and with phosphate: before and after phosphate testing.....89

6-2 Protonated amine cage surrounding a phosphate ion. 90

6-3 Modeled system of the phosphate binding polymer. 91

6-4 FTIR spectrum of glutaraldehyde crosslinked gelatin, via microwave irradiation: without phosphate, and with phosphate. 91

7-1 Synthetic route used to obtain a guanylated polymer. 95

7-2 Zwitterionic interaction of phosphate with a guanyl group. 95

7-3 SEM images of uncrosslinked gelatin, native, guanylated without phosphate, and guanylated with phosphate 98

7-4 Predicted proximity of 4 phosphate ions within the polymer structure, and a guanine derivative self assembly into G-ribbon, G-quartet, and G-quadruplex formed by stacking of G-quartets around a column of cations 99

7- 5 Glutaraldehyde crosslinked gelatin microspheres prepared via microwave irradiation, room temperature surface guanylation: after guanylation, after template extraction, and after phosphate uptake testing. Without phosphate, and with phosphate 100

7-6 Glutaraldehyde crosslinked gelatin microspheres prepared via microwave irradiation, heat initiated surface guanylation: after guanylation, after template extraction, and after phosphate uptake testing. Without phosphate, and with phosphate. 100

7-7 Glutaraldehyde crosslinked gelatin microspheres prepared via emulsion polymerization, room temperature surface guanylation: after guanylation, after template extraction, and after phosphate uptake testing. Without phosphate, and with phosphate 102

7-8 Glutaraldehyde crosslinked gelatin microspheres prepared via emulsion polymerization, heat initiated surface guanylation: after guanylation and after template extraction. Without phosphate, and with phosphate. 102

7-9 FTIR spectrum of surface guanylated gelatin crosslinked with glyceraldehyde. 103

8-1 The synthetic pathway followed for the development of the gelatin microspheres. 108

8-2 The synthetic pathway followed for the development of the molecularly imprinted gelatin microspheres. 108

8-3 Phosphate uptake results for acid washed polymeric samples synthesized without and with the phosphate template ion. 110

8-4 Phosphate uptake results for base washed polymeric samples synthesized without and with the phosphate template ion. 110

8-5 Phosphate uptake results for room temperature guanylated polymeric samples synthesized without and with the phosphate template ion. 111

8-6 Phosphate uptake results for acid washed polymeric samples synthesized without and with the phosphate template ion. 111

8-7 Phosphate uptake in surface functionalized polymers using genipin as a crosslinking agent. 112

8-8 Phosphate uptake in surface functionalized polymers using glutaraldehyde as a crosslinking agent. 113

A-1 Hannah HI 93717 handheld photometer. 118

A-2 Actual vs. Theoretical concentrations for phosphate ion using the Hannah HI 93717 phosphate meter. 119

A-3 Calibration curve for the Hannah HI 93717 phosphate meter. 120

A-4 Phosphate uptake in Renagel® samples as measured by the Hannah HI 93717 phosphate meter. 121

LIST OF ABBREVIATIONS

μm	Micron
Å	Angstrom
ATR	Attenuated Total Reflectance
Ca^{2+}	Calcium
CSSR	Cambridge Structure Search and Retrieval
EDS	Energy Dispersive Spectroscopy
ESRD	End Stage Renal
fs	Femto second
FTIR	Fourier Transform Infrared Spectroscopy
HCl	Hydrochloric Acid
ICP	Inductively Coupled Plasma
meq	Milli equivalent
MIP	Molecularly Imprinted Polymer
MIT	Molecular Imprinting Technology
mmol	Milli mole
NaOH	Sodium Hydroxide
PO_4^{3-}	Phosphate
ps	Pico second
SEM	Scanning Electron Microscope
$T_{½}$	Half life temperature

Abstract of Dissertation Presented to the Graduate School
of the University of Florida in Partial Fulfillment of the
Requirements for the Degree of Doctor of Philosophy

SURFACE FUNCTIONALIZED AND MOLECULARLY IMPRINTED POLYMERS FOR PHOSPHATE REMOVAL IN PATIENTS WITH END STAGE RENAL DISEASE

By

Anika Odukale Edwards

December 2008

Chair: Christopher D. Batich
Major: Materials Science and Engineering

Patients with end stage renal disease (ESRD) commonly use nonabsorbable synthetic polymers to sequester excess phosphate on a large scale basis. However, the cost of these agents at 10-15 pills/day/patient, and approximately $1 USD/pill, makes them an alternative not affordable to the greater general public. Thus, the need to develop a low cost therapeutic alternative exists. One way to achieve such a system is to design surface functionalized molecules with specific molecular targeting abilities that are capable of mimicking natural binding phenomena found in living organisms. Thus, a technique for the synthesis of novel surface functionalized gelatin microparticles as oral phosphate binding agents was developed that employs the use of a modified general inverse emulsion schema, or a microwave-assisted synthetic technique, biocompatible crosslinking agents, and guanylating agents. Furthermore, this unique template capturing phenomenon was maximized by creating highly stable molecularly imprinted polymers (MIPs) that possess selective binding properties due to recognition sites within the polymer matrix. Highly crosslinked, surface tailored gelatin microspheres, on the order of 10 – 200 μm, were produced with high-affinity phosphate attracting functional groups at the polymer surface. Serum phosphate uptake was evaluated using the modified microspheres in an in-vitro milieu which simulated an *in-vivo* physiological

environment. Characterization of functionalized polymers was performed using FTIR, SEM, and ICP analytical techniques. Potentially therapeutic polymers microspheres for oral ingestion were thus realized with an effective phosphate binding ability of 1-2 meq/g polymer. This research suggests the feasibility of this novel low cost technology for the therapy of reducing phosphate levels in patients with acute renal disorders.

CHAPTER 1
INTRODUCTION

Rationale

This body of work explores selective phosphate binding polymers and their potential use in treating dialysis-related hyperphosphatemia. The ability to distinguish among molecules in solution is central to many areas of research and plays a vital role in technologies ranging from biotechnology to materials science. Though there are many synthetic approaches to address this issue, surface functionalized polymeric molecules were investigated as a vehicle for these studies due to their well established synthetic routes and chemical understanding.

Polymeric microspheres which are chemically tailored at the surface as a means to interact with specific molecules provide an elegant and efficient approach to achieve targeted molecular recognition. Surface functionalization of polymeric particles with particular molecular groups has quickly become a requirement in the treatment of polymer particles for biotechnological applications. The immobilization of a hydrophilic layer as well as the possibility of coating particles with specific ligands (e.g., saccharide moieties, lipids, proteins) provide very attractive possibilities.[1] Particles can be created by a variety of methods which allow a vast array of microspheres to be developed with customized size, shape, and composition. In addition, a broad selection of functionalities can be integrated onto the particle interface due to the availability of a large amount of functional molecular species and flexibility of manufacturing tools.

Molecular imprinting technique (MIT) is a rapidly growing application that involves the design of molecularly imprinted polymers (MIPs) to produce recognition sites whose selectivity rivals that of natural antibodies.[2] Target molecules for recognition include hormones,[3] small-molecule drugs, metal ions,[4] proteins,[5] nucleic and amino acids.[6] Therefore, MIPs potential for

enhanced stability, lower cost, and selectivity at lower concentrations in comparison to their natural derivatives make them attractive materials.[7] The creation of such "recognition sites" is based on the fundamental characteristics of a functional imprinted polymer such as: stiff structure, good accessibility of binding sites, reversible chemical binding, mechanical and thermal stability, and the ability to distinguish between molecules, even enantiomers. These properties can be controlled through the way in which the MIP is synthesized, thus production parameters are significant. A vast array of research has focused on the optimization of imprinted polymer synthesis conditions. The reaction variables studied include the type and amount of print molecule, functional monomers, cross-linking agent, chemical initiator, porogen, and all other reaction conditions involved in polymerization.[8]

A good deal of interest has been directed towards the field of MIT because of the significant role that they play in surface modification and stability.[9] Extensive studies show that one way to successfully achieve stable formation of imprinted polymers is by means of non-covalent imprinting.[10-12]

Specific Aims

Specific Aim 1: Develop and Characterize Surface Functionalized Polymers for Phosphate Removal in Aqueous Systems.

The explicit goals of this research require a logical progression of microsphere synthesis with surface immobilized species that provide potential phosphate binding in relevant aqueous milieus. Gelatin microspheres were produced and tested under various conditions for phosphate capturing ability. Assays were repeated with particles that have been crosslinked with different biocompatible agents for any positive change in phosphate sequestration. Particles were then surface functionalized with a phosphate interacting ligand (Figure 1-1), and uptake was again examined.

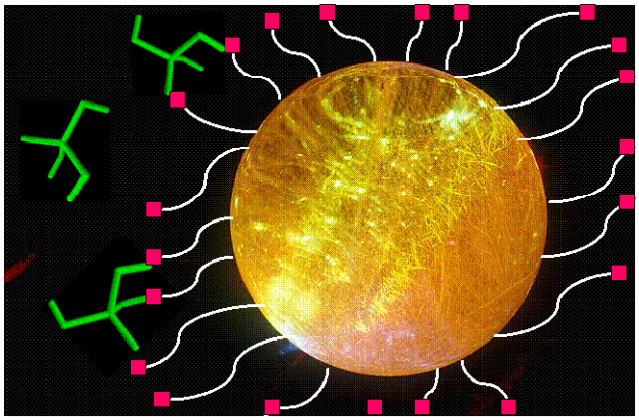

Figure 1-1. Surface functionalized (white lines with pink ends) crosslinked gelatin microsphere (gold) interacting with phosphate molecules (green) (adapted from Adobe Stock Photos).

Specific Aim 2: Develop and Characterize Molecularly Imprinted Polymers for Phosphate Removal in Aqueous Systems.

Results from Specific Aim 1 were used to define parameters necessary to synthesize insoluble phosphate-imprinted polymers. The role of each process parameter was determined, and a valid synthesis scheme was defined (similar to Figure 2).

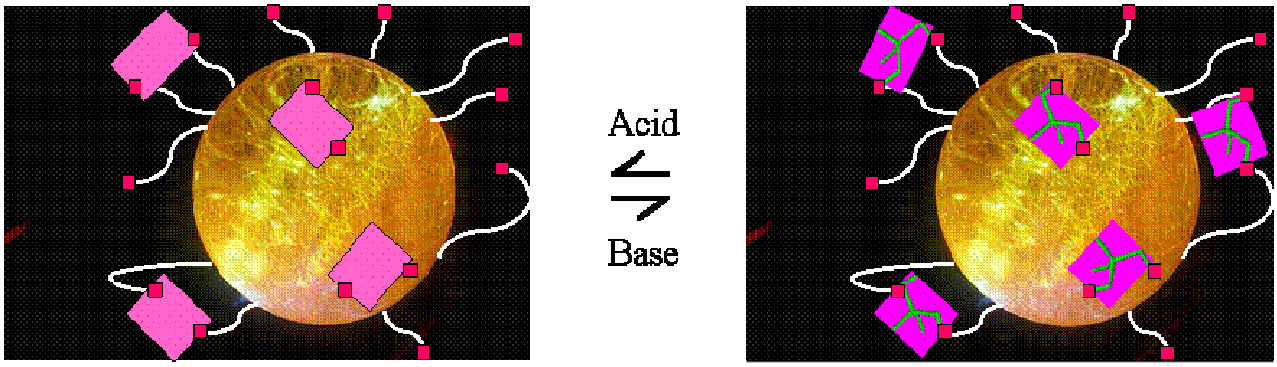

Figure 1-2. Formation of imprinted cavities for phosphate molecules in gelatin microsphere used to bind phosphate molecules (green). Magenta regions denote the rigid cavities, both within and on the surface of the gelatin sphere (gold), created by the imprinting process (adapted from Adobe Stock Photos). Surface attached functional groups are represented by the white lines with pink ends.

Specific Aim 3: Determine the Efficacy of Phosphate Uptake with these Functionalized Polymers *In-Vitro*.

Hyperparathyroidism, secondary to chronic kidney disease, has etiologic factors such as hyperphosphatemia, calcium balance, and 1,25 dihydroxyvitamin D deficiency as typical targets for intervention.[13] By examining the effect that these surface tailored insoluble polymer particles have on the binding specificity of phosphate, their potential influence on hyperphosphatemia can be determined.

To prevent hyperphosphatemia, the phosphate serum level should not exceed 400-800 mg/dL, however the average patient intake is >1 g/day.[14] Thus, the microsphere must be capable of binding and removing these excess amounts of phosphate *in-vivo*, without significant deleterious side effects, and subsequently excreted through the urinary tract and feces. *In-vitro* studies were conducted in solutions that mimic a physiological environment, and phosphate-binding efficiency was determined on a meq/ g polymer base. Data from these experiments were used to investigate the therapeutic feasibility of this surface functionalized polymer system for patients with ESRD.

CHAPTER 2
BACKGROUND

Introduction

Over the past 20 years there have been many advances in the development of MIPs, as their practical applications have far-reaching appeal. These include non-covalent and covalent imprinting and catalysis using imprinted polymers. Progression in the field has continued through the work of many researchers such as Wulff, Mosbach, and Shea.[15] Collectively, these groups have come up with a basic reaction scheme for developing highly selective, imprinted polymers. Extensive research has focused on the optimization of imprinted polymer synthesis conditions.[2] This scheme concentrated on describing how surface modified polymers were prepared for targeting phosphate ions, and examined their potential applications in chronic renal failure patients with elevated serum phosphate levels.

Emulsions

Traditionally, some of the most common methods used to prepare surface modified polymeric materials have been emulsion technology,[16] bulk,[17] and precipitation polymerizations,[18] each with its own advantages and disadvantages. Bulk polymerizations are rather straight forward, however they require an aggressive grinding and sieving step prior to use, which can destroy the binding sites and reduces reproducibility from batch-to-batch. With precipitation polymerization, there is more control over the final size and morphology of the resulting particle, which reduces the batch-to-batch variability, but they are restricted by slow kinetics and low yields.[19]

The use of surface modified polymeric resins prepared using an emulsion method has been a long standing "industry standard" for producing microspheres due to the simplicity of the process, the multiple guest binding sites created as a result of this surface functionalization

technique, and elimination of the grinding and sieving process involved in other traditional techniques as a means to expose available binding sites. The particle size and morphology are reproducible from batch-to-batch, and the monomer : template ratio can be manipulated to obtain the maximum number of template binding sited per microsphere.[20] Microspheres in the range of 1 – 200 μm will be targeted for development, Renagel® reports a 23 μm[21] average product particle size to bind phosphate most effectively. An inverse (water-in-oil) emulsion polymerization method was used to fabricate micron sized particles for investigation. Since spherical microparticles can be produced with guest binding sites on the surface, and each particle has a significant surface area, phosphate-binding phenomena should be observed.[22]

Phosphate Poisoning and Chronic Renal Failure

The irregularities of uremic bone disease are usually referred to as renal osteodystrophy, which occur in patients with chronic renal failure. The two major types of bone disorders in renal osteodystrophy include: a low-turnover osteodystrophy characterized by osteomalacia of adults and rickets of children (or renal rickets), and a high-turnover osteodystrophy characterized by osteitis fibrosa and other bone changes of secondary hyperparathyroidism; osteopenia, and osteosclerosis. Bone is a dynamic organ, constantly remodeled under the actions of the basic multicellular unit, a complex of osteoclasts and osteoblasts.[23] Osteoclasts, the cells responsible for bone resorption, originate from haematopoietic stem cells. They are recruited at a leading edge, dissolving the mineral and matrix alike, forming the Howship's lacunae. These cavities are then filled in by recruited osteoblasts, which are derived from local mesanchymal cells. However, patients with ESRD retain phosphorous, which disturbs the kidneys normal regulation cycle. This condition is highly likely to occur in ESRD patients and effects about 90% (230,000 US patients a year) of all patients on dialysis.[23]

Serum Ca^{2+} represents less than 1% of the total body calcium, however its concentration is extremely important to maintain regular cellular functions. The average person filters approximately 250 mmol of ionized calcium through the kidneys daily. Three major hormones help regulate serum Ca^{2+} metabolism: parathyroid hormone (PTH), which is excreted from parathyroid glands found in the neck, 1,25-dihydroxyvitamin D, and calcitonin. Improper maintenance of calcium and phosphorous in the blood can cause the kidneys to fail. When PTH levels decrease, calcium absorption in the gastrointestinal tract decreases, phosphate in the renal tubule increases, and stimulates 1,25-dihydroxyvitamin D production is adversely affected (Figure 2-1).[14] This results in a decrease in serum Ca^{2+}, which triggers a Ca^{2+} sensor that initiates the extraction of this mineral from the bones in an effort to raise the blood Ca^{2+} levels back to a normal concentration. If this cycle continues for long periods of time, the decrease in the Ca^{2+} in the bones causes them to weaken,[14] and also indirectly controls the excretion of urinary phosphate.[24] Chronic renal failure also prevents the kidneys from making calcitrol, which prevents the body from absorbing dietary calcium into the blood and bones.[23] Regulating the amount of blood serum phosphate levels in patients through the oral administration of phosphate binding polymers, can reduced or avoid the onset of hyperphosphatemia, which can lead to the regulation of a normal serum Ca^{2+} - PO_4^{3-} equilibrium cycle.

Current alternatives to treat hyperphosphatemia include aluminum, lanthanum, and calcium based binders, selected ion exchange resins, nonabsorbable synthetic polymers, and reduced dietary phosphate intake.[23] Significant drawbacks of the products include aluminum toxicity, hypercalcemia, and poor binding efficiency. Thus, a need exists for affordable, improved insoluble phosphate binders that can be orally administered in appropriate dosage amounts, with reduced side effects.

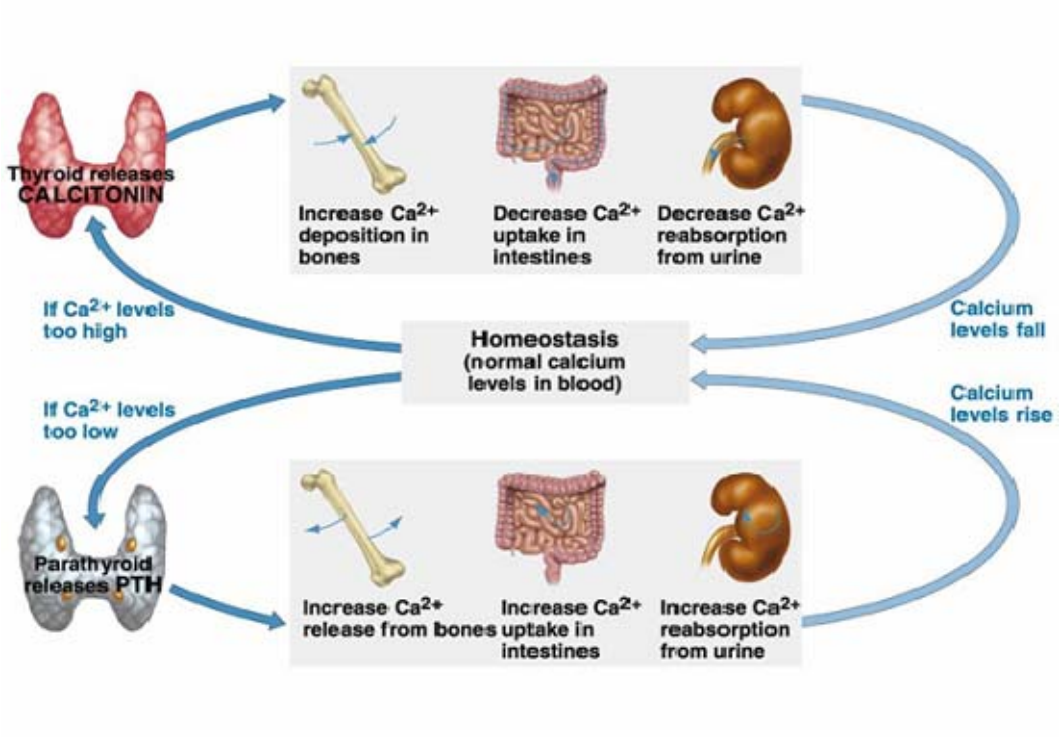

Figure 2-1. Hormonal control loop for calcium metabolism.[25]

Surface Functionalization of Polymeric Microparticles

Surface modified microspheres have been proven to have great impact applications in regards to the synthesis of new and exciting biomaterials. Characteristically, microspheres are superior materials due to their various tunable properties. Their inherent high surface area provides an ideal platform for attaching specific site attachment of ligands, which can be used in various systems in which targeted molecular recognition is paramount. Through this process, relatively inert microspheres can be altered to have precise interactions with other molecules.

Molecular Imprinting

The concept of using molecular imprinted polymers (MIPs) for chemical recognition actually originated from Linus Pauling's template-and-cast theory.[26] In the early 1940's, Pauling speculated that when an antigen is introduced into a blood system, it is recognized as a foreign object. The system creates antibodies that surround the antigen and form a rigid structure, thus

holding the antigen in place and rendering it ineffective. He described possible bonding that allows the antibodies to encase the antigen in a 3-dimensional configuration, and proposed that the antigen can eventually dissociate from the antibody structure, thus leaving behind a well-defined antigen-binding cavity. When the antigen is re-introduced to the system, it can be selectively recognized and re-trapped by the same antibody structure. Though Pauling's theory was not correct for antibodies, his idea eventually found fulfillment in the synthesis of molecular imprints.[27]

The challenge in molecular imprinting has been to determine which materials are best suited to be a molecular cast for desired template molecules and subsequent release of the template for future recognition. In addition, the determinations of the optimal processing parameters for these reactions are not yet known. Many researchers began to address this challenge in the 1970's. Gunter Wulff and his group were among the first to report the imprinting of cross-linked organic polymers as a method to synthesize molecular recognition sites in 1972.[4]

The overall concept is very simple, as shown in Figure 2-2.[28] A template molecule is introduced into a solution containing functionalized monomer, and functional groups of the monomer bind to reactive sites on the template molecule. A cross-linking agent is added to the solution and polymerization occurs around the template molecule. When the template is removed, a well-defined cavity remains in the rigid cross-linked polymer. Once re-introduced to the polymer, the template molecule is capable of selectively binding to the site and thus is "recognized".

Both non-covalent and covalent bonds can be formed between a MIP and a print molecule, which are usually the same as those that happen during the initial steps of polymer synthesis.

The major requirement in these interactions is that they be reversible.

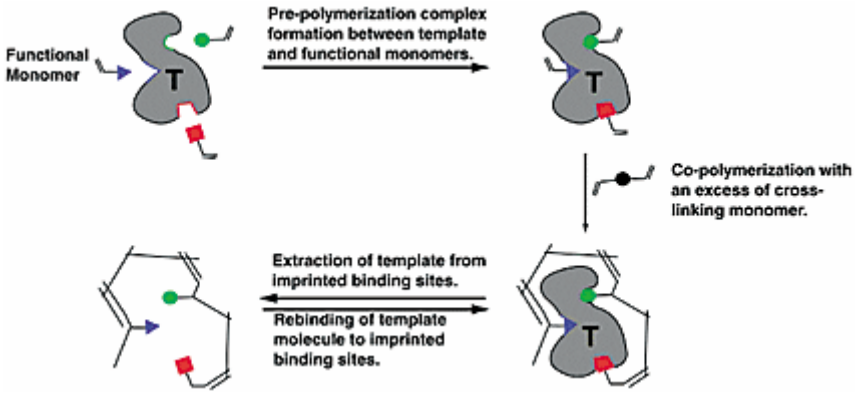

Figure 2-2. Concept of molecular imprinting of polymers.[28]

Covalent vs. Noncovalent Synthesis

For most applications, two methods are generally considered for the synthesis of imprinted polymers: the covalent and non-covalent technique (Figure 2-3).[29] Each approach has its own set of advantages and disadvantages, and the overall choice ultimately depends on the type of template molecule targeted for imprinting.

In covalent imprinting, the functional monomer and template molecule are linked together through covalent binding, and subsequently polymerized. Upon cleaving, the covalent bond is broken, and the template molecule is released from the polymer. When the guest molecule (template molecule) is re-introduced to the polymer matrix, the imprint site will recognize the molecule and bind it through the same type of covalent bond. In terms of template uptake, binding sites are only situated inside the cavity. Upon removal of the template, the cavities usually swell, which ensure a high proportion (90-95%) of reuptake after the initial removal. This concurrently facilitates a rapid mass transfer during equilibration of the template with the polymer. Upon reuptake of the target molecule, the cavity shrinks to its original volume. Advantages of using this scheme are that the monomer-template conjugates are stable and stoichiometric, which makes imprinting relatively straightforward. In addition, many

different polymerization environments can be supported due to the use of such stable covalent bonds. Disadvantages include difficult synthesis of the monomer-template conjugate, the limited number of available imprinted sites produced during synthesis, cleaving the guest molecule from the imprinted polymer can be destructive to the site, and the overall slow kinetics of the removal/binding process.[30, 31]

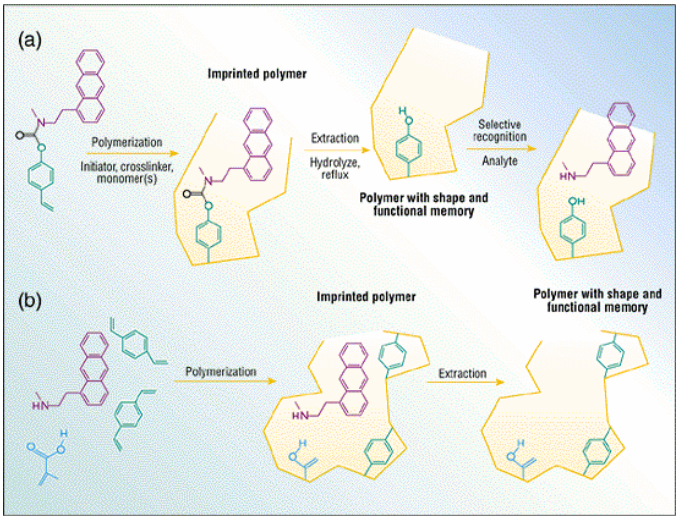

Figure 2-3. Simplified schematics of (a) covalent and (b) noncovalent imprinting procedures.[29]

With non-covalent imprinting (hydrogen bonding, electrostatic interaction, and coordination-bond formation), the functional monomer is first allowed to self-assemble around the template molecule, and then the mixture is polymerized. The guest molecule is then extracted using either an acid or a base. Once re-introduced, the guest molecule can be bound to the MIP through non-covalent interactions. Noncovalent imprinting requires a four-fold excess of binding sites in order to guarantee good selectivity. The binding sites are distributed among the entire polymer. However, only 15% of the cavities are available for reuptake of the template molecule, with the rest being irreversibly lost for use.[32] This is possibly due to the shrinking of the majority of the host sites. Advantages include eliminating the monomer-template conjugate bonding process, as required by the covalent imprinting process, easy removal of the guest

molecule from the imprinted polymer, and the kinetics of the removal/binding process is fast. Disadvantages include a loosely defined process since the stoichiometry is not strict, reaction conditions have to be clearly defined in order to maximize the number of imprinting sites developed, and selectivity of these sites is reduced due to the excess functional monomer present.[30, 31]

Noncovalent imprinting was chosen for these studies, since the easy removal of phosphate to produce the MIP, and fast binding of the molecule in-situ are paramount to the management of hyperphosphatemia in chronic renal failure patients.

MIPs are often prepared via methods such as thermal initiation, photopolymerization, or redox polymerization techniques.[33] Several advantages that thermal initiation has over the other methods are that it has faster enantiomeric separation times, thus the detection times are shorter. However, the other techniques provide slightly better adsorption capacities, which provide a medium that is more selective towards the template molecule. MIPs are superior to antibodies in terms of their enhanced affinity towards a number of important analytes, higher loading capacities, reusability, reproducibility and stability. For this reason, thermal initiation was chosen.

Radiation Polymerization

Polymerizations involving radiation initiation are becoming a popular alternative to traditional chemical initiators due to their decreased dependency on external additives to initiate polymerization. This provides a process in which "green" polymerizations can occur, which can reduce the amount of byproducts produced during synthesis. For imprinted polymers, using radiation initiation provides spatially controlled polymerization in situ, with rigid, clearly defined imprint sites. [34] Incorporation of this strategy into the imprinting regime may improve the

stability, thus the overall success, of the phosphate reuptake process with the functionalized microspheres.

Polymerizations reactions were conducted using a simple countertop kitchen microwave, which was purchased from a local department store, with remarkably great efficiency. The irradiation energy from the microwave is sufficient enough to promote radical or step growth initiation in many different polymer systems. In this study, chain crosslinking is induced to an extent that is MIT compliant.

Previous Related Work

Many research groups[31, 35, 36] have successfully developed imprinted polymers for a variety of applications in different areas of technology, which show promise for the probable success of fabricating a phosphate imprinted polymer. One such use involves MIPs as stationary phases in chromatography for chemical detection.[37, 38] Figure 2-4 shows the achievement of MIPs in enantiomeric chromatographic applications.[29]

Another practical use of imprinted polymers is in the directed nucleation of calcite. Functionalized monomers that contain a crosslinking agent are introduced to a calcite structure, and subsequently polymerized. The calcite is washed away leaving behind a well-defined imprinted polymer. The resulting imprinted "cavities" serve as preformed nucleation sites for calcite, and upon exposure to a solution of calcium chloride and sodium carbonate, rhombohedral calcite crystals are formed (Figure 2.5).[39]

MIPs have also found an interesting niche in many different bio-inspired applications, such as biomimetic glucose sensors.[40] In this technological development, a molecularly imprinted poly (allylamine hydrochloride) hydrogel was synthesized with d-glucose 6-phosphate monobarium salt as the template molecule. The resulting MIP displayed enhanced binding affinity towards glucose over fructose, indicating enantiomeric selectivity.

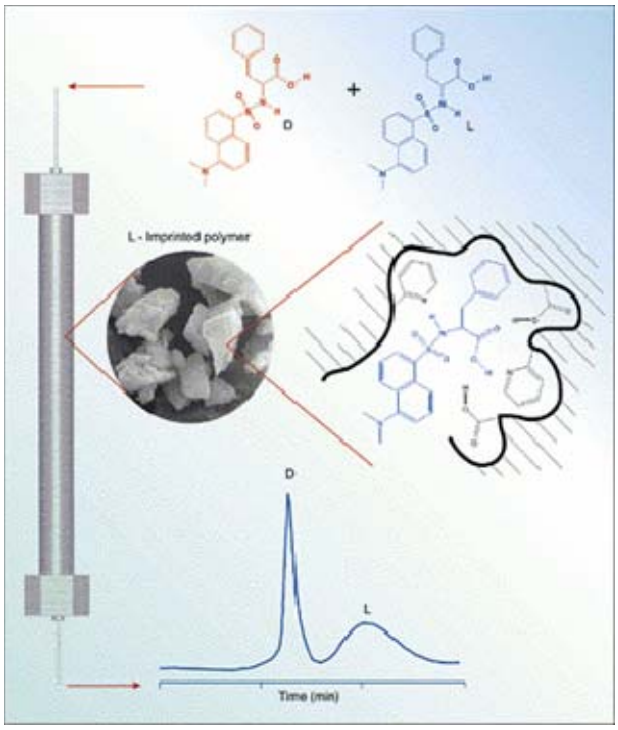

Figure 2-4. Depiction of an HPLC column packed with a MIP stationary phase used for chiral separations.[29]

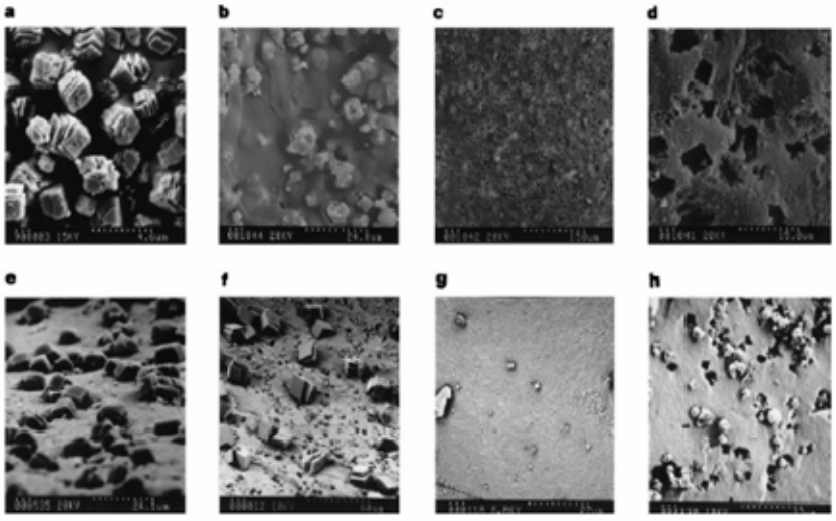

Figure 2-5. Nucleation of calcite at the polymer surface. Scanning electron micrographs (Hitachi S570) showing: a, template calcite crystals; b, Calcite imprinted polymer (PI-1) as obtained; c, d, PI-1 after HCl/CH3OH wash; e, f, nucleation of calcite crystals on PI-1; g, h, control polymers CP-1 and CP-2 respectively, after immersion in supersaturated CaCO3(aq.). [39]

The hydrogels ability to demonstrate preferential template uptake in a replicated physiological environment prove its potential use in the development of a new hand held glucose sensor device.

CHAPTER 3
RENAGEL CHARACTERISTICS

Understanding Renagel®

Phosphate binding remedies have been extensively used as a means to reduce the excess blood serum phosphate that is commonly found in individuals suffering with chronic renal failure. Sevelamer HCl is a highly effective binder due to the cationic charge of protonated amine groups, removing phosphate *in-vitro* at approximately 3 meq (288 mg/g drug).[41] Rigorous pharmacokinetics has not been published so as to describe the need for the rather high doses of this expensive medication in clinical practice. This study was designed to examine the pharmaceutical success of Renagel®, which is one of the most successful phosphate sequestering agents in current circulation. In order to provide an accurate and well-formed evaluation of the phosphate binding polymeric microspheres that have been developed for this project, a study of the effect of pH on swelling and phosphate uptake in Renagel® is presented.

Structural Properties of Renagel®

Renagel® is the trade name for the chemical Sevelamer Hydrochloride, an oral medication for patients on dialysis. Its major binding mechanism reduces the amount of excess serum phosphate that is absorbed by the intestine in patients with hyperphosphatemia, thus lowering the overall serum phosphate concentration. Sevelamer HCl is manufactured by GelTex Pharmaceuticals in Waltham, MA, and distributed by the Genzyme Corporation in Cambridge, MA.[42] It is an extremely popular phosphate binding polymer due to its exclusion of calcium or aluminum as binding agents.

Structurally, Renagel® is poly(allylamine hydrochloride) crosslinked with epichlorohydrin, containing about 40% forty percent of protonated amines separated by one carbon from the polymer main chain (Figure 3-1). The amines are partially protonated and

interact with phosphate molecules through ionic and hydrogen bonding.[43] Chemically, it is properly referred to as poly(allylamine-co-N,N'-diallyl- 1,3-diamino-2-hydroxypropane) hydrochloride. Sevelamer hydrochloride is hydrophilic, and insoluble in water[44] because of the crosslinking.

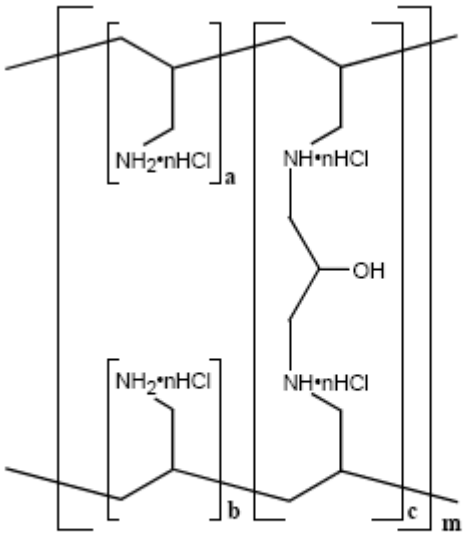

a, b = number of primary amine groups a + b = 9
c = number of crosslinking groups c = 1
n = fraction of protonated amines n = 0.4
m = large number to indicate extended polymer network

Figure 3-1. Chemical structure of sevelamer hydrochloride.[45]

Renagel® Swelling Behavioral Studies

Polymer swelling studies were also performed to examine possible influences associated with phosphate uptake.

Experimental Methods

Particles for swelling analysis were obtained by placing a Renagel tablet in 100 mL of deionized water at pH=7 for 1 hour at room temperature. This led to disruption of the tablet, and release of the smaller particles of polymer. The solution was filtered, and the particles were air dried overnight. Once dried, particles were spread over double-sided stick tape, and a flow cell was constructed (attach the tape to the middle of a microscope slide, place a bead of silicon

around the circumference of the slide, place another slide on top, and let dry for at least 24 hours). Solution flow was set to 100 mL/hr, which was regulated via a syringe pump, and attached to the flow cell through syringe needles. Swelling was monitored with an optical microscope using Zeiss imaging software. Particle swelling was analyzed after flowing solutions of 0.1M HCl at a pH level of 1, 2.5, or 7 for one hour over them. Additional trials involved a combination of solution environments to determine the effect that changing pH conditions had on swelling. This was apparent through flowing a solution of pH=7 through the cell for one hour, followed by a solution at pH=1 for an additional hour, and vice versa. Careful attention was paid to the cell to insure that it was not allowed to dry during any part of the procedure, as to maintain true swelling for the analysis.

Effect of pH on Phosphate Uptake

Polymer-based drugs present unique challenges in that they may swell or dissolve in aqueous solutions. Their efficacy can thus depend on the kinetics of ligands in solution interacting with moieties having varying degrees of hydration. Conditions or medications that impair gastric acid might then partially explain the patient-to-patient variability in the number of tablets needed to control plasma phosphate levels with ostensibly similar dietary intakes. To investigate this effect, we studied phosphate uptake by Renagel® at pH 7, after an initial incubation phase in solutions at different levels of acidity.

Incubated solutions at pH of 1, 2.3 and 7 were created to simulate potential human gastric conditions:

> Renagel® 800mg tablets were each placed unaltered in 400 ml of the incubation solution, with an n=7 for each of the 3 pH levels for 1 hour, with agitation, at 37 °C. The pH was adjusted to 7, and all fluid was removed by vacuum filtration. Phosphate uptake was then tested using a pH 7 solution simulating a gastric environment (20 mM KH_2PO_4, 80mM NaCl and 30mM Na_2CO_3) for 3 hours, with agitation, at 37 °C, and filtered. Phosphate content was assayed using atomic emission by ICP, to obtain a mean of 5 repetitions reported in this work.

Incubated solution at pH 0.3:

Experiments at acidic levels outside of the normal human gastric range were conducted to examine maximal protonation. Identical sampling and ICP measurements were performed at this pH.

Statistics: Descriptive and nonparametric statistics (2 tailed Kruskal-Willis test) were performed, with a $p < 0.05$ considered statistically significant.

Uptake values were calculated as milliequivalents, meq, which describes moles of phosphate multiplied by its valency (1.8) in solution.

Mean values were expressed to ± one SD.

Figure 3-2 illustrates tablets in a pH 7 incubation demonstrated an average phosphate uptake level of 1.85 ± 0.46 meq/g drug. This increased to 2.72 ± 0.35 meq/g with pH 2.3 incubation, and 3.13 ± 0.21 meq/g with pH 1 incubation. These changes were statistically significant: pH 7 versus either pH 2.3 ($p=0.01$) or pH 1 ($p=0.0003$); and pH 2.3 versus pH 1 ($p=0.01$). The difference between the pH 7 and pH 1 uptake was approximately 1.28 meq/g drug. This represents 123 mg phosphate/g of the medication, or an increase of 69% in binding.

The dry polymer demonstrated significant swelling of 50-70%, upon 1-hour exposure to a aqueous pH solution ranging from 1 to 7. However, not as much swelling (2-10%) occurred when a hydrated sample in a low pH acidic solution, was further exposed to a dilute HCl solution of pH 7. The majority of phosphate uptake was concluded to occur within the first hour of exposure to an aqueous environment.

Altering pH had a significant effect on the amount of phosphate uptake in our studies. Polymer swelling was examined at different solution pH levels, as to imitate small intestine conditions in-vivo. Swelling was consistent with the literature, which reports an overall increase in swelling of various polymers as the pH falls below the pKb of the molecule. Although Sevelamer's phosphate binding has been characterized at different pH levels, it is speculated that transient pre-exposure to an acidic environment enhances hydration, which may lead to an

increase in phosphate uptake. The hydrogels chains expand to their physical limit, but remain intact.

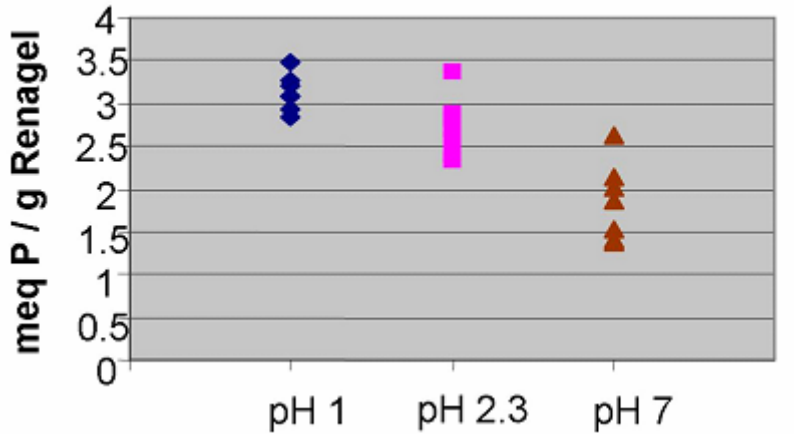

Figure 3-2. Phosphate (P) uptake in Renagel®. Solutions were at a pH of 1, 2.3 or 7, and incubated at 37 ^{o}C, to simulate human gastric conditions.

At this point there is minimal interaction between the chains, which in turn is offset by the hydrogel matrix crosslinkers. As a result, phosphate uptake is likely the result of binding to available protonated sites via diffusion of phosphate molecules into the network, from the aqueous environment, which creates an overall hydrating type effect of the polymer. These results also indicated that it may be possible for the polymer particles to crosslink to an extent such that large-scale swelling is not physically attainable.

Phosphate Binding Mechanism

Computational techniques were used to determine molecular binding in the Renagel polymer system. The established model defined the mechanism of phosphate ion capture, upon which a direct comparison was made to the expected binding phenomena in this surface modified microsphere system. A relatively simple model was designed with a dimer of Sevelamer Hydrochloride and four phosphate ions for binding simulation, which was based on electrostatic

interactions. Molecular dynamics and Monte Carlo simulations were used to determine average structure, intermolecular interaction regions, and the volume change associated with the phosphate capturing mechanism. This computational study was performed and interpreted in conjunction with Dr. Reginald Parker, formerly of Florida State University, and Dr. Jesse Edwards III, Assistant professor of Chemistry at Florida A&M University.

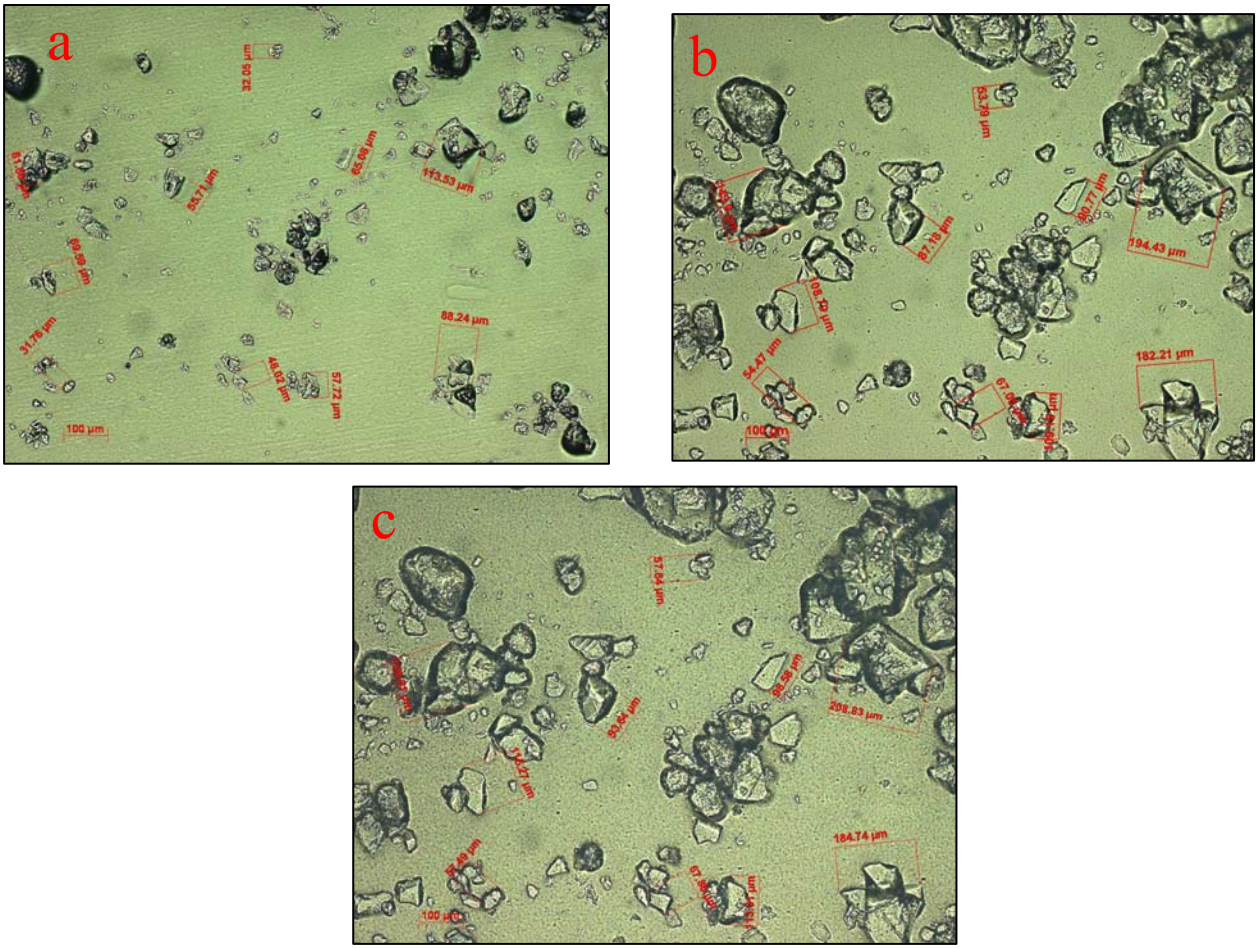

Figure 3-4. Observed swelling of dry particles (a) exposed to an acidic solution at pH = 1 for 1 hour (b), followed by additional exposure to a pH = 7 solution (c), using an optical microscope.

The amine groups in Sevelamer Hydrochloride are protonated by HCl, resulting in a set of positively charged "cages" in which phosphate anion capture occurs. The hydroxyl groups serve as additional binding sites through hydrogen bond forming interactions. Using these parameters

and a predictive model of 1.5 repeat units (Figure 3.5), molecular dynamics,[46, 47] and Monte Carlo methods, [46, 48] insight into the interactions and bonding structure of this system were defined. Monte Carlo simulations were specifically used to conduct volume calculations which can be compared to experimental swelling measurements by of this model.[49]

Molecular Dynamics

Vacuum system

Sybyl 6.9 Software[50] was used to perform minimization and molecular dynamics simulations on SGI Origin 2000 using a Tripos Forcefield. The energy of a molecule derived from a Tripos force field is defined as the sum of energy contributions that extend over all bonds, bond angles, torsion angles, and non-bonded interactions between atoms not bound to each other or to a common atom.[51] Energy minimization was calculated with Sybyl 6.9 force-field and Gasteiger-Huckel[52] charges with a non-bond cutoff distance of 8 Å using the conjugate gradient method until the root mean square deviation (RMS) < 0.05 kcal/mole/Å. An NVT ensemble[46] molecular dynamic simulation was conducted in vacuum with Gasteiger-Huckel[53] charges assigned at 300 K for 400 ps, with a time step of 1 fs. Data was collected at intervals of 200 fs.

Solvated System

The dielectric constant of the system was set to a value of 78 debye to simulate an aqueous solvated system with a homogenous field. Gasteiger-Huckel charges were assigned to the atoms of the system. Using this treatment, the large dielectric constant diminishes the coulombic interactions of the charged atoms, which allows the van der Waals interactions to be probed, absent strong coulombic effects. Thus, the effect of the van der Waals attraction on phosphate capture is determined, and the overall binding event is elucidated.

Monte Carlo

Monte Carlo simulations were used to determine the volume of each molecule. The Monte Carlo method was broken into four parts: First, a spherical shell was formed around the molecule. Second, several random values were generated as points in space, bound by the dimensions of the sphere, which allowed all derived points to fall within the sphere without necessarily having to fall within the molecule. Third, an algorithm was used to assess if the values actually fell within the molecule. Lastly, the volume of the sphere was multiplied by the ratio of points falling within the molecule to the total number of available points. The resultant product was assessed to be the aggregate volume of the molecule.

Determining the Shell Volume

The molecular systems 3-D spatial coordinates are extracted from the molecular modeling program in the CSSR format (Cambridge Structure Search and Retrieval). This layout was comprised of a numbering column, an atom identification column, spatial coordinates, connectivity matrix, the potential charge of each atom, and several other miscellaneous chemical information attributes that help define the system.

The spatial location was given in terms of Cartesian coordinates. The center of the molecule (x',y',z') was determined by averaging the values in the coordinate space. The molecule was then translated by spatial subtraction of each value by the origin. This resulted in an origin of the molecules center being set to (0,0,0). The coordinate space was subsequently transformed into spherical coordinates. The largest value of r was determined, and 2 Å were added in order to determine r_{shell}. From this, the volume of the shell was calculated.

$$V_{shell} = \frac{4}{3}\pi r_{shell}^3 \qquad (3\text{-}1)$$

Thus, the Monte Carlo method was used to extract the molecular volume based on the computationally derived shell volume.

Generating Random Numbers

The stock random number generator of Matlab® was used to generate three random numbers for each point in the simulation. The first two numbers were bound by $(-\pi, \pi)$ with angles given in radians, and the last number was bound by the radius of the shell.

Determining the Ratio

The solution technique was evaluated in iterative segments in order to maximize the efficiency of the treatment. The first step assessed the generated radius of the molecule. If the derived radius was larger than that on the existing molecule, the value was determined to be on the outside of the molecules spherical area and added only to the total count. If the value was less than those found within the molecule, it was considered to contribute to the molecule itself. In addition, radii could also contribute to the molecule if one or more points have a radius greater than the determined angle, and are within 0.07 radians (~2 degrees) of any of those points. This effective method was run several times until the ratio values (Equation 3-2) become relatively constant and reproducible.

$$ratio = \frac{count_{inside}}{count_{total}} \tag{3-2}$$

Determining the Volume of the Molecule

The ratio of molecules determined using Equation 3-2 was then used to calculate the volume of each molecule, as set up in Equation 3-3.

$$V_{molecule} = V_{shell} \times ratio \tag{3-3}$$

The volume of the molecule was found by using a nested for-loop towards the average of several runs. The first for-loop generated a ratio, while the second for-loop determined the stability of

the Monte Carlo method prediction for the volume of the molecule. The method was deemed valid of it had a covariance less than 3%.

Results

Results compared the actual experimental swelling measurements to calculated values obtained from running the simulations. Molecular dynamic simulations were used to create a model of the average structure of the proposed system interacting with four triphosphate ions. The derived average structure was used in a Monte Carlo simulation to calculate the volume of the model system. The percent change of volume (% swelling) was calculated by comparing the volume difference of the model system with and without the presence of phosphate ions.

The space filled representation of the model system (Figure 3-4) suggested that approximately 75% of the phosphate ions were trapped in the amine cages found in the center of the system, and the remaining phosphate ions oriented at a surface amine site on the model molecule. This was a strong indication that Van der Waals interactions were the primary binding forces for the phosphate ion capturing mechanism in this model system. More specifically, these results supported the notion that this was a zwitterionic interaction. Zwitterions carry both formal positive and negative charges that, in essence, compensate for each other making the overall molecule electrically neutral. Their association was polar in nature.

Further examination was performed by plotting the interatomic distances between various nitrogen and phosphate atoms, and evaluating the dynamic motion of the amine groups and sequestered phosphate ions.

Interatomic distances were isolated choosing specific nitrogen (Nitrogen 126) and phosphorous (Phosphorous 237) atoms, which are listed in Figure 3-6. The atom labels represent the atom type and number for the total selected system. The data demonstrated that system stabilized and maintained a bond distance between 2.7 – 4 Å upon the resolution of the

reorganization energy. In addition, the plot illustrates a system adjustment around 480 ps, which allows the Nitrogen - Phosphorous separation to fall below 3.5 Å. Eventually the system adjusted back to an average separation of approximately 3.5 Å. This provided a mechanism for hydrogen bonding between the phosphate ions and the hydrogen atoms on the amine groups through a zwitterion association.

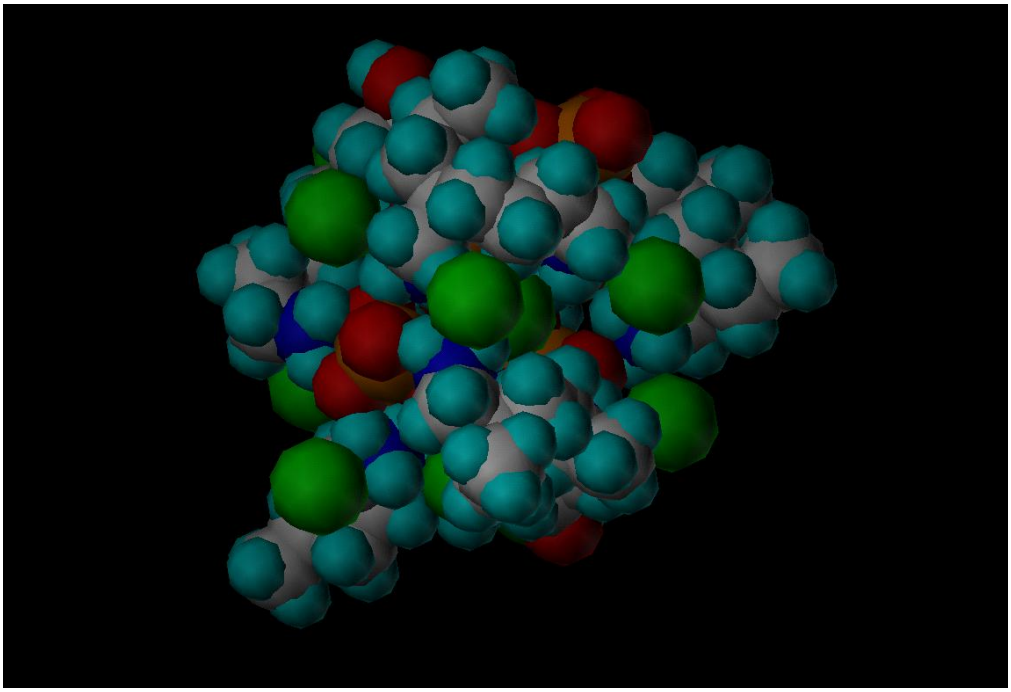

Figure 3-5. Van der Waals representation of the space filled model system with four phosphate ions bound to the polymer. The green spheres represent chloride ions (counter ions to amines), light blue spheres are hydrogen atoms, dark blue spheres are nitrogen atoms, red spheres are oxygen atoms, and the orange spheres are phosphate ions.

Figure 3-7 represents a similar type of plot, except the distances of Nitrogen 204 and Phosphorous 237 was calculated. In this example the nitrogen group was bound to the end of the polymer, which allowed more freedom in the wagging motion in comparison to the previous calculation. This allowed the phosphate motion to be held constant, thus the resulting motion was attributed to the amines ability to wag in and out of the proximity of the phosphate. The periodic interatomic separation between the phosphate ion and the amine nitrogen were due to

the flapping motion of the amine on the polymeric tail and varied between a separation of 5 Å for 200 ps to below 4.3 Å for 400 ps.

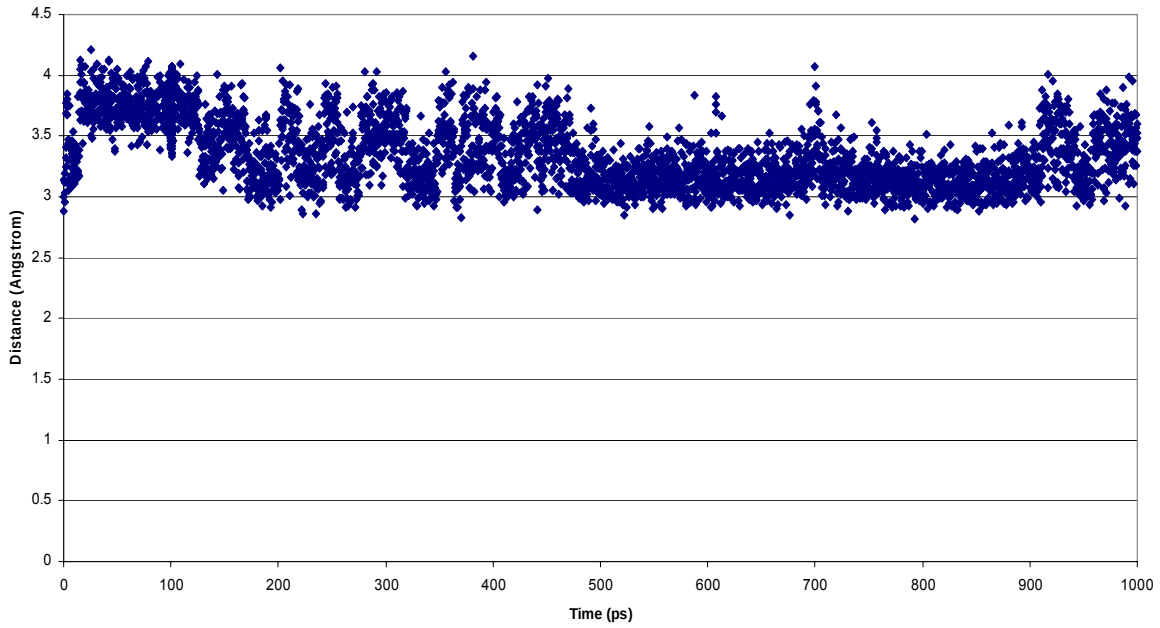

Figure 3-6. Interatomic distance between Nitrogen (126) and Phosphorous (237) in the model system Renagel® and four triphosphate ions, with an N-P separation adjustment of the system at about 480 ps.

The reorganization and stabilization that occurred during the simulation was represented in Figure 3-8, which expressed the interatomic distance between Nitrogen (89) and Phosphorous (237), which display typical behavior for amine groups and phosphate ions in the central cages of the polymer. After the reorganization of the polymer, the molecular separation was maintained at a distance which was roughly 3.5-4 Å.

Tables 3-1 and 3-2 show values of various interatomic separations obtained from the results of a NVT ensemble simulation in vacuum for the four phosphate ion system. Phosphate ions bound in the central region of the polymer exhibit nitrogen-phosphorous separations on the order of 3-4 Å, which indicated minimal movement of these sequestered phosphates.

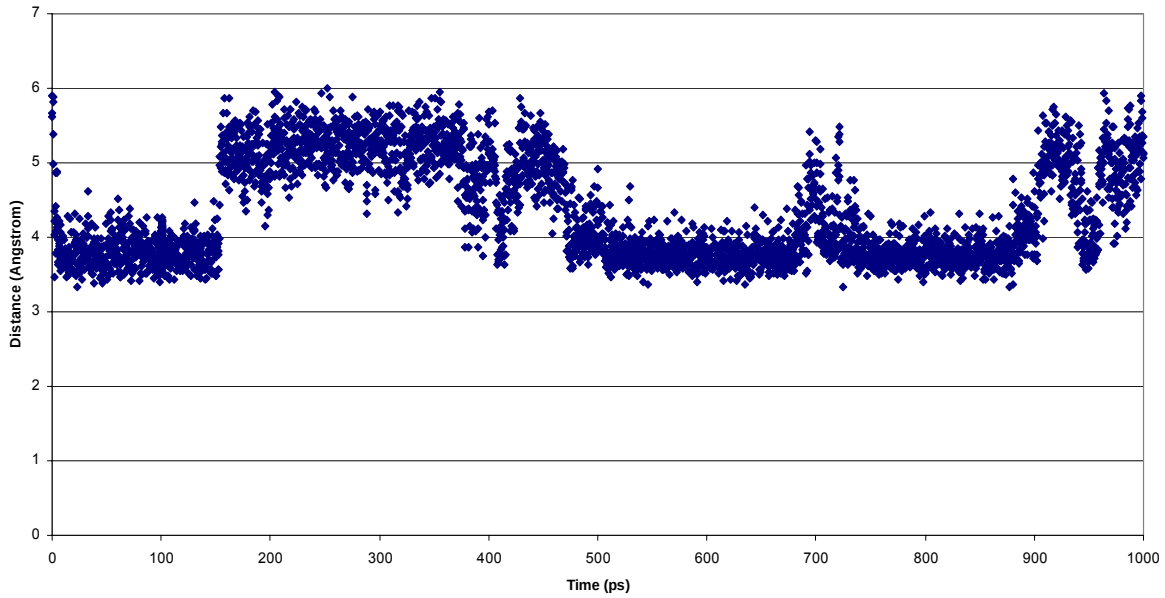

Figure 3-7. Interatomic distance between Nitrogen (204) and Phosphorous (237) in the model system Renagel® and four triphosphate ions. This figure shows the periodic motion of end amine group flapping in and out of the proximity of the Phosphorus 237 atom of a triphosphate ion.

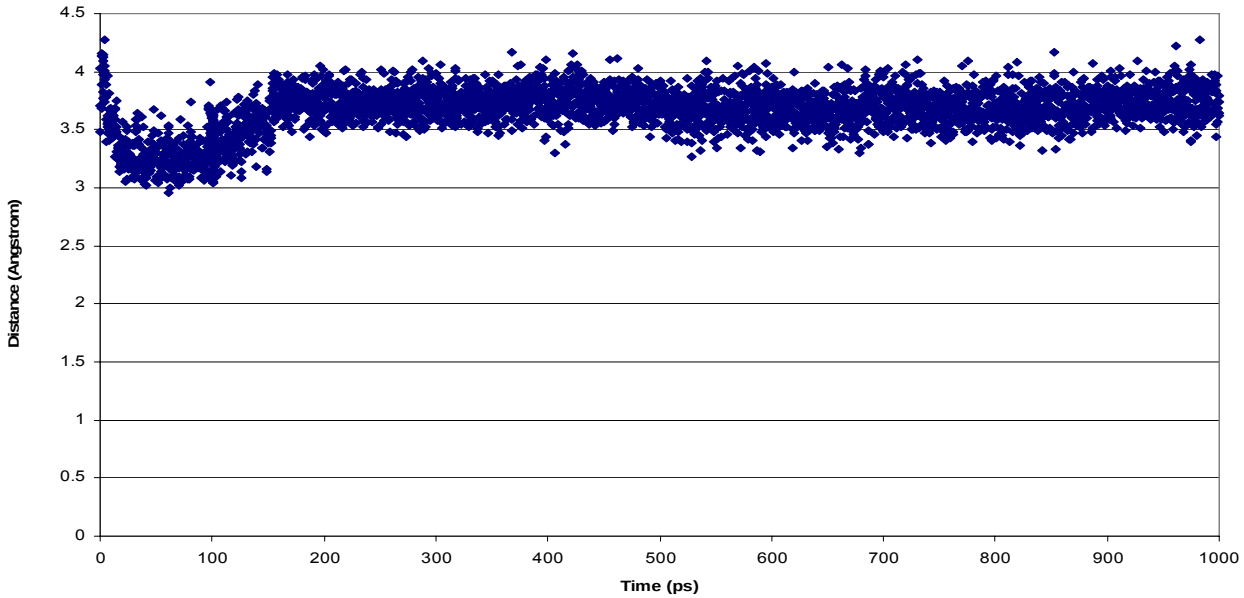

Figure 3-8. The change of interatomic distance between N(89) and P(237). Shown is the reorganization and stabilization that occurred during the simulation. An interatomic separation of approximately 3.5-4 Å was maintained after the reorganization of the polymer.

Figure 3-9 shows the stable separation between Phosphorous 237 and Phosphorous 216 of about 6-7 Å when measuring the distances between a set of interior (captured) phosphate ions, which remained constant after the stabilization of the simulation.

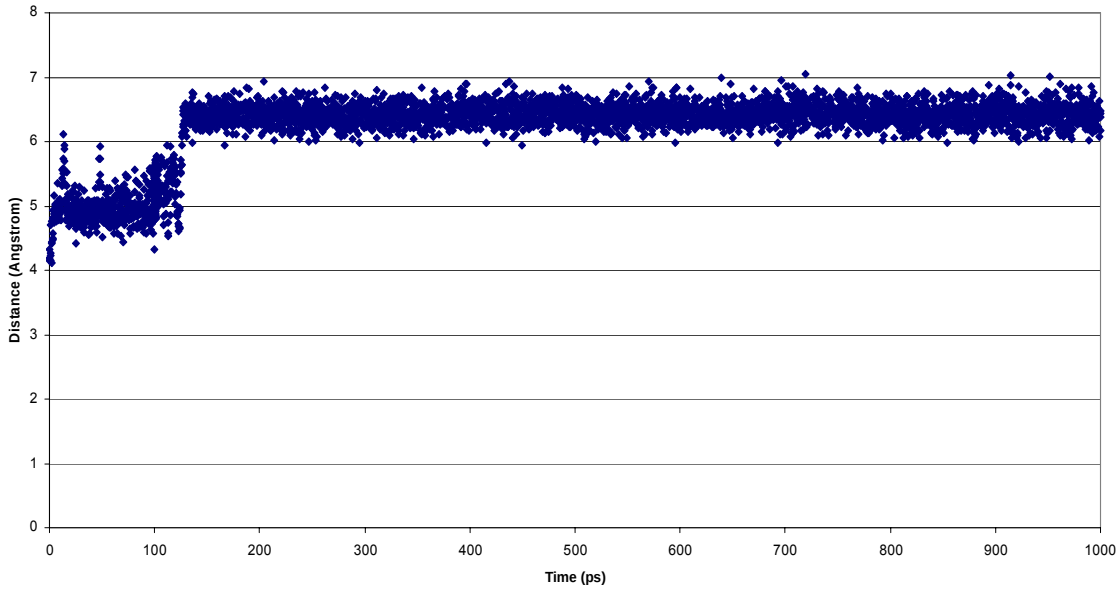

Figure 3-9. The P(237)-P(216) interatomic separations versus simulation time. The plot shows a stable separation after about 100 ps between 6-7 Å.

This separation was constant between all of the phosphorus atoms within the phosphate ions confined to the center of the polymer.

Due to the large dielectric constant in the simulated solvated system, considerable reorganization takes place before being stabilized. Equation 3-4 is used to compute the coulombic interactions, which significantly decrease.

$$U = \frac{q_1 q_2}{D r^2} \qquad \text{(where D is the dielectric constant)} \qquad (3\text{-}4)$$

In Table 3-1 the standard deviation of the nitrogen - phosphorous separations for the centrally captured phosphate amines was relatively low, where as the deviations in Table 3-2 were much higher due to the mimicked solvation using the change in dielectric from 1 to 78 debye. This was due to the fact that the binding of phosphate is attributed to van der Waals

interactions, which required structural rearrangement within the polymer to properly incorporate the phosphates in an amine cage. Table 3-2 summarizes such results.

Table 3-1. Interatomic distance values (mean, standard deviation, high, and low) for the NVT ensemble simulation in vacuum for four phosphate system with dielectric 1 debye.

NVT Ensemble 4 PO4 dielectric=1 Interatomic Distances [Nitrogen - Phosphorous, Phosphorous - Phosphorous, Hydrogen - Chlorine] (Å)				
Atom Types and ID Number	Mean	Standard Deviation	High	Low
N126-P237	3.35	0.28	4.21	2.82
N39-P237	3.16	0.18	4.02	2.76
N89-P237	3.66	0.19	4.27	2.96
N30-P237	3.35	0.14	3.81	2.92
N81-P237	3.13	0.12	3.73	2.69
N204-P237	4.33	0.68	6.00	3.34
N102-P2421	3.15	0.11	3.63	2.79
N204-P242	3.36	0.16	4.00	2.78
N165-P242	4.10	0.17	5.32	3.49
N89-P226	3.44	0.42	5.12	2.86
N165-P226	3.08	0.09	3.51	2.79
N188-P226	3.19	0.13	4.03	2.81
N139-P226	5.84	1.03	7.01	2.97
N201-P216	3.03	0.14	3.82	2.71
N16-P216	3.29	0.23	4.56	2.82
N65-P216	3.18	0.17	4.30	2.74
P237-P216	6.21	0.53	7.04	4.12
P226-P242	5.90	4.09	0.19	4.88
Cl106-H143	3.19	0.13	4.03	2.81

The calculated average volume from the molecular dynamic simulation of the solvated four phosphate systems produced a percent swelling of 140% which was good agreement with some of the extreme values of the experimental results.

Conclusions

Molecular dynamic and Monte Carlo simulations were used to develop a simple model of phosphate binding events in the Renagel® polymer. Our results showed an average swelling value of 25% in vacuum and over 140% in water during the simulations, which were relatively

consistent with experimental results of between 10-200%, with the average being approximately 50-60%. Data was also obtained using these simulations that support the view that the predominant molecular interactions in this system are via van der Waals forces, specifically zwitterionic in nature.

Table 3-2. Interatomic distance values (mean, standard deviation, high, and low) for the NVT ensemble with dielectric 78 debye to mimic a solvated system (H2O). This system shows the capture of four phosphates internally and externally for several hundred picoseconds.

NVT Ensemble 4 PO4 dielectric=1 Interatomic Distances [Nitrogen - Phosphorous, Phosphorous - Phosphorous, Hydrogen - Chlorine] (Å)				
Atom Types and ID Number	Mean	Standard Deviation	High	Low
N16-P223	10.22	2.23	21.41	6.72
N131-P228	4.52	0.97	9.28	3.19
N84-P228	4.59	1.06	9.40	3.37
N96-P228	5.55	0.78	8.45	3.70
N144-P228	9.19	1.04	13.67	4.06
N155-P228	10.48	1.42	14.61	4.54
N77-P228	7.82	0.89	12.33	6.01
N77-P202	4.69	1.59	10.59	3.03
N177-P202	5.66	2.28	12.81	3.19
N62-P202	8.52	4.84	20.28	3.24
N155-P202	5.92	2.70	14.42	3.39
N119-P202	12.44	1.99	15.98	4.73
N77-P223	6.40	3.49	20.10	3.15
N119-P223	9.88	3.78	21.27	3.36
N29-P212	4.99	1.12	11.35	3.42
N37-P212	4.76	1.17	12.46	3.32
P223-P212	9.80	2.77	18.99	5.73
N77-P212	4.91	0.74	8.18	3.26
N29-P223	8.00	3.72	17.18	3.40
P228-P202	9.41	1.66	12.27	4.16
P223-P228	8.47	1.96	17.60	4.91

These results exemplify the capture mechanism of the phosphate ions with minimal electrostatic interactions, which will be used to envisage the various forms of the protonated phosphate ion available for uptake in the synthesized surface altered polymers. The simulated

polymer model indicates that internally, amine cages form around the phosphate in the center of the polymer for binding events, while the external capture of the phosphates is accomplished through interactions about one of the P-O bonds with the amines on the exterior of the polymer. These results are used in subsequent chapters to structure the method of phosphate capture that occurs in the different MIPs that are produced, and to and support the use of molecular imprinting technology in this research.

CHAPTER 4
POLYMERIZATION PARAMETERS

Experimental Design and Material Selection

The main goal of this research was to develop a robust system in which a functionalized polymer could be synthesized for the selective binding of phosphate ions. Upon modification of this polymer, and other process parameters, the polymer could be produced and applied to *in-vitro* and *in-vivo* testing. This novel technique may be especially valuable in the development of resorbable polymer technology in which highly selective chemical recognition is possible and, due to the highly crosslinked nature of the host polymer, the system degradation will be minimal. This is especially important for *in-vivo* applications, where the polymer must remain in tact while removing the molecule of interest in a gastrointestinal environment. *In-vivo* processing of these polymers would include oral ingestion, processing through the digestive tract, binding of phosphate in the gastrointestinal tract to prevent phosphate from being absorbed, and eventual urinary and bowel excretion. Gelatin was chosen as a potentially useful candidate.

Granular gelatin was weighed and placed in a reaction vial with a predetermined amount of boiling water, whose pH had been adjusted to approximately 7.4, until it dissolved. Potassium phosphate monobasic (KH_2PO_4) was added to the gelatin solution for phosphate containing samples only, otherwise the control sample was the viscous gelatin blend alone. The gelatin mixture was slowly added to a round bottom flask containing common grade oil (vegetable, corn, etc.) at 60^{o} C to create a water-in-oil emulsion, where no additional emulsifier was required. The reaction flask was stoppered with a rubber septa, purged with a nitrogen stream, and allowed to stir for approximately 60 minutes to allow a stable emulsion to form. 10 – 50% w/v of the crosslinking agent was added, and the blend was mixed for an additional amount of time. Upon visible formation of microspheres, the crosslinked mini emulsion was aggressively washed in

order to remove any residual amount of crosslinking agent.

The potassium phosphate monobasic, Type B (225 bloom) bovine gelatin, 50% w/v glutaraldehyde, D,L-glyceraldehyde (≥90%), and cottonseed oil all came from Sigma-Aldrich chemical company. The crosslinking agent, genipin, was ordered from Wako Chemicals. All chemicals were used as received. The common grade oil, either vegetable or olive, was purchased from the local grocery store.

Synthesis Parameters

Template Molecule

The choice of guest molecule depends on the use of the intended polymer.[54, 55] However, studies show that imprinting of small molecules is more successful than that of larger biological molecules, such as proteins, because their size and fragility make it almost impossible to apply either of the two classical approaches using covalent or noncovalent binding approaches.[56] With this in mind, careful consideration must be taken to ensure that the system chosen is compatible with a successful molecular templating strategy. For targeting phosphate, potassium phosphate monobasic was chosen.

According to well established polyprotic acid data based on phosphoric acid, the phosphate ion can exist in four different molecular forms (Figure 4-1), depending on the number of hydrogen atoms that are protonated. This can be affected by the pH of the surrounding solution, as predicted by the Henderson-Hasselbalch Equation:

$$\mathrm{pH} = \mathrm{pK}_a + \log_{10} \frac{[\mathrm{A}^-]}{[\mathrm{HA}]} \qquad (4\text{-}1)$$

which is the equivalent of:

$$\mathrm{pH} = \mathrm{pK}_a + \log_{10} \left(\frac{[\mathrm{base}]}{[\mathrm{acid}]} \right). \qquad (4\text{-}2)$$

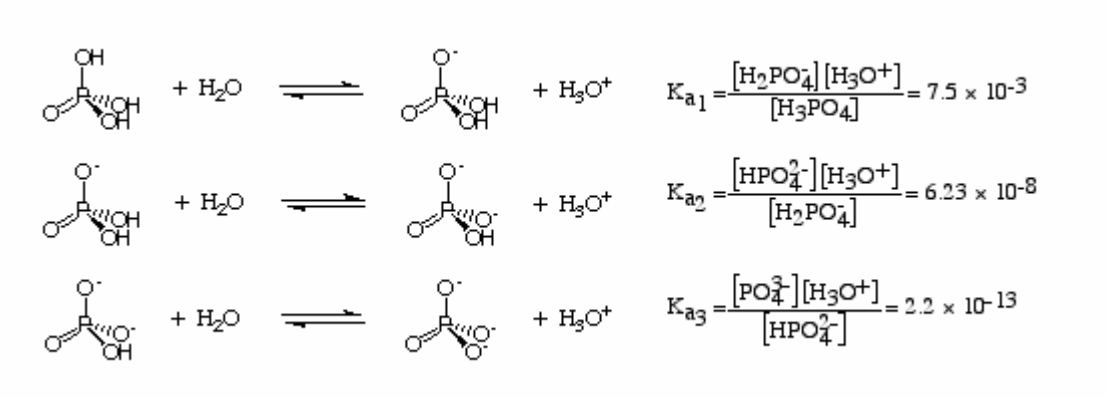

Figure 4-1. Common polyprotic molecular structures of the phosphate ion. There are three hydrogen atoms that dissociate at different pH values; thus, phosphoric acid has three pK_a values.

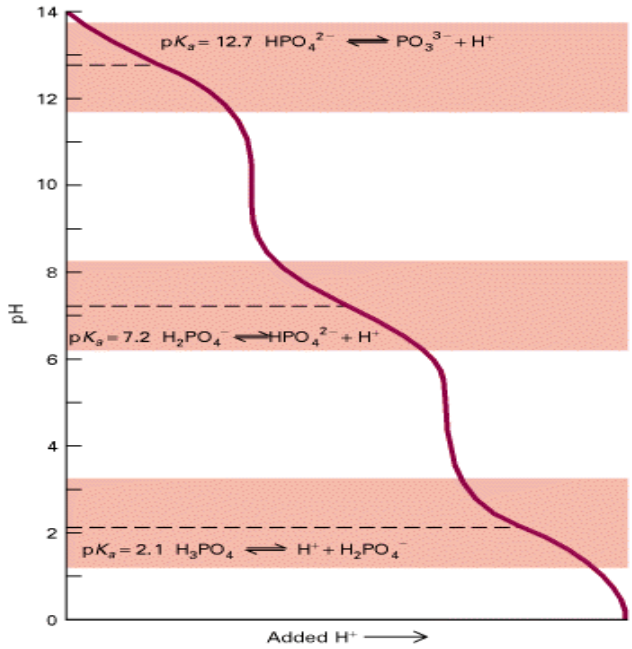

Figure 4-2. Titration curve for phosphoric acid. Phosphoric acid (H_3PO_4) has three hydrogen's and therefore three midpoints at pH 2.1 (pK_1), pH 7.2 (pK_2), and pH 12.4 (pK_3).[57]

To generate *in-vitro* assays that mimic the human *in-vivo* gastric environment, phosphate uptake trials were run at pH = 7.4, which meant that the expected phosphate ion available for binding was primarily in the form of $H_2PO_4^-$ (80%) with some HPO_4^{2-} (20%). These values were obtained from extrapolations using Figure 4-3.[58]

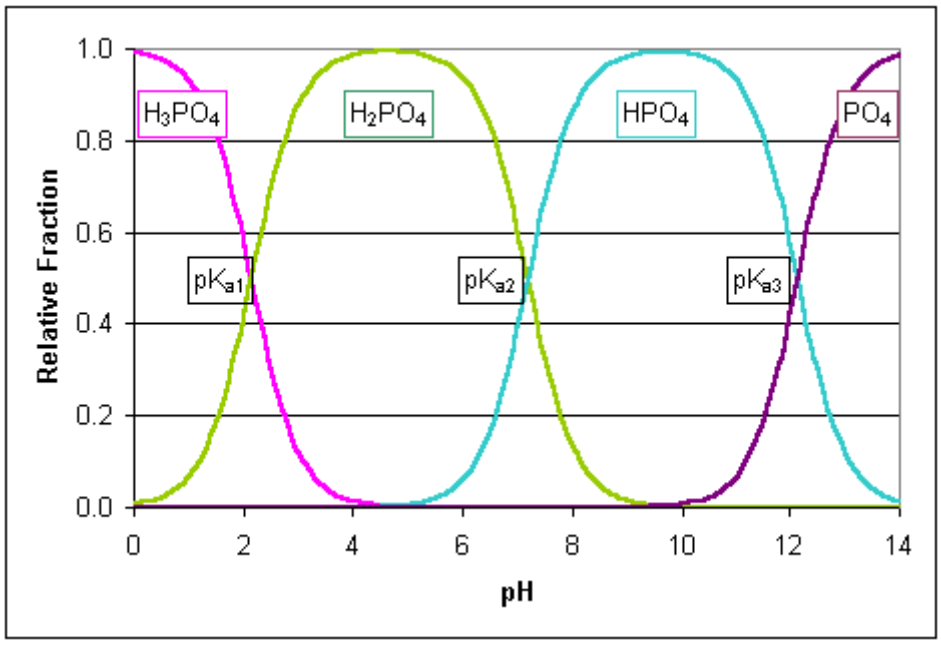

Figure 4- 3. Relative fractions of the various forms of phosphate at different pH levels.

Functional Monomer

The monomer system was chosen based on its ability to remain intact with the other components (template, crosslinker, etc.) upon polymerization, and remain biologically inert. The system varies with the intended use of the nonabsorbable polymer, as well as the type of imprinting or surface functionalization technique used.

One of the major concerns with developing this type of polymer for *in-vivo* use was biocompatibility, which has been a major problem with traditional synthetic routes that use potentially toxic crosslinking agents. The original plan was to develop the system which would be refined so that it was biocompatible, which led to the thought of simply starting with a known material that would suit this purpose. Common monomers extensively used as recognition networks include methacrylic acid, itaconic acid, acrylamides, 4-vinyl pyridine, and acrylamide.[59] After some consideration, gelatin was identified as a logical, well studied substance with over 100 years of biocompatible use in humans, which was used as the main functional monomer backbone that would provide enhanced rebinding selectivity.

The industrial preparation of gelatin is through thermal denaturation of collagen from animal skin, bones, and the less common fish scales.[60] Its structure is mostly comprised of glycine (arranged every third residue) and proline. Gelatin contains extended left-handed proline helix conformations incorporated with 300 to 4000 amino acids. Gelatinous solutions undergo coil-helix transitions and then aggregate, causing the formation of higher level pyrrolidines, which results in the formation of stronger gels.

The approximate amino acid (Figure 4-4) composition of gelatin is: glycine 21%, proline 12%, hydroxyproline 12%, glutamic acid 10%, alanine 9%, arginine 8%, aspartic acid 6%, lysine 4%, serine 4%, leucine 3%, valine 2%, phenylalanine 2%, threonine 2%, isoleucine 1%, hydroxylysine 1%, methionine and histidine <1% and tyrosine <0.5%. These values vary, depending on the source of the raw material and processing technique.[61.]

There are two main types of gelatin; Type A, which is derived from porcine skin, and Type B, which is a bovine derivative. Type A usually undergoes an acid pretreatment, while Type B is exposed to an alkaline pretreatment in which asparagines and glutamine residues are converted to their respective acids and results in higher viscosity. Gelatin is amorphous and amphoteric, thus has a broad range of materials applications.

Gelatin based materials have recently found biomaterial applications for use in bioadhesives, wound dressing material, and bone substitute. Gelatin is a natural polymer which has a low antigenicity and is biodegradable. However, gelatin is limited by the fact that it rapidly swells and dissolves in aqueous environments, which ultimately leads to rapid *in-vivo* degradation.[62]

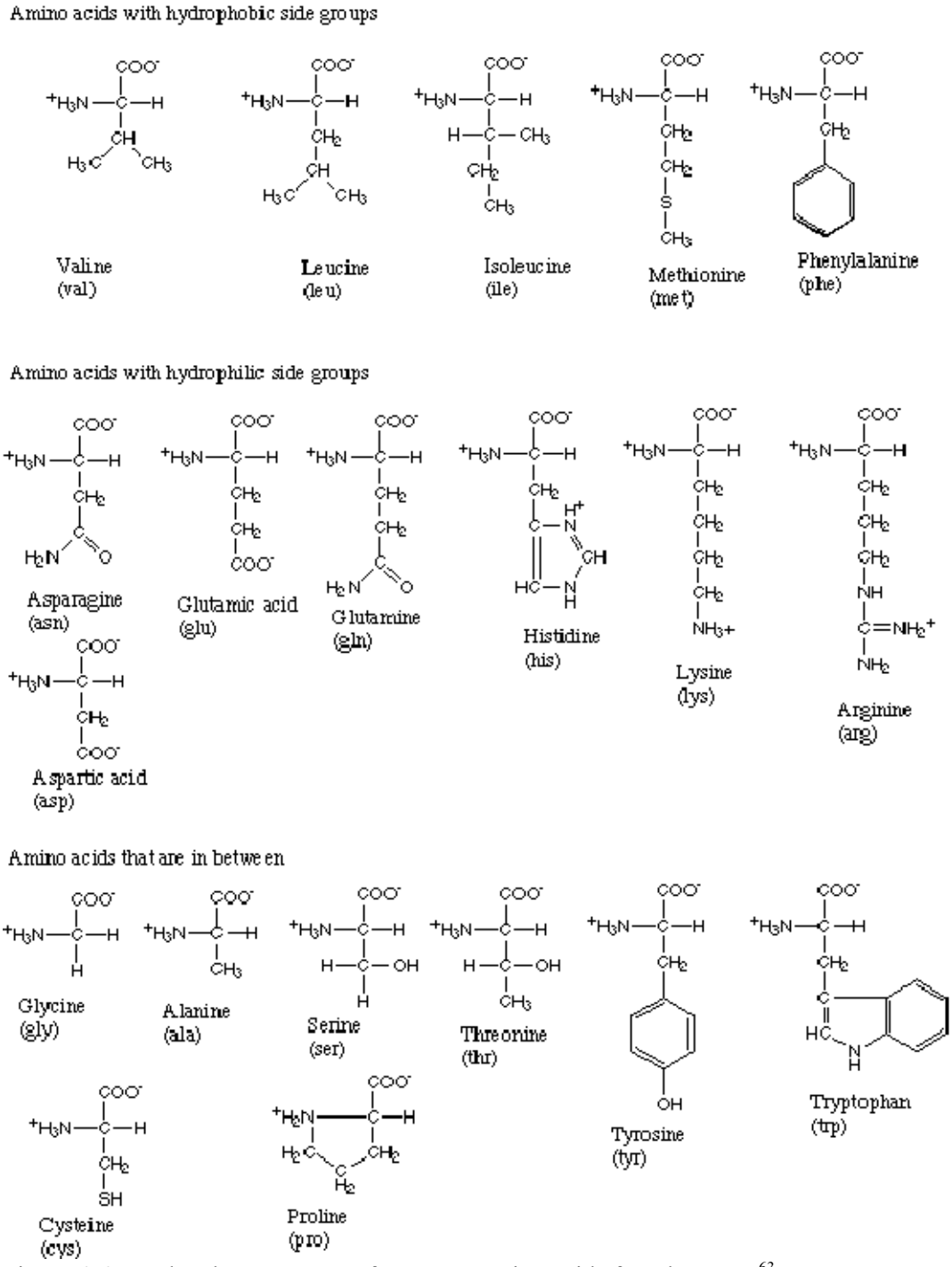

Figure 4-4. Molecular structures of common amino acids found *in-vivo*.[63]

One way to address this issue is to treat the gelatin with crosslinking materials. Chemical crosslinking can be achieved by creating bonds between functional groups of amino acids, such

as transglutaminase to link lysine to glutamine residues, and glutaraldehyde to link lysine to lysine.[64]

The experimental design used for this work is based on the notion that phosphate groups will bind to the arginine groups on the gelatin chain. Upon the addition of the crosslinking agent, there should be "spontaneous" reactions with the amino acids, which will hold the template in place.

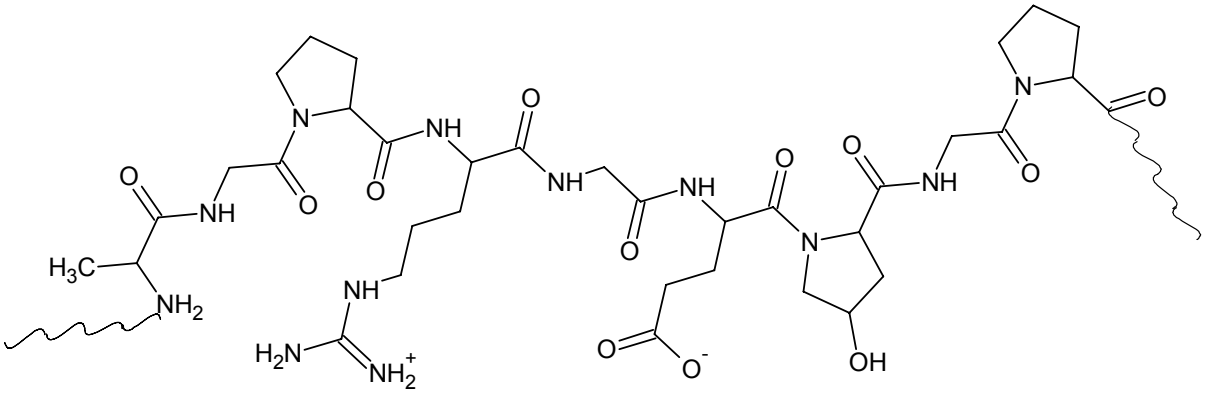

Figure 4-5. Structure of Gelatin

Crosslinking density is obviously affected by the amount of crosslinking agent available, but it is believed that every possible crosslink site will not react.

Initiator

In developing templated microspheres for various applications, the viscosity of the product must be a tunable property. Though a solid, rigid polymer may be desired, extraction and subsequent use may be more difficult than that of a more porous and flexible hydrogel-like product. Temperature, duration of polymerization, stirring speed, and altering the type and amount of initiator all affect polymer rigidity. The amount of initiator has an influence on the number of attachment sites and hence the amount of target molecule that is capable of binding to the polymer.[65] This will also effect the rate in which polymerization is initiated and terminated, which assists in determining the final composition of the templated polymer.

For these reasons, thermal initiation was chosen to induce polymerization. In this instance, the temperature at which polymers begin to crosslink depends on the physical properties of the crosslinking agent, and not the half-life, $T_{½}$, of the potential initiator used.[66] It is also important to note that the binding of monomers to templates can cause a reduction in chain termination, thus an overall increase in reaction rate. Ultimately, the amount of crosslinked, imprinted polymer that produced is strongly affected by the polymerization temperature.

Crosslinking Agent

Gelatin microsphere swelling was dictated by the extent of crosslinking between the polymer chains. The greater the degree of crosslinking, the shorter the bond distance of the chains, which causes a more dense spherical structure.[67] Thus the type and amount of crosslinker used has a significant affect on the overall microstructure.

The major requirement for specific ion imprinting is that the host polymers possess rigid guest-binding sites that are stable under a host of chemical environments. The crosslinking agent is primarily responsible for this feature in that it influences the solubility of the polymer in solvents,[68] which allows the them to be used in many different technical applications.

In molecular imprinting, selectivity is also mainly influenced by the type and amount of crosslinking agent used. Below a certain amount of crosslinking in the polymer (≈10%), selectivity usually is not observed due to the unstable nature of the cavities. Typically, selectivity steadily increases when crosslinking is greater than 10%, and between 50-60%, an unexpectedly high increase in selectivity occurs.[69] Varying the type and amount of crosslinker used directly controls the structure and environment around the guest-binding site. The crosslinking agent used should be similar in structure to the type of the host monomer in order to provide adequate random copolymerization, and evenly distribute functional sites throughout the polymer network.

The molar stoichiometry of the crosslinking reagent to the functional monomer is also an important controlling property of the final templated structure.[70] When the crosslinker is in great excess, the imprint sites become too close together and actually hinder receptor recognition. In the other extreme, not enough imprint sites are formed, and specific template recognition is not possible. The amount of cross-linker used is usually between 25 - 80% by weight, depending on the combined weight of crosslinking and monomer. Glutaraldehyde, genipin, glyceraldehyde and dextran were thoroughly investigated as crosslinkers because they have been reported in literature as being effective crosslinking agents for proteins, especially gelatin. The crosslinker used during synthesis should provide mechanical and thermal stability, good wettabity in most rebinding media, rapid mass transfer with good recognition properties, and be biologically compatible.

Genipin crosslinked microspheres

Genipin is a naturally occurring crosslinking agent used commonly for proteins, collagen, gelatin, and chitosan. It is derived from geniposide, present in fruit of Gardenia jasmindides Ellis. It has a low acute toxicity, and is significantly less toxic than many other commonly used synthetic cross-linking regents.[71]

The structure of genipin (Figure 4-6) was discovered in the 1960's by Djerassi. It has a molecular formula of $C_{11}H_{14}O_5$, a molecular weight of 226.227 g/mol, and contains a dihydropyran ring.[72] Genipin itself is colorless but it reacts spontaneously with amino acids to form blue pigments. It is soluble in ethanol, methanol, acetone, and slightly soluble in water.[71] The components of the Gardenia fruit have been used in traditional Chinese medicine and as a blue colorant by food industries in East Asia. It is also used for pharmaceutical purposes because it is a naturally occurring, biodegradable molecule with low cytotoxicity. Recent explorations into the use of genipin crosslinked gelatin (Figure 4-7) for the use as a bioadhesive,

wound dressing, and as bone substitutes, have shown it to have potential as a new and safe crosslinking agent.

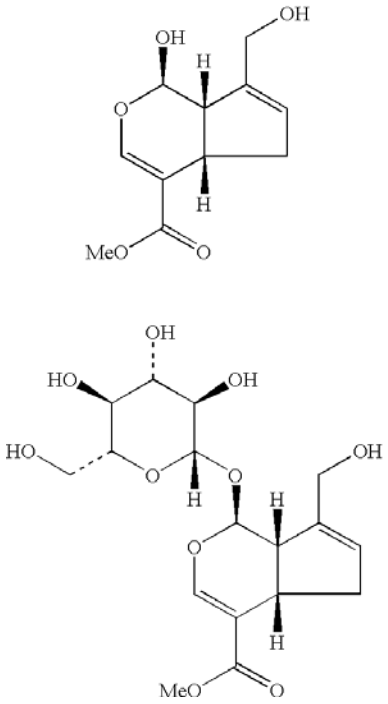

Figure 4-6. The molecular structure of Genipin (top) and Geniposide (bottom).

Glutaraldehyde crosslinked microspheres

Glutaraldehyde has a wide variety of industrial uses as a disinfectant, preservative, fixative, crosslinking agent, and as a chemical intermediate in the synthesis of pharmaceuticals and pesticides. It is also used for industrial water treatment and as a chemical preservative. However, it can be toxic upon degradation, causing severe eye, nose, throat and lung irritation, as well as headaches, drowsiness and dizziness.[73]

Glutaraldehyde is an oily liquid at room temperature (density 1.06 g/mL). It has a molecular formula of $C_5H_8O_2$, and a molecular weight of 100.11 g/mol.[74] It is a colorless liquid with an overpowering smell.

Glutaraldehyde is frequently used in biochemistry applications as an amine-reactive

homobifunctional crosslinker, and has been the gold standard used for crosslinking gelatin (Figure 4-9) for decades. Crosslinking happens through the reaction of the aldehyde group of glutaraldehyde and the free amino groups of lysine or hydroxylysine amino acid residues[75] on the gelatin chain. The oligomeric state of proteins can be examined through this application. It is miscible in water, alcohol, and benzene.

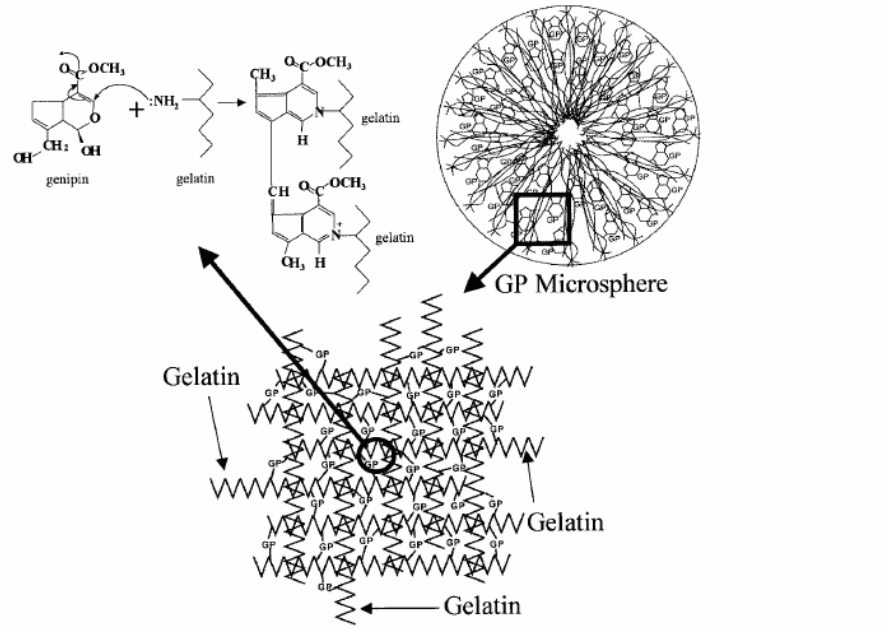

Figure 4-7. Crosslinked structures of genipin crosslinked gelatin microspheres[76]

Figure 4-8. The molecular structure of glutaraldehyde.

Dextran

Dextran is a branched polysaccharide composed of glucose, with the main chains being formed by 1α→6 glycosidic linkages and the side branches are attached by 1α→3 or 1α→4 linkages (Figure 4-10). Dextran is a bacterial product whose structure is dependent on its inherent source. It is also used commercially as food additives, an anti-platelet, and increases the volume of blood in plasma.[77]

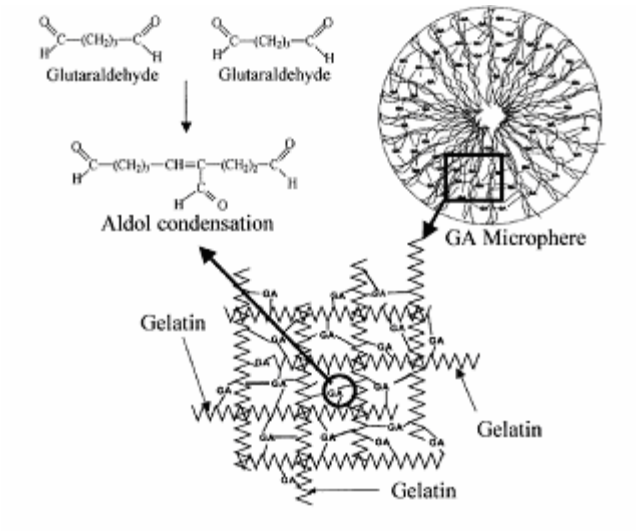

Figure 4-9. Crosslinked structures of glutaraldehyde crosslinked gelatin microspheres[76]

Dextran has a molecular formula of $n(C_6H_{10}O_5)$, is water-soluble, and been found to have an average molecular weight of 75,000 in its purified form. Lower weight dextrans display slightly less branching[78, 79] and have a more narrow molecular weight distribution. Dextrans with molecular weights greater than 10,000 have highly branched characteristics and as the weight increases, the dextran molecules attain greater symmetry.[80] At molecular weights below 2,000 dextran has a rod-like behavior,[81] while those with 2,000≤ molecular weight ≥ 10,000 exhibit the properties of an expandable coil.

The primary crosslinking of gelatin by dextran occurs through a Schiff base formation between the ε-amino lysine groups and the hydroxylysine residues of gelatin and the free aldehyde.[82]

D,L-glyceraldehyde

Another nontoxic alternative to chemically crosslinking gelatin along the macromolecular chains is through the use of D,L-glyceraldehyde (Figure 4-12). Recent studies show the successful crosslinking of chitosan microspheres using d,l-glyceraldehyde,[83] and its proposed

broad application as a biocompatible crosslinking agent for protein microspheres.[84] Glyceraldehyde is also a metabolic product of fructose in the human organism, which indicates complete biocompatibility. It has a crystalline appearance, chemical formula of $C_3H_6O_3$, and a molecular weight of 90.08 g/mol. As an aldehyde, crosslinking mainly occurs through lysine residues.

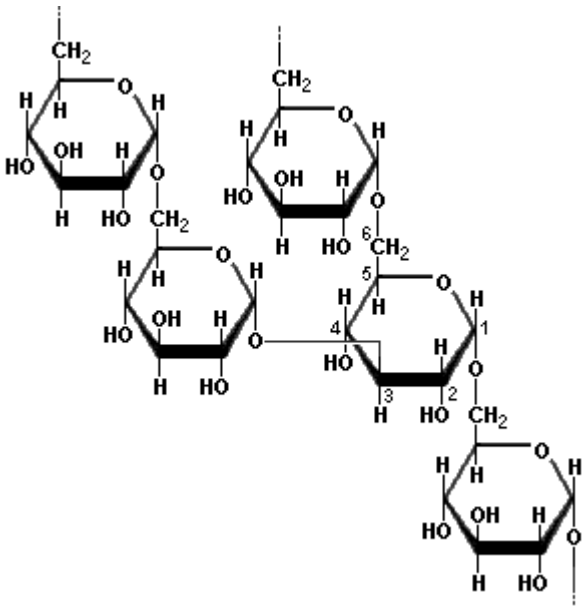

Figure 4-10. Molecular structure of dextran.

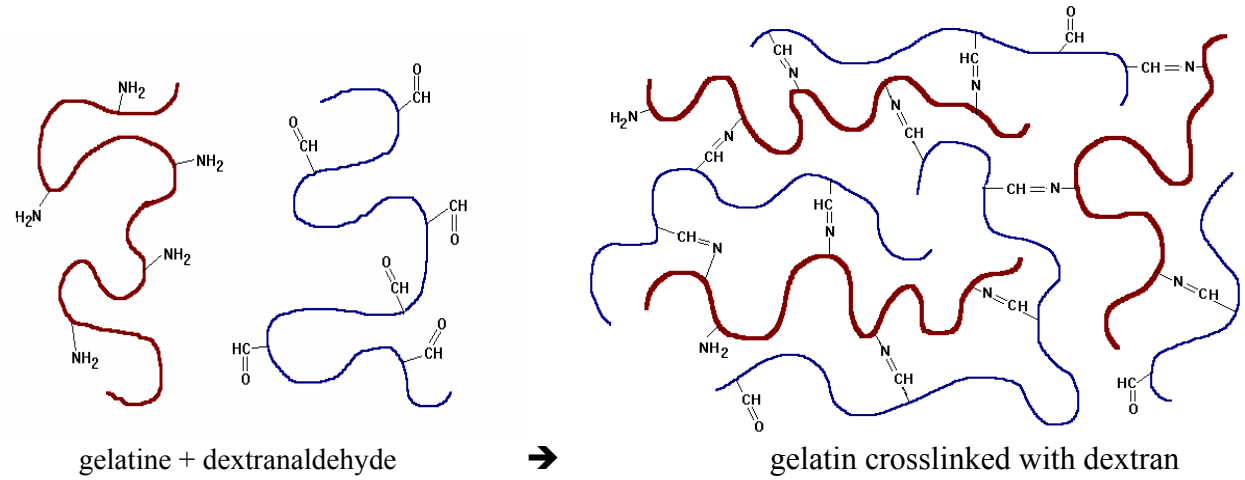

Figure 4-11. Preparation of gelatine hydrogels crosslinked with partially oxidized dextrans.[85]

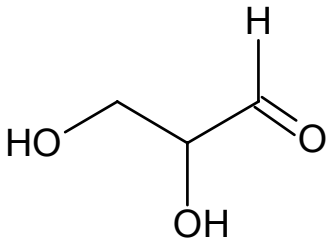

Figure 4-12. Molecular structure of D,L-glyceraldehyde.

It has been demonstrated that, on average, natural polymers crosslinked with glyceraldehydes do not swell as much as those using glutaraldehyde.[83] The extent of crosslinking can vary, depending on the amount of crosslinking agent used and the crosslinking time period.

Porogen

The use of solvents in polymerization is central to the success of the imprinting process, and vary depending on the imprinting technique employed. Though an important application of solvents is that they dissolve components for polymerization, greater significance is placed on the role that they play in creating porous structures.[86, 87]

During polymerization, solvent molecules are incorporated into the polymer structure, and removed during the post-treatment process, leaving behind a porous space. Without this, the polymer would be too rigid and dense, making template binding impossible due to too few accessible cavity sites. The solvent used during polymerization affects the selectivity of template recognition in that it may either enhance or destabilize the specific interactions that lie at the center of the imprinting effect.

Another role of porogens is that they disperse the heat of reaction associated with polymerization.[88] Without this, the temperature of reaction for the polymerization would increase, which may create detrimental side effects that could impede or terminate the reaction. The porogen should be the least polar solvent capable of dissolving the components of the

mixture as to maximize the non-covalent interactions between the template and functional monomer. Acetone and water will be used as porogens for microsphere synthesis.

Determine the Efficacy of Phosphate Uptake with the Polymers *in-vitro*

Once the polymer system was defined in Specific Aim 1, examination of the effect that the polymers had on the binding specificity of phosphate, and their possible influence on hyperphosphatemia, was determined. This was accomplished by determining the amount of phosphate the surface modified microsphere could bind, and ascertaining if this was sufficient enough to reduce the excess amount of phosphate in patients with chronic renal failure.

Assessment of the Reaction Parameters

The gelatin monomer system from specific aim 1 was modified until a functionalized polymer sphere was fabricated in which extraction and reuptake of the template was optimized. This included adjusting each of the parameters described for synthesis. Success was established by identifying polymers that could bind solution phosphate at a minimal level of 1.00 mEq/ g polymer.

Recovery

The success of polymer imprinting was determined through *in-vitro* analysis in an aqueous phosphate milieu. Once synthesized, the polymer was washed with an acidic or basic solution in order to extract most of the phosphate present during synthesis. The concentration of the phosphate ion in each successive wash was probed using ICP, UV/VIS, or a handheld phosphate meter. Once extracted, the polymer was washed with deionized water to remove any excess solvents from the system, and dried in-vacuo overnight to eliminate excess moisture.

In-Vitro Analysis of Phosphate Uptake in the Functionalized Polymer

For *in-vitro* studies, 800 mg of the polymer were placed in 400 mL of a pH = 7 solution of 20 mM phosphate, 80 mM sodium chloride, and 30 mM sodium carbonate, which mimicked the

conditions of the small intestine,[89] for a period of 3, 24, and 48 hours. An aliquot of the test solution was collected and the concentration analyzed using either ICP or a Hanna high range hand held phosphate meter. The amount of phosphate bound to the polymer was calculated by subtracting the phosphate found in the filtrate solution from the original phosphate present.

$$[PO_4^{3-}{}_{Bound}] = [PO_4^{3-}{}_{Initial}] - [PO_4^{3-}{}_{Final}]$$

Instrumentation

The instrumentation used for analysis were: ICP and IR at the Particle Engineering Research Center (PERC), SEM at the Major Analytical Instrumentation Center (MAIC), UV in the Goldberg laboratory, and the phosphate meter in the Batich lab. All facilities were located on the campus of the University of Florida.

ICP

Inductively coupled plasma was used to determine the concentration of phosphate in the collected aqueous washes of the test samples. A calibration curve was constructed using a phosphorous standard, and the phosphate test samples were analyzed against this.

UV/VIS

Ultraviolet visible spectroscopy was also used with an EnzChek phosphate assay kit E-6646 (Molecular Probes) to quantify the inorganic phosphate in solution. The absorbance peak of the substrate appeared around 330 nm against a calibration curve prepared at a 360 nm absorbance.

Phosphate meter

A HI 93717 phosphate high range phosphate meter (Hanna Instruments), was used for the fast and direct analysis of phosphate concentrations in mediums inclusive of, but not limited to water. The reagent sets for analysis were included with the instrument.

Characterization of bulk polymer

Scanning Electron Microscopy (SEM)

Due to the expected small size of the imprint sites, the polymer was imaged using scanning electron microscopy (SEM) with EDS capability, in order to examine the morphology and possible molecular content of the sample. The particles were mounted on aluminum stubs, attached to the surface using double-stick tape, and coated with gold prior to imaging.

Infrared (IR)

Fourier transform infrared spectroscopy (FTIR) analysis, using a Perkin Elmer Spectrum 100 Series FTIR spectrometer, was used to investigate the sample composition by determining the presence and type of bonds in the molecule using attenuated total reflectance (ATR). ATR-IR is used to probe the surface of materials. Samples were measured at room temperature in the range of 4000 – 6000 cm^{-1} at a resolution of 4 cm^{-1}.

CHAPTER 5
GELATIN MICROSPHERES VIA EMULSIFICATION

Water in Oil Emulsions

A water-in-oil emulsion system, commonly referred to as an inverse emulsion, was chosen due to its known ability to produce fast and relatively simple polymer particles of high molecular weights, and to allow a rapid transfer water laden spheres to the aqueous phase.[90]

In water-in-oil emulsions, an aqueous solution of a water soluble monomer is emulsified in a hydrophobic medium (Figure 5-1). Emulsification is dependent on the reaction temperature, concentration of the ingredients, and can be initiated through the introduction of either a water or oil soluble chemical. The attraction of the synthetic scheme used in these experiments is that the reaction is thermodynamically driven, thus a chemical initiator is not required. Instead, a water soluble crosslinking agent was used to control the extent of crosslinking, producing a dispersion of spheres. In addition, an emulsifier free emulsion was carried out, which does not require the use of a surfactant.

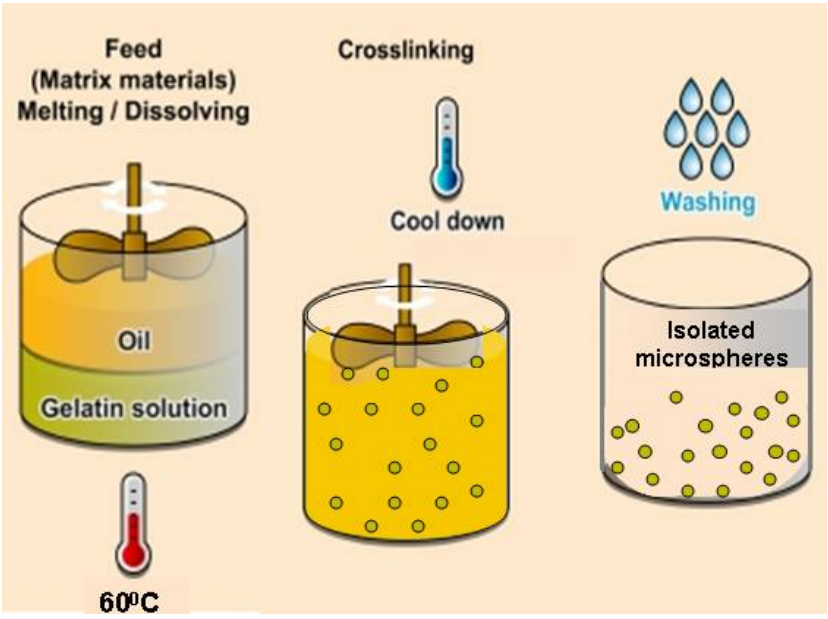

Figure 5-1. An inverse emulsion system.

Reverse phase emulsions mainly transpire within the monomer swollen particles, contain a discontinuous aqueous phase which usually has two or more droplet size distributions,[91] provide high polymer solids with reduced oil content, low bulk viscosity, and high physicochemical stability. However, these particles are on average less stable than those prepared by the more common oil-in-water emulsion technique due to the electrostatic forces involved.

In this formulation, the aqueous solution contains the phosphate and/or gelatin, and oil is the nonpolar phase, which is a simple hydrocarbon medium. Smaller size drops can be affected by many different variables, such as the rate of stirring, duration of reaction, decreasing the interfacial tension, or by the concentration of the components in the water phase. Some of these variables have a greater influence on the emulsion polymerization process more than others, however they can all be modified to achieve the best product characteristics.

To better understand the physicochemical formulation concerns of a water-in-oil emulsion system, a set of parameters are examined which are indicative of the nature of the components. Although emulsions are not in equilibrium, the length of the reaction often leads to a physicochemical type equilibrium in which the formulation determines the properties and phase behavior[92] of the mixture.

In the past 50 years, researchers have made intensive efforts to characterize the physical and chemical behavior of emulsion polymerizations, resulting in the identification of the HLD (Hydrophilic Lipophilic Deviation), which is a measure of the relative affinity of the surfactant for the aqueous and oil phase. At HLD = 0 the surfactant affinities are exactly matched, and a minimum interfacial tension is attained, as sought in enhanced oil recovery processes.[93] Since surfactants are not used in this specific application, it was assumed that the system was functioning at the HLD = 0 level, thus the apparent performance was based on the features

provided in Figure 5-2,[91] which summarizes a survey of data available in literature.[94, 95]

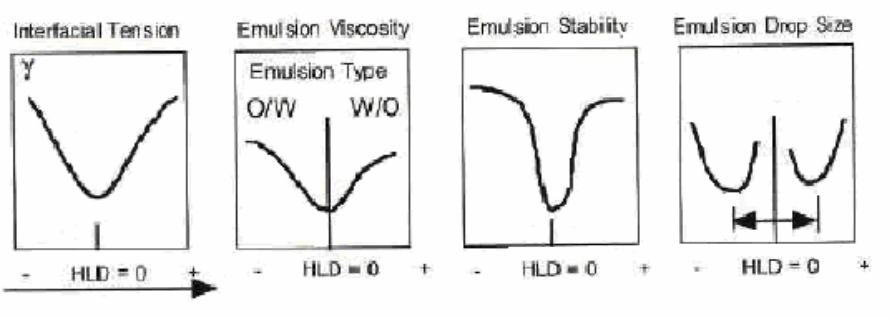

Figure 5-2. Interfacial tension and emulsion variations versus formulation (as HLD) at near unit water-to-oil-ratio.

Thus the interfacial tension of the particle, the emulsion viscosity, and the emulsion drop size should all be at their minimum values, which provide a state for maximum efficiency for the reaction. It is important to recognize that as the emulsion stability concomitantly decreases, the drops coalesce instantly upon contact, which favors a larger particle size. Ultimately, this mixed phase phenomena results in a bimodal distribution of drops. This effect can be addressed by increasing the stirring energy, which widens the area where the decreasing tension produces smaller drops, thus favoring the production of a decrease in microsphere size.

Crosslinked Gelatin Microspheres

Synthesis of Gelatin Microspheres

A modified synthetic scheme[96] was developed for gelatin microsphere fabrication. Dissolve 2.5g of 225 Bloom bovine gelatin in 10 mL of deionized water at 100 ^{o}C, whose pH has been adjusted to 7.4 using dilute NaOH or HCl solutions, and place in an ultrasonic water bath at 60 ^{o}C. The gelatin completely dissolved, resulting in a viscous solution. 10 mM of potassium phosphate monobasic is added to the sample for imprinting, while the sample that did not contain phosphate served as the control. The solution was added dropwise to 20 mL of vegetable oil at 60 ^{o}C, and the mixture was placed in an oil bath at 60 ^{o}C. Stir for approximately 1 hour, upon

which a clearly defined gelatin emulsion was apparent. The emulsion was placed in a water bath at 4-13 ^{o}C, while stirring, for 30 minutes. Particles were dehydrated by adding 30 mL of cold (4 ^{o}C) acetone to the solution, and allowed to stir for 30-60 minutes. They were filtered, rinsed with precooled acetone, and vacuum dried overnight in order to remove any residual water or oil left on the particles.

Some particles were crosslinked using different amounts of crosslinking agent in order to determine if the appropriate amount to use for microsphere formation concurs with the established parameters detailed earlier in Chapter 4. Once the optimum amount of crosslinker to use was ascertained, it will be the standard for future experiments.

Crosslinking Gelatin Microspheres with Genipin

Genipin is a naturally occurring crosslinking reagent for gelatin with very low cytotoxic effects.[97] For this reason, there has been a recent significant shift towards using it as an alternative to other crosslinking agents that are known to be cytotoxic.

2.0 g of the gelatin microspheres were placed in 20 mL acetone/water (2:1, v/v) mixture at pH = 7.4., to which was added 300 mg of genipin to the mixture and stirred for 15 hours at 4-10 ^{o}C, or until crosslinking was evident by a pigment change of the protein to a dark blue color. The solution was then allowed to stir at room temperature for 10 hours. The resulting microspheres are filtered, rinsed with cold acetone, and dried under vacuum overnight. The resulting product will be a rigid, dark blue microsphere.

Genipin crosslinked gelatin microspheres were prepared using 2, 15, and 75% (w/w) genipin. The samples were prepared using pure gelatin (control), and gelatin with phosphate microspheres.

Crosslinking Gelatin Microspheres with Glutaraldehyde

The most commonly used crosslinking reagent for gelatin is the synthetic reagent

glutaraldehyde due to its efficiency in crosslinking collagen based materials, and its relatively cheap cost.[98] However, glutaraldehyde is often considered to be cytotoxic due to the release of formaldehyde upon degradation. Nevertheless, many articles cite the use of glutaraldehyde crosslinked gelatin microspheres as being relatively safe *in-vivo*, providing that their synthesis includes a rather vigorous washing procedure to remove unreacted reactant. Even so, there has been a widespread shift from its use to crosslinking agents that are known to have little to no cytotoxic side effect.

Gelatin spheres can be crosslinked with glutaraldehyde during the emulsion process. Uncrosslinked particles were prepared, as described above, and stirred for an hour in the pre-chilled acetone. 30 mL of 25% glutaraldehyde (w/v) in DI water was added, and allowed to stir overnight. The appearance of burnt orange colored spheres were present after several hours of mixing. The particles were then be filtered, washed with 100 mL portions of ethanol to terminate crosslinking reaction, and washed with DI water. The microspheres were then dehydrated by adding 30 mL of cold (4 ^{o}C) acetone to the solution, and allowed to stir for 30 minutes. The supernatant was filtered off, and the particles washed with precooled acetone. The spheres were dried overnight in vacuo.

Crosslinking Gelatin Microspheres with additional agents

In an effort to provide a thorough analysis of crosslinked gelatin polymers that have potential *in-vitro* and *in-vivo* applications, dextran and glyceraldehyde were used as crosslinking agents with low toxicity.

Dextran

Oxidized dextran can form a cross-linked gelatin network through sugar mediated cross-linking, which can reduce the dissolution of gelatin.[99] Uncrosslinked gelatin microspheres were prepared using an inversion emulsion scheme, and crosslinked using 15% w/w dextran dissolved

in 3 ml of DI water. Crosslinking was carried out 5 ^{o}C for 24 hours. The resultant white powdery-like microspheres were rinsed several times with precooled acetone, and allowed to dry in vacuo for 24 hours.

Glyceraldehyde

Uncrosslinked gelatin microspheres were prepared in the usual fashion, and crosslinked using 2% w/v glyceraldehyde since a highly crosslinked polymer was desired. Crosslinking was carried out in an acetone-water mixture (40:20, v/v) at 5 ^{o}C for 24 hours. The resultant bright pumpkin colored microspheres (darker burnt orange if phosphate is used) were rinsed several times with precooled acetone, and allowed to dry in vacuo for 24 hours.

Gelatin Microsphere Processing

Removal of the Template

After the spheres were crosslinked, extraction of the phosphate template molecule was performed with a simple washing procedure. Assays were performed on acid washed and base washed microspheres to determine the most effect template extraction procedure to provide the most suitable polymeric microenvironment for the phosphate binding mechanism. Since 100% crosslinking was not attained, there should be amines remaining from arginine groups on the gelatin chain on the surface and within the polymeric particle (Figure 5- 3), both of which should be available for phosphate uptake.

Base Wash Extractions

Approximately 200 mg of the gelatin polymer sample was measured, placed in 20 mL of a 1:1 solution of 0.1 M NaOH: MeOH, and allowed to stir for 45 minutes. The solution was decanted off, and the procedure was repeated two more times. The solution was decanted, 20 mL of DI water was added, adjusted to pH = 7 and allowed stir for 30 minutes. The particles were filtered,

rinsed with neutral DI water, and dried overnight in a vacuum oven at room temperature. Particles were then used for phosphate uptake trials.

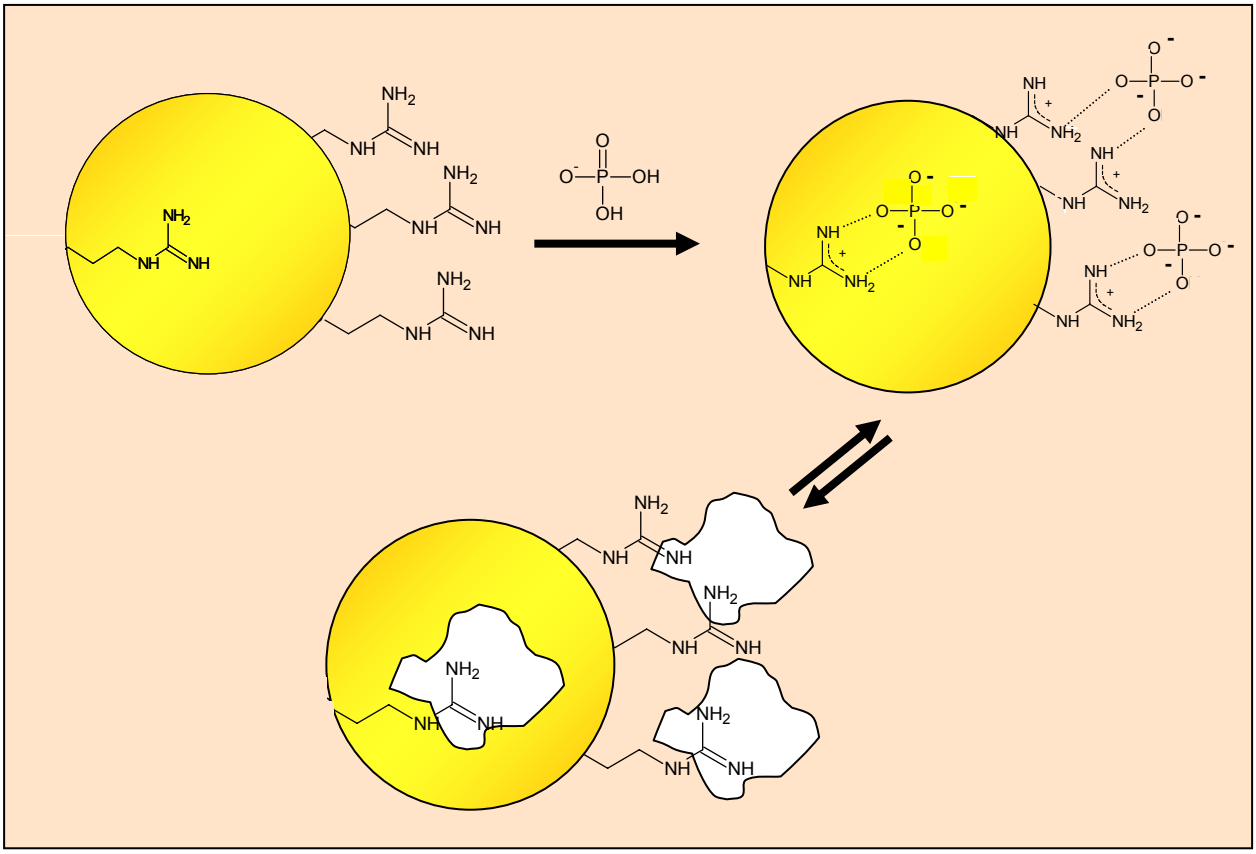

Figure 5- 3. Template removal from the active binding site.

Acid Wash Extractions

Measure approximately 200 mg of polymer sample. Place sample in 20 mL of a 1:1 solution of 1 M HCl: H_2O. Let stir for 30 minutes (agitate occasionally if a rotating apparatus is not available). Decant off solution and take reading on the phosphate meter. Repeat process two more times. Add 20 mL of DI water. Adjust to pH = 7. Let stir for 30 minutes. Filter particles, rinse with neutral DI water, and dry particles overnight in a vacuum oven. Particles are then used for phosphate uptake trials.

Results

Water-in-oil emulsions have proven to be a relatively simple and straightforward method used to prepare crosslinked gelatin microspheres.

Gelatin Inverse Emulsions

Initially, gelatin microspheres prepared via w/o emulsions were synthesized and evaluated for compositional information using SEM and ATR-IR. These non-crosslinked samples dissolved during the *in-vitro* testing at 37 ^{o}C, as expected.

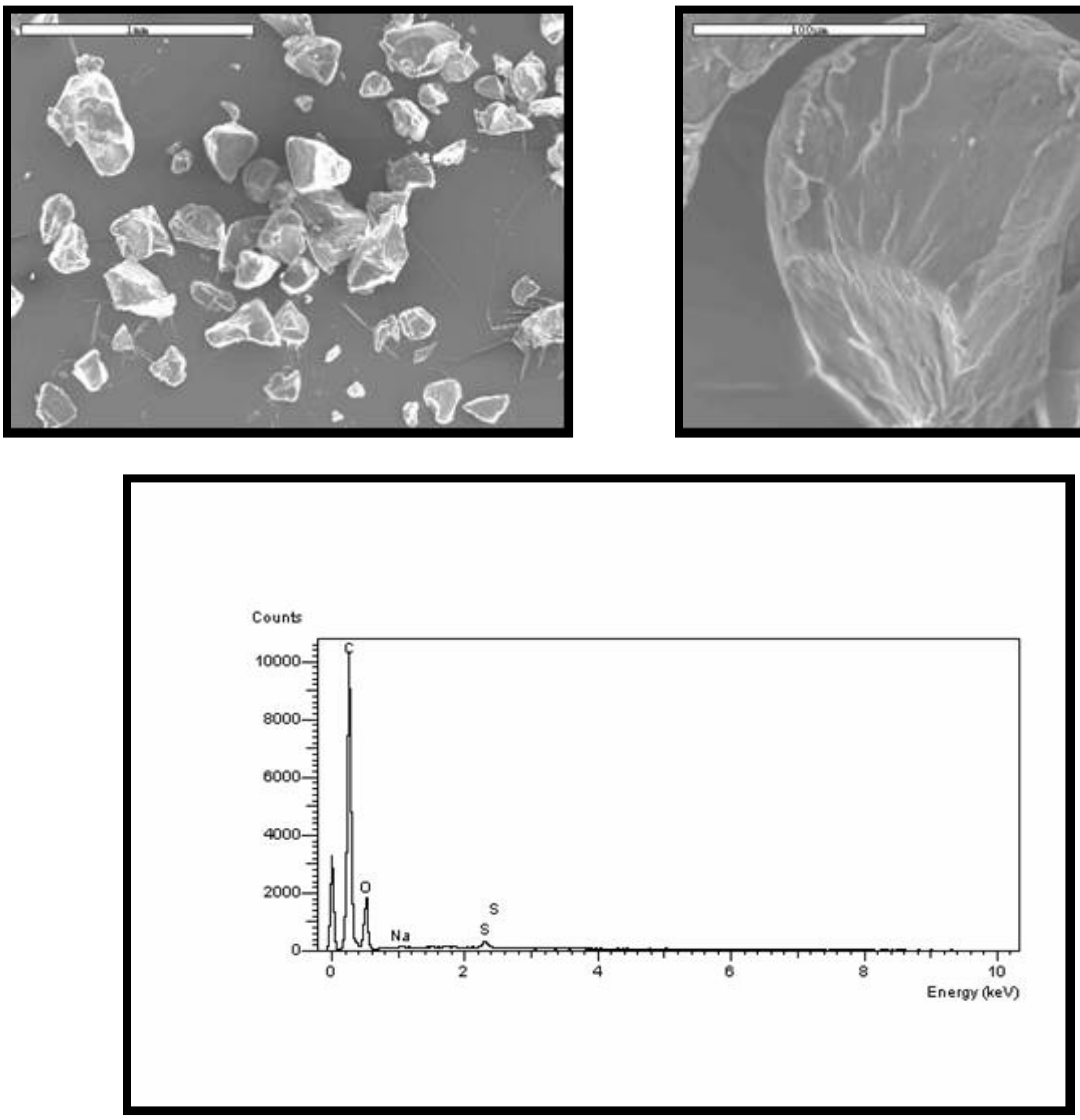

Figure 5-4. SEM and corresponding EDS analysis of raw Type B (bovine) gelatin.

SEM analysis provided a sound survey of the change in the size and morphology of the gelatin as it was exposed to different processing conditions. One noticeable feature was the decrease in particle size from the raw gelatin to the gelatin spheres. This could be attributed to the fact that the gelatin was dissolved in a hot water medium and placed in hot oil under turbid stirring conditions.

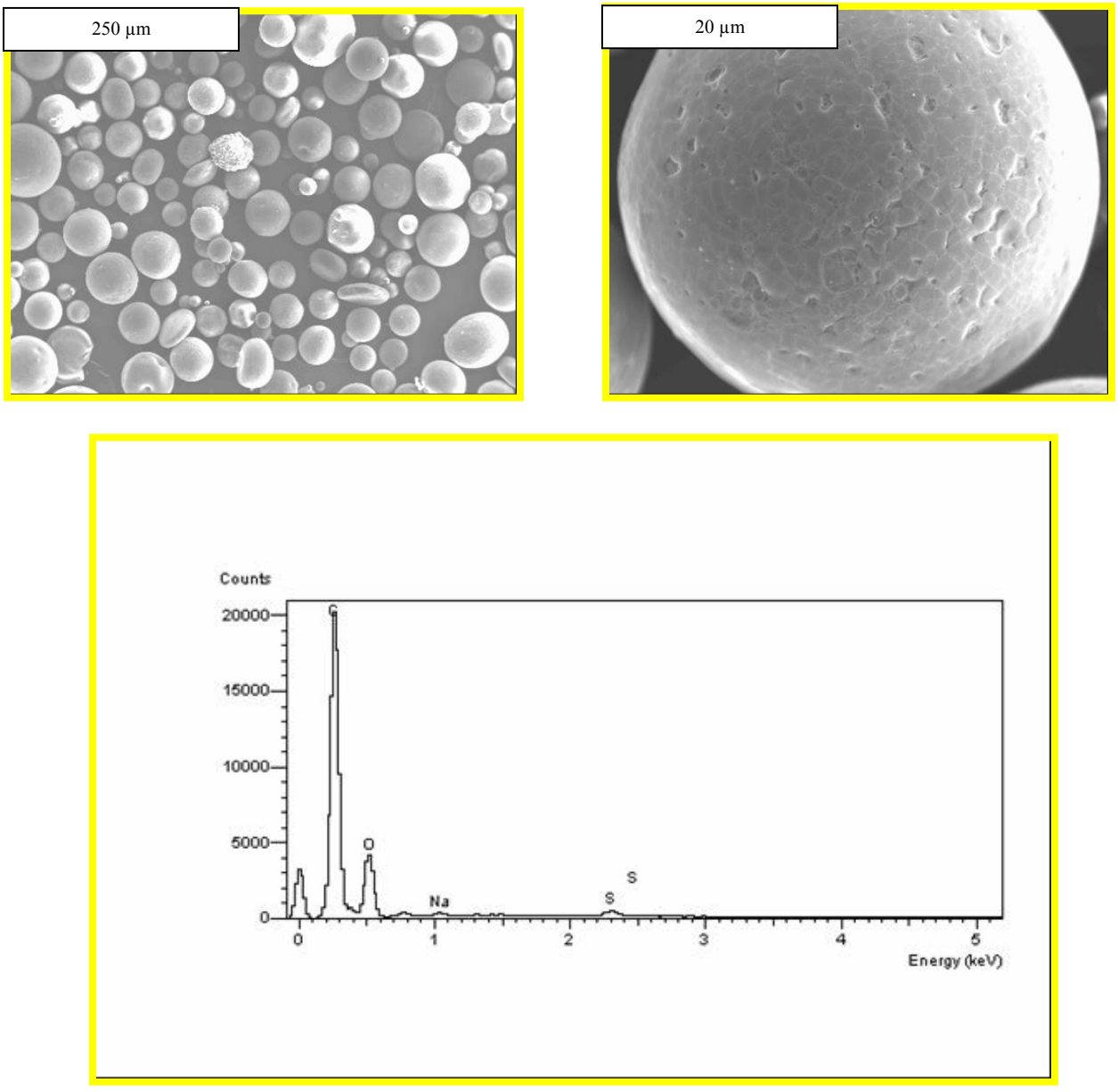

Figure 5-5. SEM and corresponding EDS analysis of gelatin microspheres prepared via water in oil emulsion.

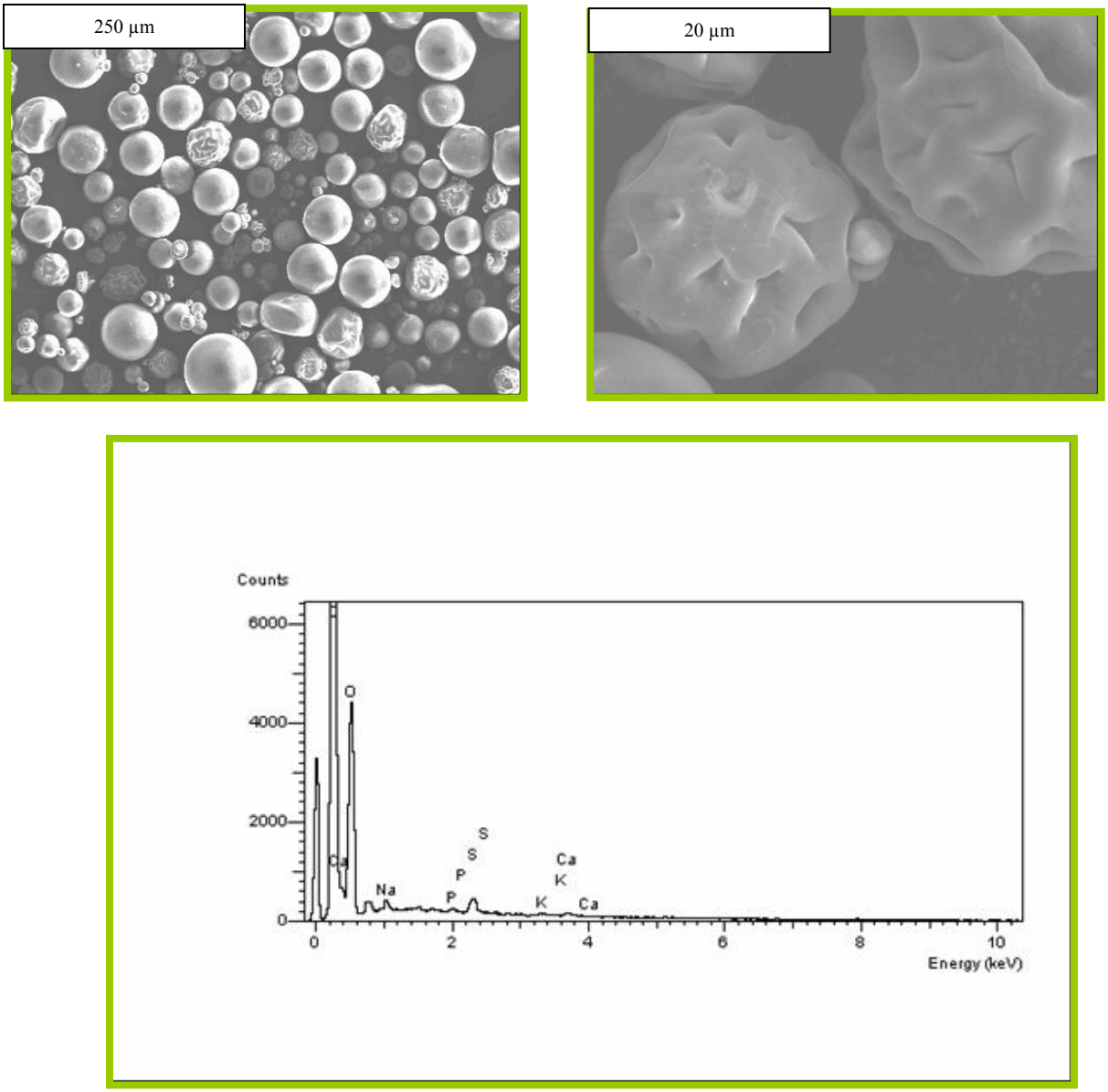

Figure 5-6. SEM and corresponding EDS analysis of gelatin microspheres containing phosphate, prepared via water-in-oil emulsion polymerization.

This procedure allowed the formation of a "new" gelatinous material whose size could be altered. Also, the microspheres that contained phosphate had several "puckered" looking spheres, which may have been the result of bound phosphate ions in the gelatin chain.

EDS, while indicating the presence of phosphate in the gelatin containing polymer

particles, did little more than confirm the presence of a large amount of carbon and oxygen. Therefore, EDS analysis was discontinued.

IR spectral analysis was used to monitor the change in the gelatin structure as it is processed. In general, the amide bonds in protein α-helices absorb around 1660–1650 cm^{-1}, β-sheets at 1640–1620 cm^{-1} and near 1675 cm^{-1}, β-turns in the range 1695–1660 cm^{-1}, and unordered structures and α-helices at 1650–1640 cm^{-1}.[100] Therefore, the amide I band region (≈ 1650 cm^{-1}) was closely monitored for possible changes in the gelatin secondary structure as different processing methods and crosslinking agents were used. The amide II band (≈1550 cm^{-1}) positions were analyzed to get information about the environment and hydrogen-bonding characteristics of the peptide CNH bonds. The amide III band (≈1240 cm^{-1}) intensity was monitored as an indication of intermolecular associations between the gelatin and the crosslinking agent.

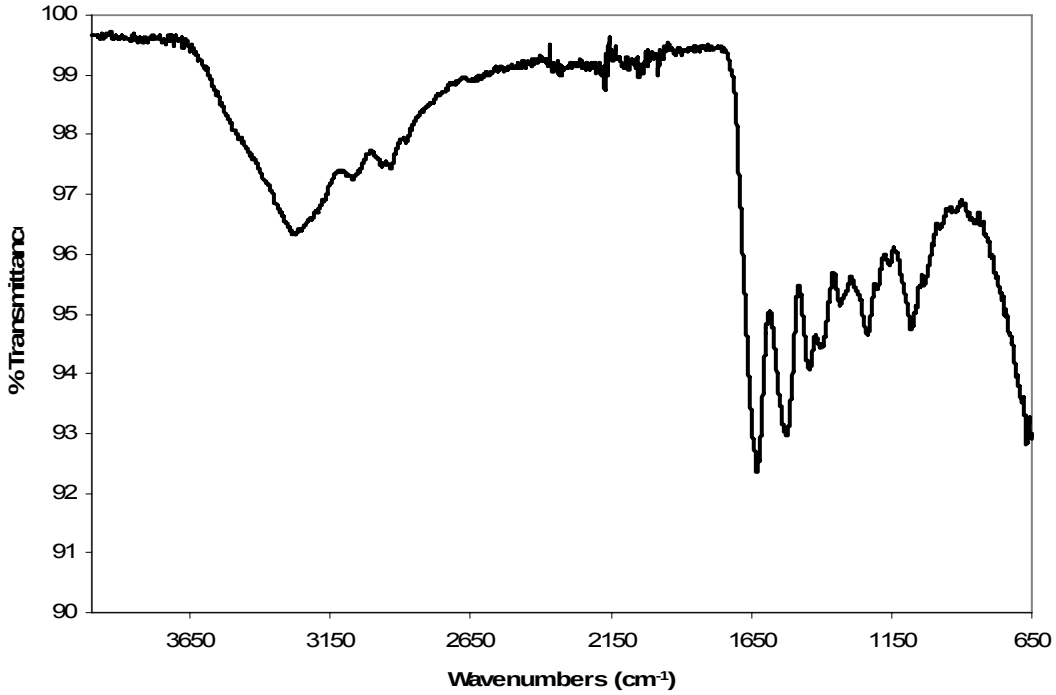

Figure 5-8. FTIR spectrum of unprocessed Type B (bovine) gelatin.

The raw Type B (bovine) gelatin showed characteristic peaks at 3514 cm^{-1}, 3313 cm^{-1}, and 3071cm^{-1} due to -NH stretching of secondary amide. The amide I band region contains amide carbonyl C=O stretching at 1680 cm^{-1} and 1630 cm^{-1}, with some contribution of C-N stretching and C-C-N deformation. The amide II region has -NH bending at 1526 cm^{-1} and C-N stretching at 1542 cm^{-1}. There is also -NH out-of-plane wagging at 670 cm^{-1}, C-H stretching at 2924 cm^{-1} and 2853 cm^{-1}, C-C stretching and C=N ring stretching at 1452 cm^{-1} (Figure 5-8).

It can be observed from the spectrum of the processed gelatin spheres in Figure 5-9, that the peaks remain similar to those of the unprocessed particles, indicating no apparent change in structure.

The gelatin microspheres containing phosphate in Figure 5- 10 illustrate the first noticeable difference in the increase of the peak intensity, and the peak at 1030 cm^{-1} confirms the presence of the phosphate ion.

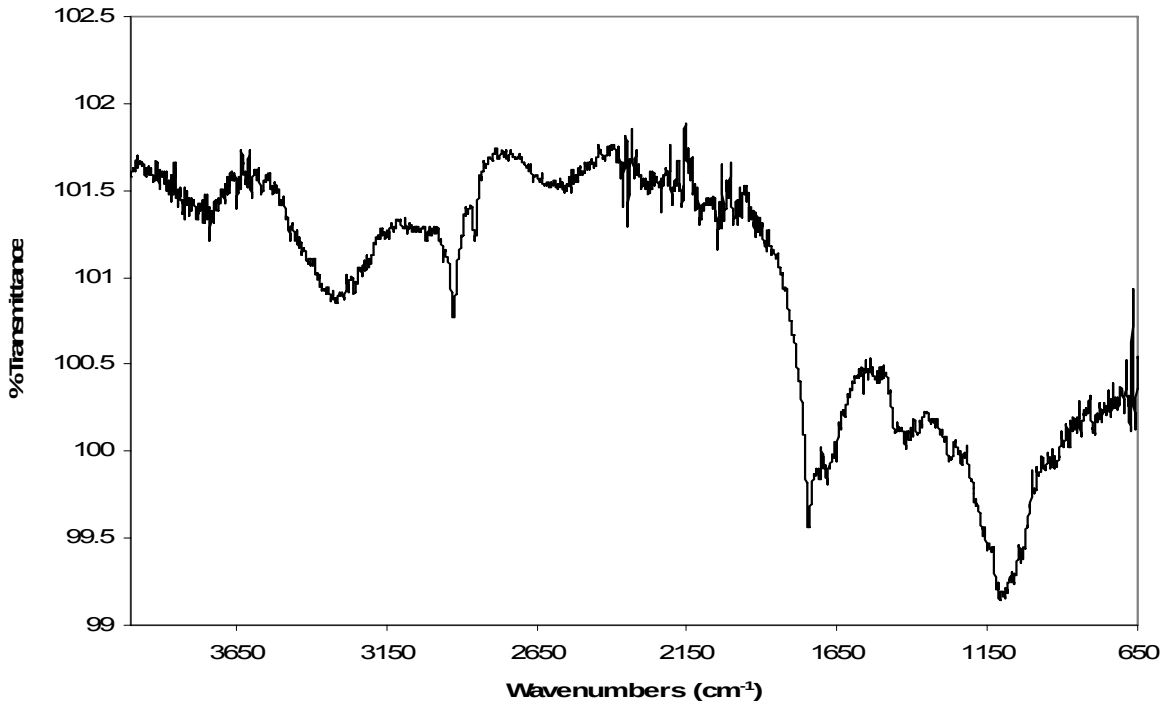

Figure 5-9. FTIR spectrum of gelatin microspheres via water-in-oil emulsion.

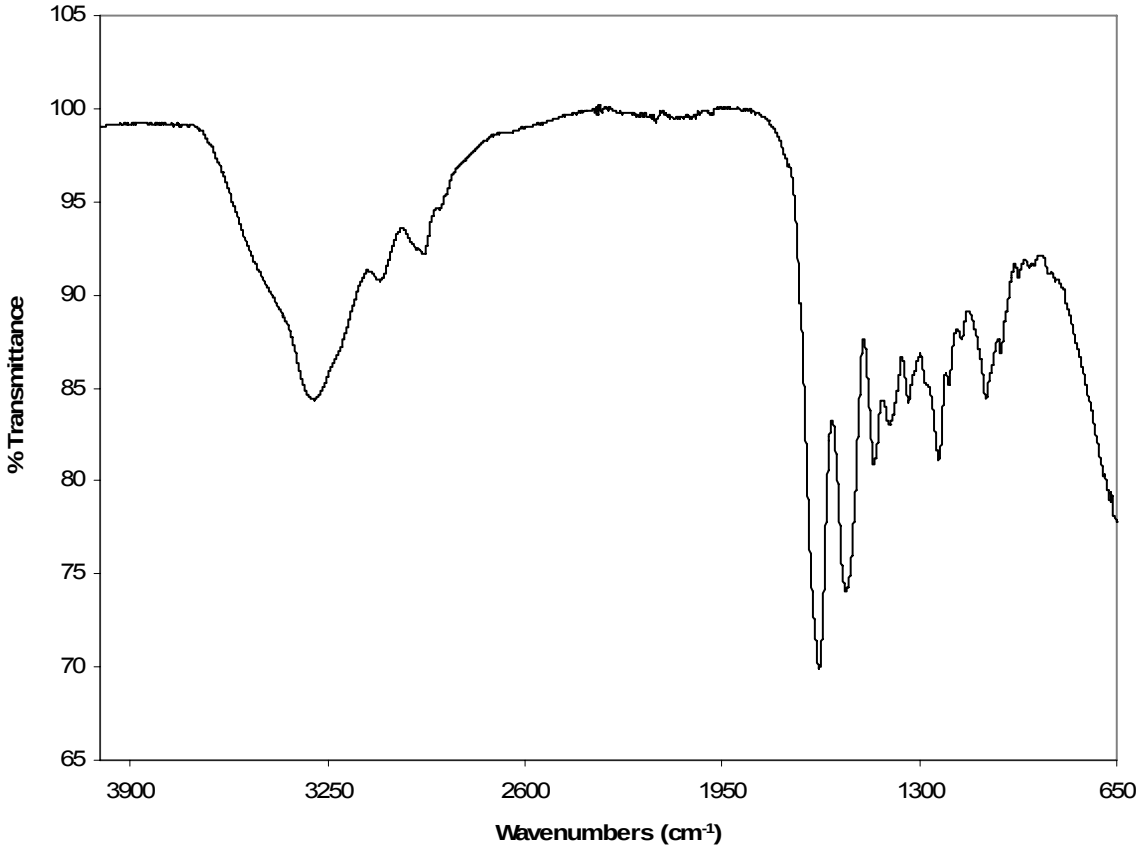

Figure 5-10. FTIR spectrum of gelatin microspheres containing phosphate via water-in-oil emulsion.

Figure 5-10 showed that there was a noticeable increase in the intensity of the spectral peaks when the phosphate was added to the gelatin. This was rather unexpected since the presence of template molecules should have a minimal effect on a non-crosslinked structure. The gelatin content was anticipated to be similar. This difference could simply be due to a difference in contact of the sample with the crystal on the IR.

Genipin Crosslinked Gelatin Polymerization

Gelatin was crosslinked with 2%, 15%, and 75% genipin in order to probe the stability of the particle. The physical appearance of the resulting crosslinked spheres varied. When using 2% genipin, the particles were cloudy blue, semi-opaque, gel-like particles. The 15% crosslinked particles were dark blue and spherical, and the 75% particles were dark blue, small,

and very rigid. Upon washing with a 1:1 mixture of HCl : DI water, the 2% particles dissolved, while the 15% and 75% particles remained intact, though hydrated.

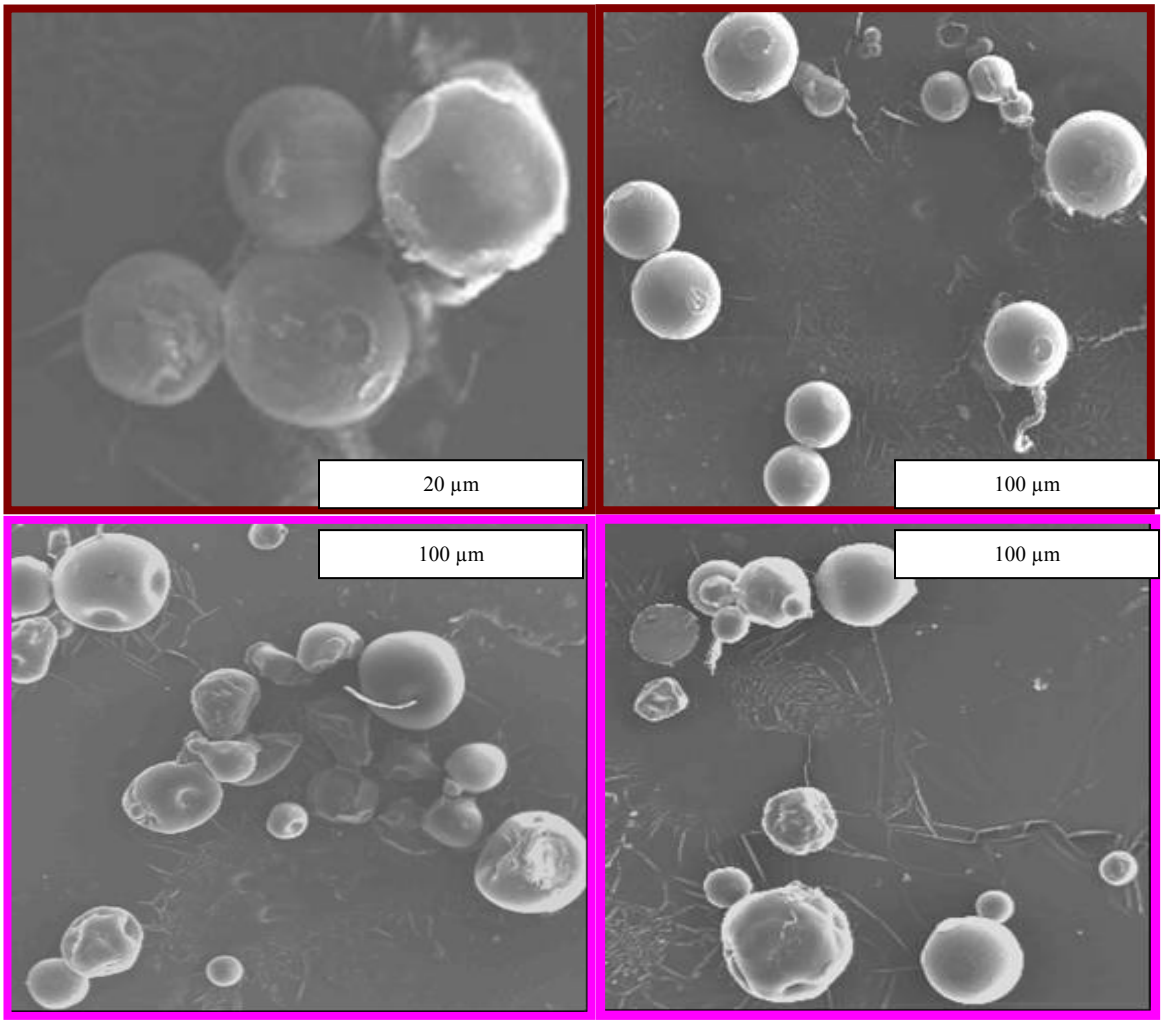

Figure 5-11. Gelatin microspheres crosslinked with 15% genipin without phosphate (top): before (right) and after (left) phosphate testing, and with phosphate (bottom): before (right) and after (left) phosphate testing.

Genipin crosslinked microspheres FTIR spectra indicated an increase of the ratio between the amide I (1627 cm^{-1}) and amide II (1532 cm^{-1}), and a C-O vibration around 1080 cm^{-1}, which are all indicative of crosslinking in the sample. Typical gelatin peaks remained, however the intensity of the spectra increase. The peak at 1030 cm^{-1} confirmed the presence of the phosphate ion.

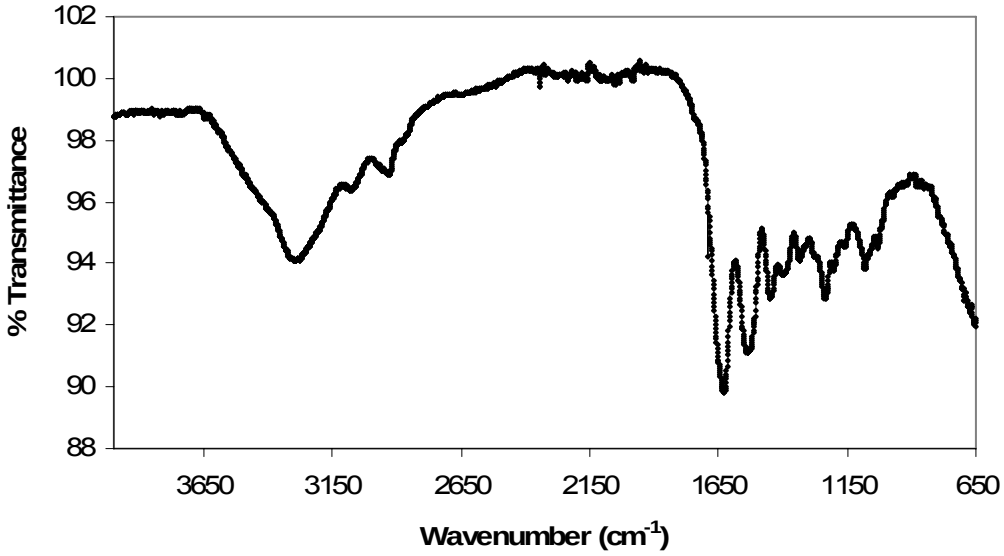

Figure 5-12. FTIR spectrum of genipin crosslinked gelatin microspheres.

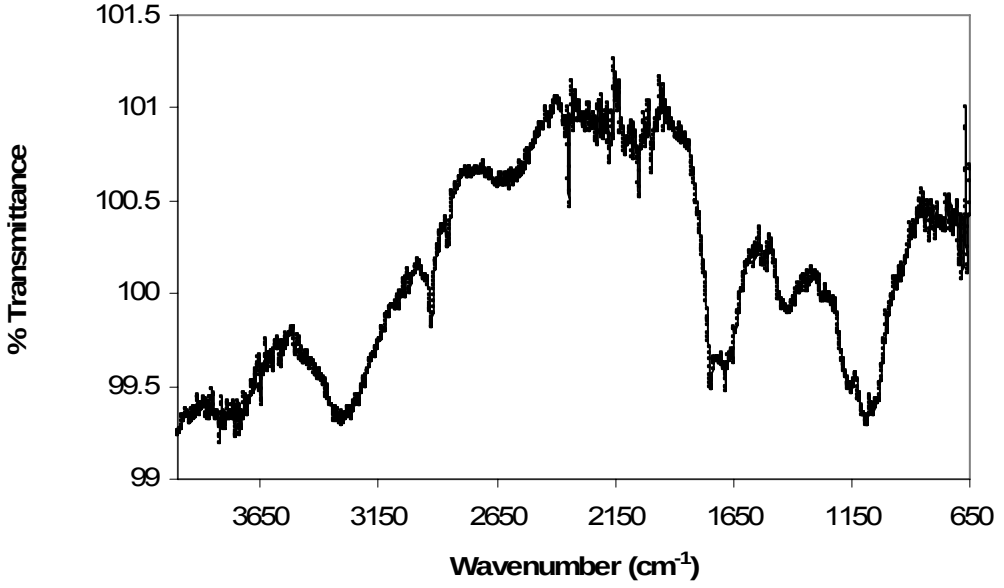

Figure 5-13. FTIR spectrum of genipin crosslinked gelatin microspheres containing phosphate.

Glutaraldehyde Crosslinked Gelatin

The glutaraldehyde crosslinked gelatin microspheres were confirmed by the presence of characteristic peaks at 2925 cm^{-1} and 1744 cm^{-1}, which represent C-H stretching of methyl and

methylene groups, and C=O stretching[101], respectively. The C-O vibration around 1080 cm^{-1} is indicative of crosslinking in the sample. Typical gelatin peaks remained, however the intensity of the spectra increase. The peak at 1030 cm^{-1} confirms the presence of the phosphate ion.

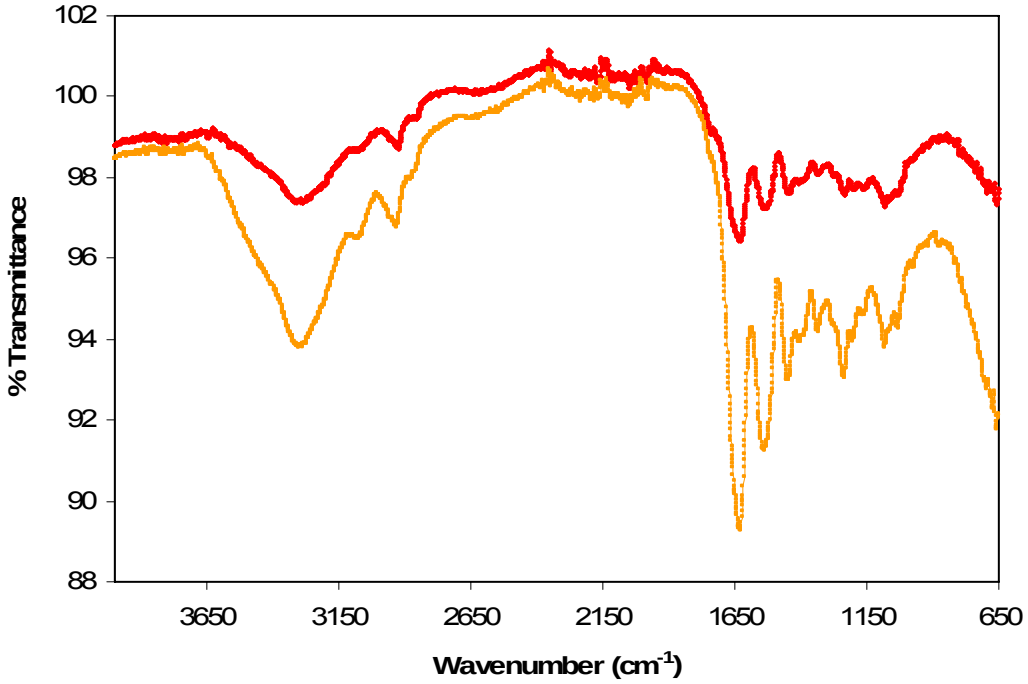

Figure 5-14. FTIR spectrum of glutaraldehyde crosslinked gelatin without phosphate (top), and with phosphate (bottom).

Many of the subsequent spectra taken were very similar in appearance, due to the strong presence of the gelatin bands, with slight differences in characteristic peak appearance. For this reason, the band appearance will be reported for each sample, but the FTIR spectra will not be presented.

Dextran Crosslinked Gelatin

Typical dextran spectra exhibit wide absorption bands in the region of vibrations of hydroxyl groups (3700-3000 cm^{-1}), and a band of stretching vibrations of CH-groups with the main maximum at 2920 cm^{-1}. The dextran crosslinked gelatin microspheres were confirmed by the presence of hydroxyl groups around 3080 cm^{-1} and 3007 cm^{-1}, and characteristic peaks of

gelatin, however the intensity of the spectra increase. The presence of phosphate was indicated by a peak at 1015 cm^{-1}.

Glyceraldehyde Crosslinked Gelatin

The typical spectra of glyceraldehyde display absorption bands in the region of 2956, 2924 and 2855 cm^{-1} corresponding to C-H stretch vibration bands, and a C=O band at 1743 cm^{-1}. The glyceraldehyde crosslinked gelatin microspheres were confirmed by the presence of peaks at 2925 cm^{-1} and 1744 cm^{-1}, which represent C-H stretching of methyl and methylene groups, and C=O stretching, respectively. The C-O vibration around 1080 cm^{-1} is indicative of crosslinking in the sample. Characteristic peaks of gelatin were displayed, however the intensity of the spectra increase. The presence of phosphate was indicated by a peak at 1015 cm^{-1}.

Phosphate uptake trials were performed in the usual manner. A stock solution of 20 mM phosphate, 80 mM NaCl, and 30 mM Na_2CO_3 was made to mimic conditions in the small intestine environment, and adjusted to pH = 7.4 to replicate physiological conditions. Microspheres were exposed to this solution for 3-48 hours at 37 ^oC.

Table 5-1 displays results for phosphate uptake in the gelatin polymers. Each reported value represents the average of 3 samples. Overall, the results demonstrate no significant phosphate uptake by the polymers crosslinked using various reagents.

Conclusions

The 2% genipin crosslinked samples did not have enough crosslinker in them to remain intact for these studies. Thus, upon heating, they simply became extremely hydrated and microsphere swelling occurred so much so, that the matrix formed a hydrogel like material, which hindered mixing during the phosphate uptake trials. The 75% crosslinked samples were crosslinked at such a high degree, that the matrix is too closed in, which actually restricts the phosphate ion from entering. Also, using such an excess of genipin makes the production of

these polymers cost prohibitive for the intended applications. The results obtained using the 15% genipin crosslinked structure appears to be a feasible line to continue. Though appreciable phosphate uptake does not occur, the physical characteristics indicate that it may be possible to manipulate the surface of this polymer in future experiments.

Table 5-1. Phosphate uptake in gelatin crosslinked microspheres that have been either acid or base washed prior to trials.

Sample	Acid treatment	Base treatment	48 hour uptake mEq / g polymer
2% Genipin	✓		swelled to a gel
2% Genipin		✓	swelled to a gel
2% Genipin w/ Phosphate	✓		swelled to a gel
2% Genipin w/ Phosphate		✓	swelled to a gel
15% Genipin	✓		0.15 ± 0.04
15% Genipin		✓	0.14 ± 0.06
15% Genipin w/ Phosphate	✓		0.41 ± 0.35
15% Genipin w/ Phosphate		✓	0.08 ± 0.07
75% Genipin	✓		0.23 ± 0.12
75% Genipin		✓	0.00
75% Genipin w/ Phosphate	✓		0.00
75% Genipin w/ Phosphate		✓	0.00
25% Glutaraldehyde	✓		0.45 ± 0.24
25% Glutaraldehyde		✓	0.43 ± 0.45
25% Glutaraldehyde w/ Phosphate	✓		0.73 ± 0.35
25% Glutaraldehyde w/ Phosphate		✓	0.83 ± 0.14
Dextran	✓		dissolved in wash
Dextran		✓	dissolved upon heating
Dextran w/ Phosphate	✓		dissolved in wash
Dextran w/ Phosphate		✓	dissolved upon heating
Glyceraldehyde	✓		0.00
Glyceraldehyde		✓	0.00
Glyceraldehyde w/ Phosphate	✓		0.90 ± .060
Glyceraldehyde w/ Phosphate		✓	0.68 ± 0.34

Glutaraldehyde and glyceraldehydes crosslinked spheres expressed a trend towards increased levels of phosphate binding in the samples prepared with the phosphate “imprints”, thus, these materials will be further surface modified as well.

The dextran crosslinked samples most likely undergo hydrolysis during the base wash and heating of the acid treated samples, which is why they dissolve. It is likely that this polymer is unsuitable for any type of heat processing, even if the surface could be favorably modified for binding phosphate ions.

CHAPTER 6
MOLECULARLY IMPRINTED POLYMERS

Microwave Fabricated Gelatin Microspheres as Phosphate Binding Agents

Biomimetic sensors can be tailored for use *in-vivo* and *in-vitro*. These mechanisms can be utilized in areas such as detecting the presence of cells that cause tumors cancer chemotherapy, or monitoring the amount of glucose in the blood stream in diabetic patients.[40] The extensive list of in-vivo applications of MIPs, without significant patient side effects, show that it is feasible to design phosphate MIPs for oral administration for patients with chronic renal failure.

A novel microwave-assisted technique has been developed for the synthesis of molecularly imprinted gelatin microparticles as oral phosphate binding agents on the order of 10 – 200 μm, is described. After extraction of the template molecule, an imprint cavity of specific shape and memory remains in the polymer.

Crosslinked Gelatin Microspheres via Microwave Radiation

Thermal denaturation has been examined as a way in which proteins can be physically crosslinked.[102] Extended dehydration of gelatin at elevated temperatures and reduced pressures have been known to induce the spontaneous formation of interchain amide links[103] within the matrix. Crosslinking occurs through a condensation reaction between a free carboxyl group on the gelatin backbone and an amino acid on an adjacent chain. However, crosslinking can take more than 24 hours under ambient conditions, which can be accelerated by the use of microwave radiation.

Previous studies have shown that gelatin can be thermally crosslinked after 10 minutes using a CEM microwave oven (model MAS 7000) with an inlet temperature of 250 ^{o}C .[104] Such an oven was not available for experiments, so trials were simulated using a regular, department store purchased, small kitchen microwave (1.2 kW Samsung Simply microwave oven, model

#MW5470W).

This procedure was developed to investigate the synthesis of molecularly imprinted polymers via microwave treatment, in order to decrease the synthetic reaction time in comparison to standard step-growth or radical polymerization procedures.[105] With success, an alternative synthetic route was provided that is cheaper, more time efficient, and can be performed under a gentler chemical environment as compared to traditional schemes. A major benefit of this particular regime was that particles prepared this way may allow increased imprinted sites for binding. However, in order to comply with the ideal of highly crosslinked MIPs, crosslinking agents will be used as well.

Microwave Treatment

500 mg of gelatin microspheres, produced as previously described, were placed in a glass vial containing 2 ml of a 1:1 (v/v) mixture of acetone : crosslinking agent (a polar medium was used to obtain uniformity of microwave energy during the trial). The vial was placed in a microwave for the determined amount of time (≥2 minutes), with a glass microscope slide loosely placed on top, as to prevent total solvent evaporation. The microspheres were collected and washed five times in 10 ml acetone, or until the supernatant was clear (cloudy indicates excess glutaraldehyde still being released). The particles were then washed once with 1:1 solution of 0.1 M NaOH: MeOH, three times with DI water, filtered, and rinsed with acetone. The spheres were dried at room temperature, in-vacuo, in order to remove any residual moisture.

Results

Gelatin Emulsion Microspheres

Using plain gelatin spheres for the microwave treatment resulted in particles that appeared to have low crosslinking density character at about 25 minutes, and started to “cook” around 30 minutes. Spheres expanded, took on a ‘rice crispy’ like appearance, and had a pungent odor. A

slight decrease in swelling was apparent after 40 minutes of microwave time, and a definite crosslinked form occurred around 50 minutes. This was indicated by the slight darkening in color of the sphere which is associated with the slight reduction in particle diameter. However, particles eventually swell upon long term exposure to water (≥ 24 hours). Thus, it was apparent that, in order to accomplish the synthesis of this type of crosslinked gelatin without using a crosslinking agent, the microwave technique reported in literature should probably be used. Therefore, since crosslinking could not be established using the Samsung microwave, the overall feasibility of crosslinking gelatin particles without the use of a chemical crosslinking agent could not be determined at this time .

Genipin and Glutaraldehyde Crosslinked Microspheres

The experiment was repeated using genipin and glutaraldehyde as crosslinking agents. Noticeable crosslinking appeared to happen in less than 2 minutes using glutaraldehyde, which was associated by the change in color of the spheres to burnt orange, and the emergence of a pungent smell. Visible crosslinking is notably minimal when microwaving genipin for as long as 10 minutes, thus the production of these polymeric microspheres was discontinued.

The glutaraldehyde crosslinked particles were processed using different amounts of crosslinking agent in order to determine if the appropriate amount to use for microsphere formation concurs with the established parameters detailed earlier in Chapter 4. Once the optimum amount of crosslinker to use was ascertained, it was established as the standard for future experiments.

SEM highlighted several interesting morphological features that suggest phosphate binding in the microspheres (Figure 6-1). The microspheres synthesized without phosphate appeared to be relatively smooth on the surface, even after they had been tested for phosphate uptake. This indicated minimal phosphate binding within the sample. Conversely, microspheres created with

phosphate showed a “textured” surface prior to uptake trials, and an agglomeration of microstructures on the surface of particles after uptake testing.

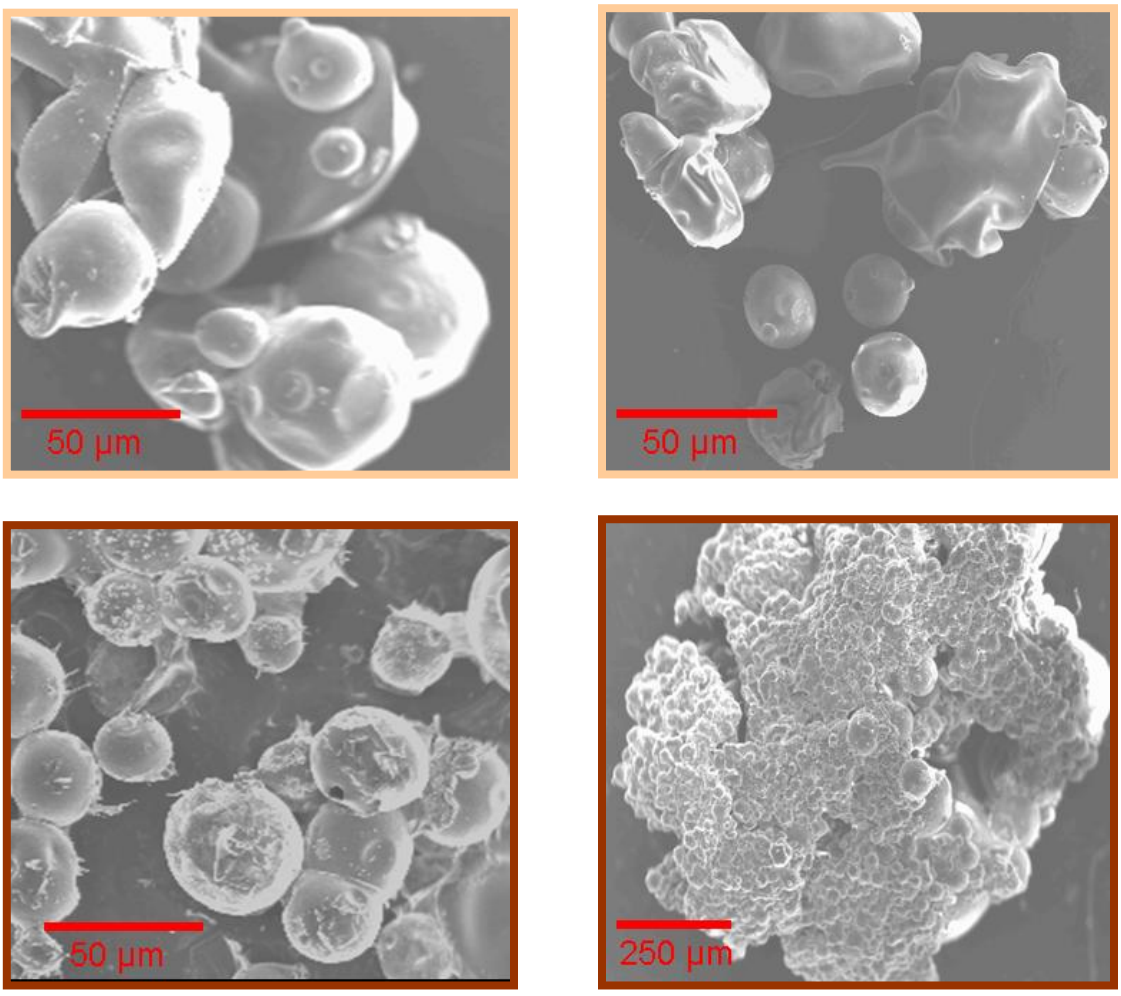

Figure 6-1. SEM of gelatin crosslinked microspheres via microwave processing without phosphate (top): before (left) and after (right) phosphate testing, and with phosphate (bottom): before (left) and after (right) phosphate testing.

The mechanism for phosphate binding in the gelatin microspheres for this study was proposed in Chapter 4. This could be further explained by comparing the SEM in Figure 6-2 to the modeled system. Figure 6- 2 illustrates the way in which phosphate is bound by a protonated amine cage, and Figure 6-3 demonstrates multiple phosphates bound by the microsphere structure, which resemble the imprint sites for the template. It was reasonable to conclude that there were recognition sites within the polymer as well as on the surface. If phosphate was

bound at the surface, it could function as a nucleation site for additional phosphate ions to grow from. Individual phosphate ions are too small to be visible through SEM, however phosphate clusters at the surface of the microsphere will appear mineralized. This phenomena was seen in the images.

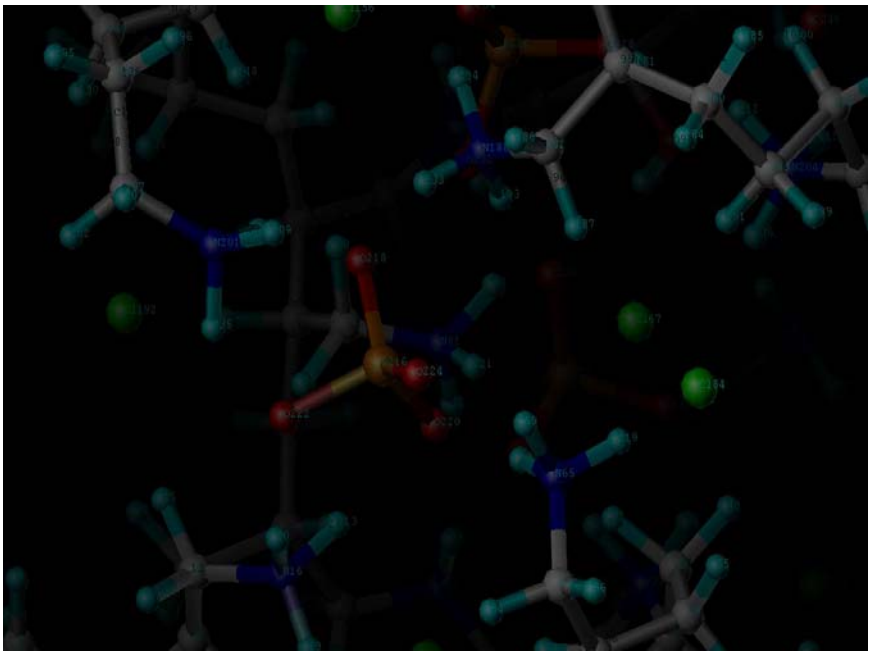

Figure 6-2. Protonated amine cage (blue) surrounding a phosphate ion (red/orange).

The glutaraldehyde crosslinked gelatin microspheres were confirmed by the presence of characteristic peaks at 2925 cm^{-1} and 1744 cm^{-1}, which represent C-H stretching of methyl and methylene groups, and C=O stretching[101], respectively. The C-O vibration around 1080 cm^{-1} is indicative of crosslinking in the sample. Typical gelatin peaks at 1630 cm^{-1}, 1535 cm^{-1}, and 1237 cm^{-1} (amide I, amide II, and amide III, respectively) were represented in the spectra, and the presence of phosphate is shown around 1030 cm^{-1}.

The microspheres that were acid washed prior to phosphate uptake testing had largely similar IR spectra, however there were small band shifts, which may be attributed to the presence of phosphate.

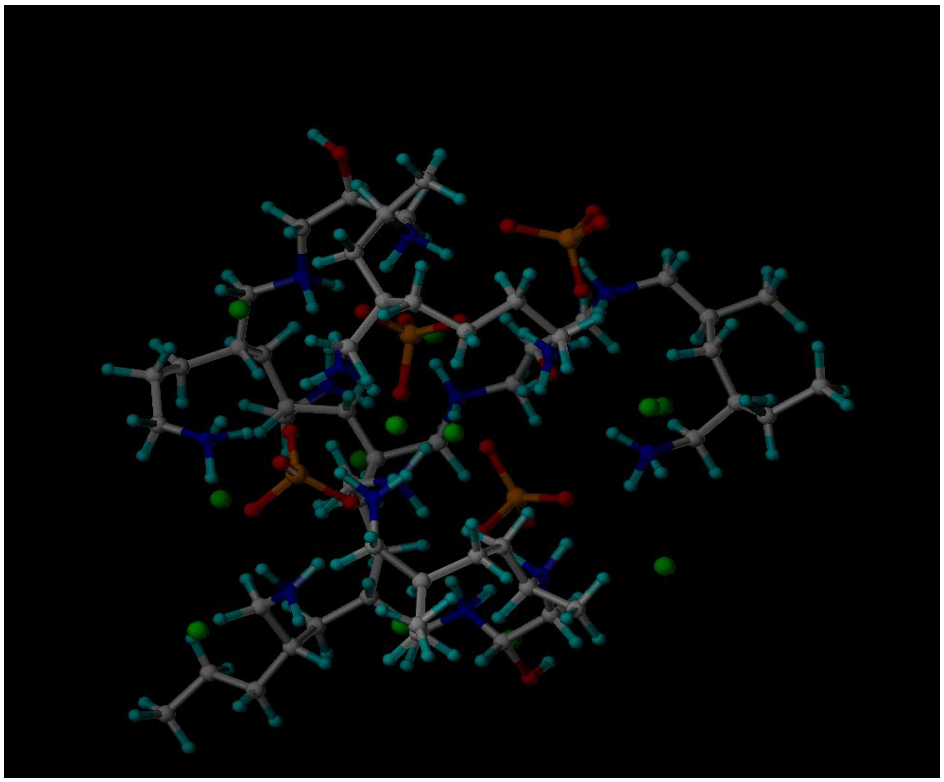

Figure 6-3. Modeled system of the phosphate binding polymer.

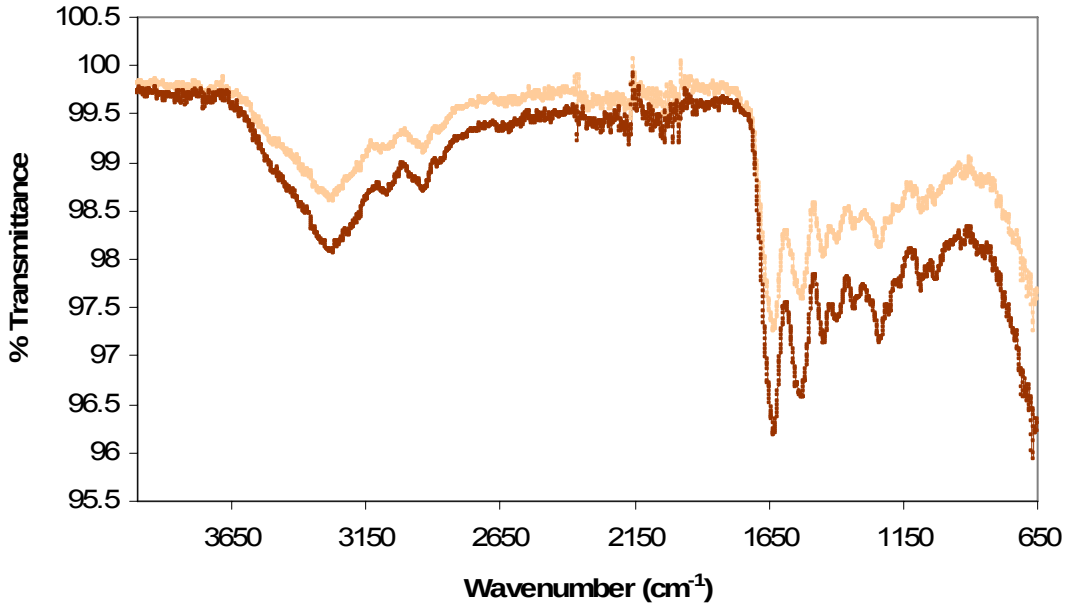

Figure 6-4. FTIR spectrum of glutaraldehyde crosslinked gelatin, via microwave irradiation: without phosphate (top), and with phosphate (bottom).

The microspheres that were base washed prior to phosphate uptake testing had largely similar IR spectra. The peaks for the particles that did not contain phosphate appear less intense in comparison to those that did contain phosphate, however peak ratio analysis indicated that they there was no significant difference in the spectra.

Phosphate uptake trials were performed in the usual manner. A stock solution of 20 mM phosphate, 80 mM NaCl, and 30 mM Na_2CO_3 was made to mimic conditions in the small intestine environment, and adjusted to pH = 7.4 to replicate physiological conditions. Microspheres were exposed to this solution for 3-48 hours at 37 ^{o}C.

Table 6-1. Phosphate uptake in microwave irradiated gelatin crosslinked microspheres that have been either acid or base washed prior to trials.

Sample	Acid treatment	Base treatment	48 hour uptake mEq / g polymer
10% Glutaraldehyde	✓		0.20 ± 0.04
10% Glutaraldehyde		✓	0.61 ± 0.54
10% Glutaraldehyde w/ Phosphate	✓		1.05 ± 0.85
10% Glutaraldehyde w/ Phosphate		✓	0.62 ± 0.40
25% Glutaraldehyde	✓		0.23 ± 0.32
25% Glutaraldehyde		✓	0.39 ± 0.24
25% Glutaraldehyde w/ Phosphate	✓		1.98 ± 1.38
25% Glutaraldehyde w/ Phosphate		✓	0.95 ±0.38
40% Glutaraldehyde	✓		0.45 ± 0.24
40% Glutaraldehyde		✓	0.60 ± 0.13
40% Glutaraldehyde w/ Phosphate	✓		0.82 ± 0.68
40% Glutaraldehyde w/ Phosphate		✓	1.07 ± 0.24

Table 6-1 displays results for phosphate uptake in the gelatin polymers. Each reported value represents the average of 3 samples.

Conclusions

There were several noticeable trends that emerged for the microspheres after phosphate testing. First, the phosphate binding capacity increased as the amount of crosslinking agent increases. This was accurate in terms of information represented in the literature. In order to produce an efficient MIP, a high degree of crosslinking must be present such that a non-

destructible template cavity is formed that allows multiple binding and extraction events. However, polymers that are too highly crosslinked restrict template recognition, and crosslinking that is too low to not provide a mechanically stable enough environment for template sequestration. The 40% w/w glutaraldehyde composition seemed to provide a feasible formula for creating MIPs via microwave irradiation. Though there was a great degree of error associated with the 25% w/w acid treated sample, the uptake was so great, that it could not be ruled out as an insignificant result. Second, the based washed microspheres displayed overall enhanced phosphate binding in comparison to their acid washed counterparts. This indicated that the base wash provided an environment that was more conducive to removing the phosphate ions from the imprinted polymer, thus providing additional available binding sites for ion extraction from solution.

CHAPTER 7
GUANYLATED POLYMERS

This chapter describes a technique for the synthesis of novel guanylated gelatin microparticles as oral phosphate binding agents. Using modified processing schemes, various biocompatible crosslinking agents, and high affinity phosphate binding functional groups, highly crosslinked, tailored, gelatin microspheres on the order of 10 – 200 μm were produced.

Previous experiments performed involving the use of gelatin, crosslinked with either genipin, glutaraldehyde, glyceraldehyde, or dextran have shown limited phosphate binding capacity during uptake trials. Thus, the need for adding a functional group to the gelatin backbone to increase phosphate uptake became a forefront consideration.

To address this issue, a guanidine derivative was chosen to structurally modify the gelatin microspheres. Guanylating reagents are compounds that chemically transform a specific reactive group, in this case an amine, into guanidine. This reaction can take place in organic solvents as well as water, and usually under relatively mild conditions. One major set back with the use of guanidines is that they are highly basic, with a pKa of 12.5, and highly nucleophilic.[106] However, this same feature allows them to be fully protonated under physiological conditions[107], which provides a foundation for its ligand-receptor interaction.

Recent applications of guanidine derivates include biocidal polymers,[108] bile acid sequestrants,[109] and potential gene delivery carriers.[107] There has also been interest and some success in using amidinium based monomers in molecular imprinting[110-113] for phosphonates.

1-H-pyrazole-1-carboxamidine hydrochloride was chosen as the guanidinating reagent for the direct preparation a gelatin-guanidinium compound, which reacts with an amine group on the polymer according to the following general scheme in Figure 7-1. The primary amines are readily converted, while secondary amines usually require heat to initiate guanylation.[114] The

pyrazole byproduct is soluble in water, which allows the insoluble guanylated polymer to be easily removed.

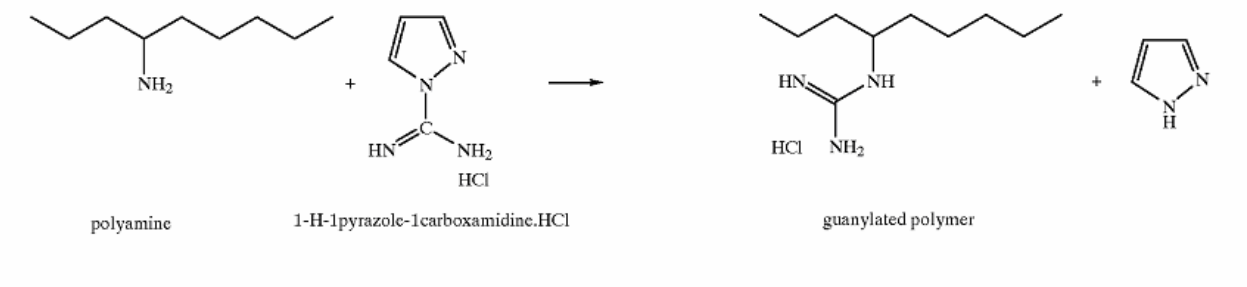

Figure 7-1. Synthetic route used to obtain a guanylated polymer.

In turn, the guanidine group can form a strong association with the external oxygen groups on the phosphate ion, which make binding possible. The use of guanidinium groups for oxyanion recognition and binding[115] has attracted a great deal of interest over the past years. Their ability to sequester these ions through cationic and hydrogen bonding through Zwitterionic interactions make them unique biocompatible binding agents.

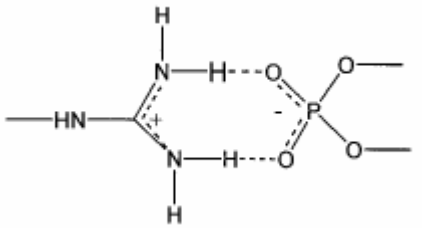

Figure 7-2. Zwitterionic interaction of phosphate with a guanyl group.

The synthesis of low molecular weight guanidinium compounds has been extensively reported in literature. However, there is only a small body of work that has inspected the synthesis of polymeric guanidinium salts.

Functionalized Gelatin Microspheres via Guanylation

The first step in this synthetic route was to prepare previously described crosslinked gelatin microparticles for surface functionalization. Due to the basic nature if the 1-H-pyrazole-1-

carboxamidine, the spheres were first base treated – which resulted in a freebase surface environment that was more amenable to the high pKa of the guanylating agent. There were two approaches to particle synthesis: noncrosslinked gelatin microspheres were prepared for guanylation modification and subsequently crosslinked for molecular imprinting, and the already crosslinked gelatin particles were surface guanylated. SEM and IR were used for surface morphology and bond characterization.

In the typical IR spectrum of guanine−HCl, bands at 2725 cm^{-1}, 2520 cm^{-1}, and 2485 cm^{-1} represent N-H stretching of weak NH^{+}-Cl^{-} intermolecular hydrogen bonds.[116] The absence of these characteristic peaks indicated molecular conversion.

Imprinted Gelatin Microspheres

Room Temperature Guanylation

A freebase sample of uncrosslinked gelatin was prepared by placing 1.5 g of the microspheres in 30 mL of acetone, and NaOH was used to adjust the solution to a pH of 12. The solution was stirred for 1 hour, rinsed 3 times with DI water, and dried overnight in vacuo. A cloudy white solution of 20 mM 1-H-pyrazole-1-carboxamidine: 10 mM KH_2PO_4 in a water : acetone (1:2) mixture was adjusted to pH = 7.4, and stirred for 3 hours under nitrogen in order to form a complex between the guanidine and the phosphate. The freebase gelatin particles were added to the guanidine mixture, which was purged with nitrogen and turned clear after 1 hour. The reaction was allowed to stir for 24 hours at room temperature, under a nitrogen stream, cooled to room temperature, filtered, and washed 3 times for 20 minutes in 25 mL acetone. The sample was then washed with a 1:1 solution of 0.1 M NaOH: MeOH, neutralized with DI water, filtered, and dried in vacuo. The final product was off white and spherical. In addition, this sample was further processed by crosslinking.

Heat Assisted Guanylation

A freebase sample of uncrosslinked gelatin was prepared by placing 1.5 g of the microspheres in 30 mL of acetone, and NaOH was used to adjust the solution to a pH of 12. The solution was stirred for 1 hour, rinsed 3 times with DI water, and dried overnight in vacuo. A cloudy white solution of 20 mM 1-H-pyrazole-1-carboxamidine: 10 mM KH_2PO_4 in a water: acetone (1:2) mixture was adjusted to pH = 7.4, and stirred for 3 hours under nitrogen in order to form a complex between the guanidine and the phosphate. The freebase gelatin particles were added to the guanidine mixture, which was purged with nitrogen and turned clear after 1 hour. The reaction was allowed to stir for 24 hours at 60 ^{o}C, under a nitrogen stream, cooled to room temperature, filtered, and washed 3 times for 20 minutes in 25 mL acetone. The sample was then washed with a 1:1 solution of 0.1 M NaOH: MeOH, neutralized with DI water, filtered, and dried in vacuo. The final product was off white and spherical. In addition, this sample was further processed by crosslinking.

Surface Guanylated Gelatin Microspheres

The surface guanylated gelatin microspheres were prepared both with and without the introduction of heat, as described in the previous section. However, crosslinked spheres synthesized according to the descriptions in Chapters 5 and 6 were used instead of the uncrosslinked gelatin microspheres. These guanylated moieties are further treated with an acid or base to remove the template as described in Chapter 5.

Results

Imprinted Polymers

Uncrosslinked gelatin microspheres were prepared and guanylated so that they could be further crosslinked and processed as MIPs. Batches of control gelatin microspheres, which did not contain phosphate, and spheres that contained the phosphate template molecule, were

synthesized. Because the uncrosslinked microspheres are susceptible to hydrolysis and degradation under heat, these batches were guanylated at room temperature. For this same reason, *in-vitro* phosphate uptake testing was not possible. As a result, these materials were probed using SEM and FTIR instruments.

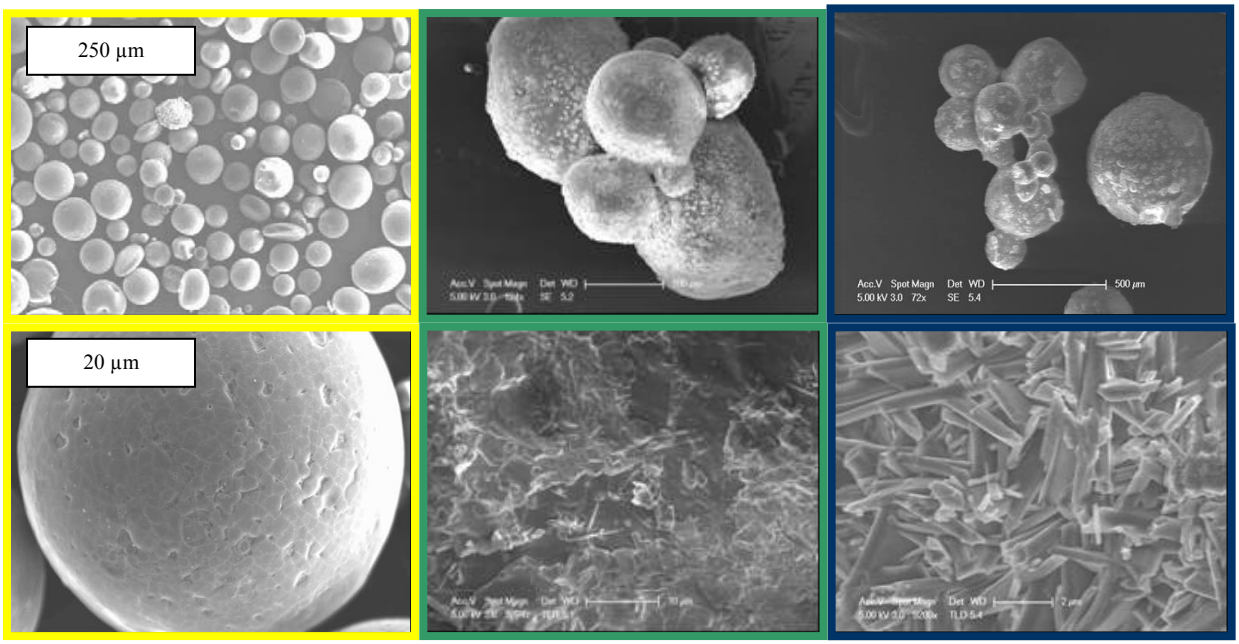

Figure 7-3. SEM images of uncrosslinked gelatin, native (left), guanylated without phosphate (middle), and guanylated with phosphate (right). Bottom images are magnified versions of top images.

SEM analysis provided visual evidence concerning the modification of gelatin side chains using guanylating agents. Raw, uncrosslinked gelatin spheres have relatively smooth surfaces in comparison to the gelatin microspheres that have been guanylated, which have rough and bumpy surfaces. The guanylated particles that are supposed to have bound phosphate in them had a rough and bumpy surface as well, however the magnification of these samples clearly show the presence of crystal shaped rods on the surface, which were believed to be phosphate. The SEM images are taken of microspheres that have been used in phosphate uptake trials, and subsequently air dried. Thus, the bound phosphate in solution becomes more concentrated at the

surface, which contributes to the amount of crystals that are imaged.

This visual phenomenon can be explained by the suggested phosphate ion binding model proposed in Chapter 3. With the proposed close proximities of all of the phosphate binding events (Figure 7-4) it is possible that there are template ion "cages" that stack on top of each other, thus promoting the nucleation and upward growth of phosphate crystals. It is proposed that these cages can also orientate themselves to form G quartets.

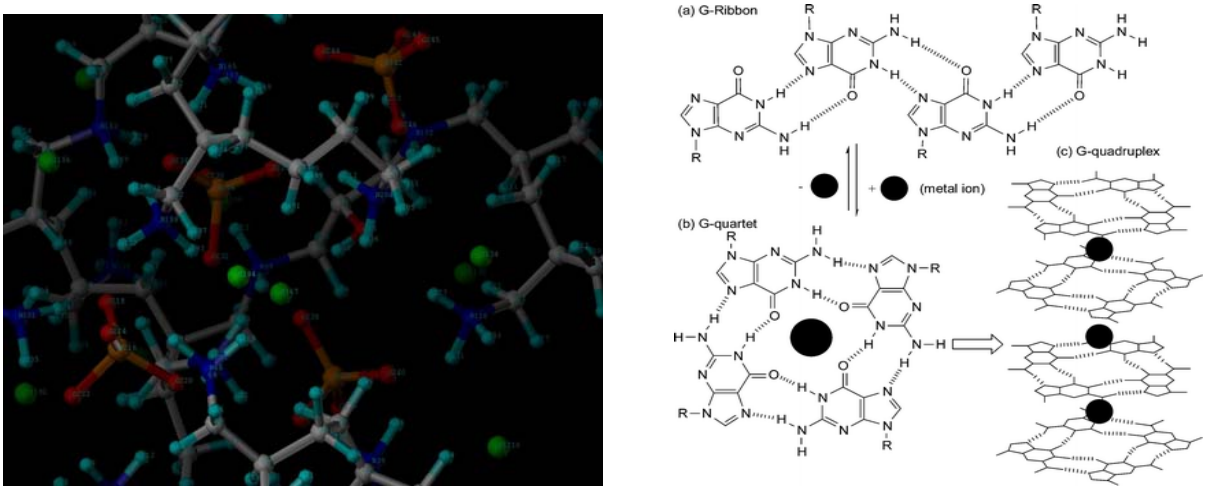

Figure 7-4. Predicted proximity of 4 phosphate ions within the polymer structure (right), and a guanine derivative self assembly into (a) G-ribbon, (b) G-quartet, and (c) G-quadruplex formed by stacking of G-quartets around a column of cations.[117]

DNA and RNA are guanine rich, which allows them to form inter- and intramolecular four-stranded structures, referred to as G-quartets.[118, 119] G-quartets evolve from the association of four guanine bases into a cyclic Hoogsteen H-bonding arrangement (Figure 7-4). The G-quartets stack on top of each other to give rise to tetrad-helical structures, which would explain the presence of the phosphate crystal structures. The stability of G-quartet structures depends on the presence of the monovalent cations, which promote formation and increase stability, and the concentration of the G-rich moieties.

Glutaraldehyde

The uncrosslinked, guanylated gelatin microspheres were further processed by crosslinking

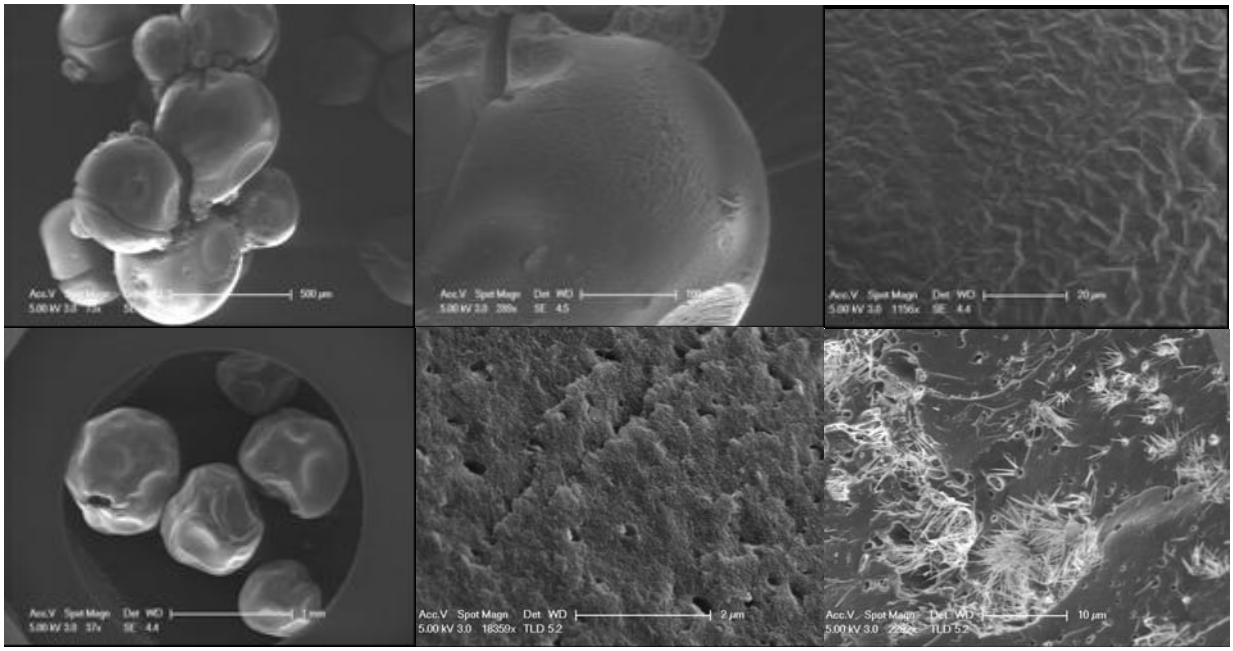

Figure 7- 5. Glutaraldehyde crosslinked gelatin microspheres prepared via microwave irradiation, room temperature surface guanylation: after guanylation (left), after template extraction (middle), and after phosphate uptake testing (right). Without phosphate (top), and with phosphate (bottom).

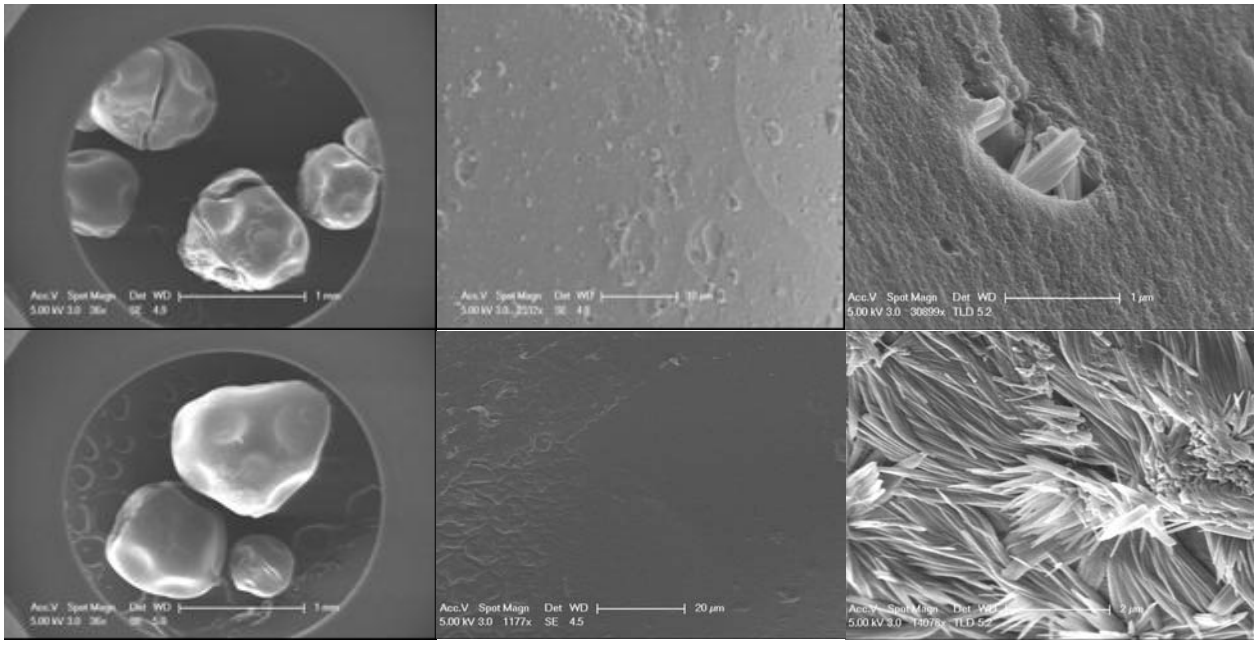

Figure 7-6. Glutaraldehyde crosslinked gelatin microspheres prepared via microwave irradiation, heat initiated surface guanylation: after guanylation (left), after template extraction (middle), and after phosphate uptake testing (right). Without phosphate (top), and with phosphate (bottom).

with glutaraldehyde according to the microwave irradiation procedure (Chapter 6). Resultant polymeric particles were dark burnt orange spheres. The spheres have a translucent off-white surface hue.

We used SEM to visually confirm the change in microsphere morphology as it is processed from guanylation to template extraction, and ultimately tested in a phosphate ion solution. Pitting is present in several of the samples where the template was extracted, which suggested that phosphate ion binding was successful. The visible crystals on the surface of the particles represented the presence of phosphate, which was most likely both bound by the gelatin polymer sphere as well as physisorbed on the surface.

Surface Modified Crosslinked Polymers

Samples of gelatin crosslinked microspheres were taken and guanylated either with or without the use of heat, as detailed in the above section.

Genipin

The uncrosslinked, guanylated gelatin microspheres were further processed by crosslinking with genipin according to the reverse emulsion procedure that was thoroughly described in Chapter 5. The resultant polymeric particles were dark teal, with either spherical or chunk like shapes.

Glutaraldehyde

SEM was used to visually confirm the change in microsphere morphology as it is processed from guanylation to template extraction, and ultimately tested in a phosphate ion solution. Samples that were guanylated or viewed after template extraction had relatively smooth surfaces, which indicated that there was not a considerable change in the surface structure of the sample between processing steps. The visible crystals on the surface of the particles after uptake testing represented the presence of phosphate.

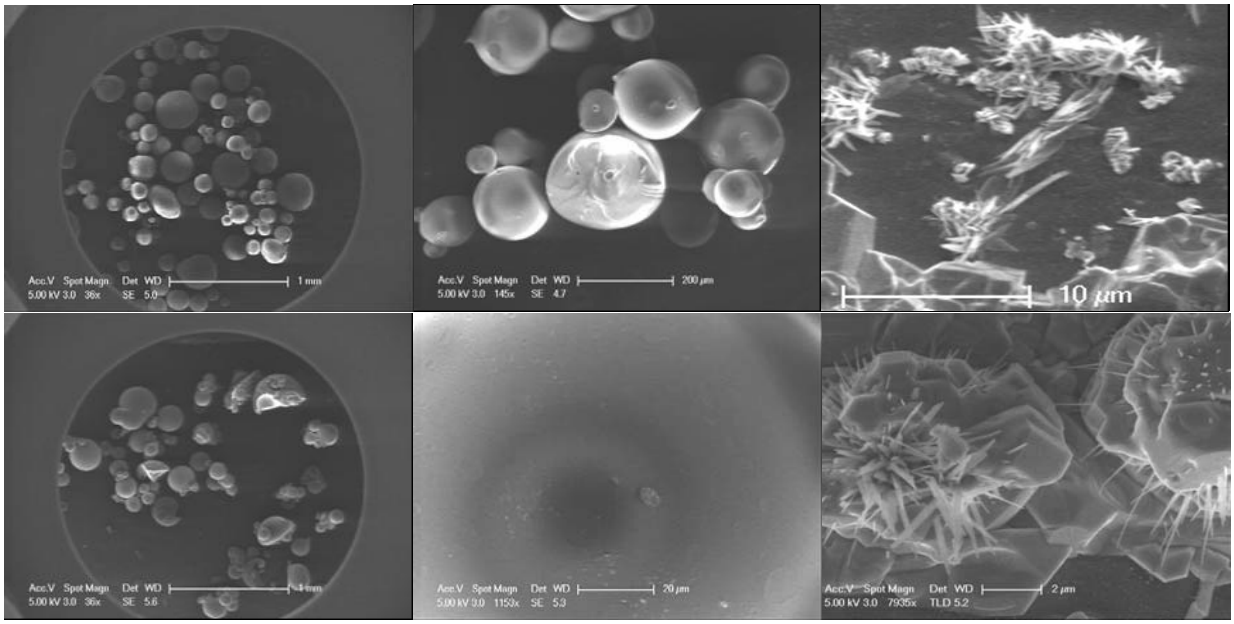

Figure 7-7. Glutaraldehyde crosslinked gelatin microspheres prepared via emulsion polymerization, room temperature surface guanylation: after guanylation (left), after template extraction (middle), and after phosphate uptake testing (right). Without phosphate (top), and with phosphate (bottom).

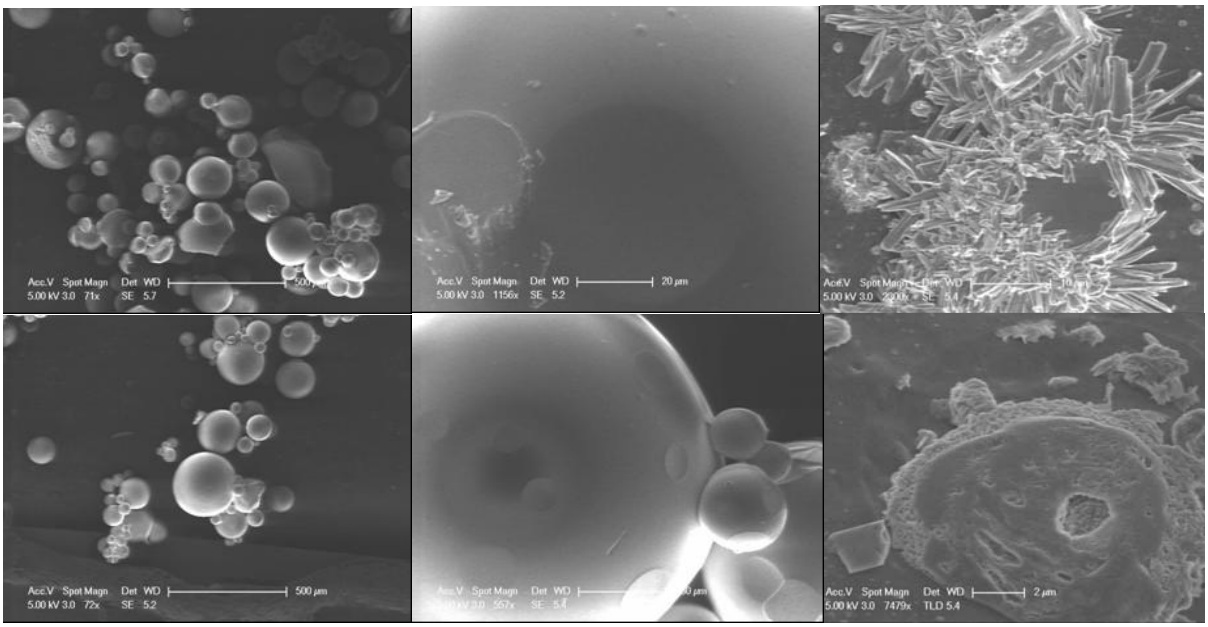

Figure 7-8. Glutaraldehyde crosslinked gelatin microspheres prepared via emulsion polymerization, heat initiated surface guanylation: after guanylation (left) and after template extraction (right). Without phosphate (top), and with phosphate (bottom).

In samples that did not contain phosphate in the original composition, the presence of the crystals most likely is the result of physisorption. In samples that did contain phosphate in the original composition, the presence of the crystals was most likely due to phosphate both bound by the gelatin polymer sphere as well as physisorbed on the surface.

Glyceraldehyde

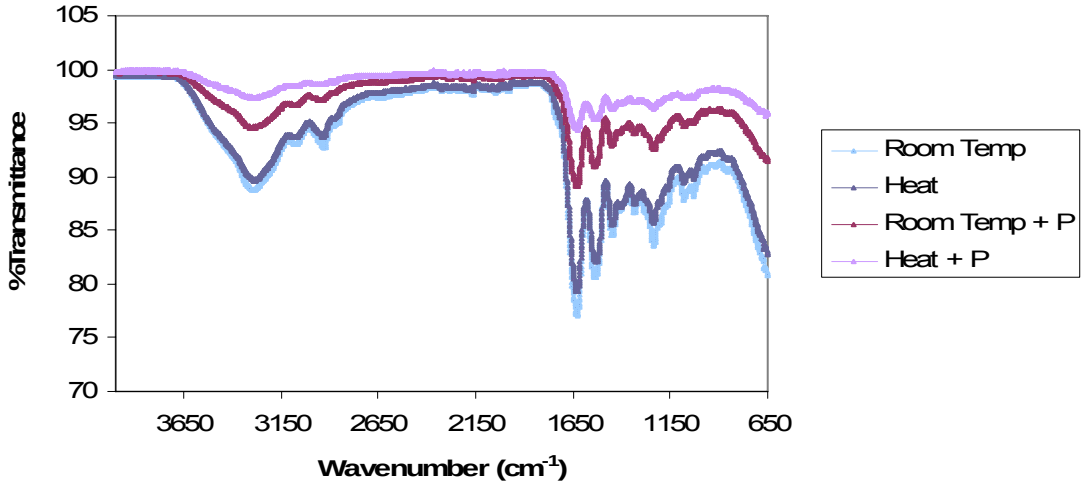

Figure 7-9. FTIR spectrum of surface guanylated gelatin crosslinked with glyceraldehyde.

The typical spectra of glyceraldehyde display absorption bands in the region of 2924 and 2855 cm^{-1} corresponding to C-H stretch vibration bands, and a C=O band at 1743 cm^{-1}. The glyceraldehyde crosslinked gelatin microspheres were confirmed by the increase in intensity in the 2925 cm^{-1} peak, which represented C-H stretching of methyl and methylene groups, and C=O stretching, respectively. The C-O vibration around 1080 cm^{-1} is indicative of crosslinking in the sample. Characteristic peaks of gelatin are present.

Phosphate uptake trials were performed in the usual manner. A stock solution of 20 mM phosphate, 80 mM NaCl, and 30 mM Na_2CO_3 was made to mimic conditions in the small intestine environment, and adjusted to pH = 7.4 to replicate physiological conditions. Microspheres were exposed to this solution for 3-48 hours at 37 ^{o}C.

Conclusions

Microspheres that were glutaraldehyde crosslinked using microwave irradiation were processed to produce a molecularly imprinted product. Though phosphate uptake occurred in these samples, the variability in the heat treated trials was great, and the significant error associated with the standard deviations demonstrated that this procedure should be discontinued. However, room temperature guanylated microspheres indicate reasonable phosphate binding in the 25% crosslinked batch, even though uptake is below the previously established minimum "success" value. This indicated that polymer imprinting is achieved through this synthetic pathway. Template recognition may have been hindered by probable small size, buried position, and or spatially restricted position of the imprinted site, which are all reported common problems with MIP rebinding studies.

Glutaraldehyde crosslinked microspheres, prepared by an inverse emulsion process, were surface guanylated and the phosphate binding capacity was measured. Interestingly enough, the heat treated microspheres were able to attract phosphate to a greater degree in comparison to the room temperature processed particles. In addition, the heat processed samples containing phosphate had less phosphate uptake in them than did the samples that did not contain phosphate. The reverse trend was seen in the room temperature processed samples.

Table 7-1 displays results for phosphate uptake in the gelatin polymers. Each reported value represents the average of 3 samples.

SEM images of the guanylated glutaraldehyde crosslinked samples support the data. A particularly remarkable physical feature of the samples after phosphate testing is that the imprinted microspheres appeared to have phosphate emanating from within the microstructure, and the surface modified spheres appeared to have phosphate attached onto the surface. This would verify the viability of imprinted and surface templated techniques.

Table 7-1. Phosphate uptake in surface functionalized and molecularly imprinted gelatin crosslinked microspheres prepared by either emulsion or microwave irradiated.

Sample	Room Temperature	Heat	48 hour uptake mEq / g polymer
Emulsion Processed			
15% Genipin	✓		0.62 ± 0.09
15% Genipin		✓	0.14 ± 0.14
15% Genipin w/ Phosphate	✓		1.19 ± 0.18
15% Genipin w/ Phosphate		✓	0.32 ± 0.05
25% Glutaraldehyde	✓		0.68 ± 0.26
25% Glutaraldehyde		✓	1.08 ± 0.02
25% Glutaraldehyde w/ Phosphate	✓		0.90 ± 0.23
25% Glutaraldehyde w/ Phosphate		✓	0.63 ± 0.17
Glyceraldehyde	✓		0.73 ± 0.21
Glyceraldehyde		✓	0.34 ± 0.17
Glyceraldehyde w/ Phosphate	✓		0.79 ± 0.48
Glyceraldehyde w/ Phosphate		✓	0.11 ± 0.07
Microwave Irradiated			
10% Glutaraldehyde	✓		0.87 ± 0.42
10% Glutaraldehyde		✓	1.07 ± 0.16
10% Glutaraldehyde w/ Phosphate	✓		0.85 ± 0.29
10% Glutaraldehyde w/ Phosphate		✓	1.78 ± 1.62
25% Glutaraldehyde	✓		0.21 ± 0.15
25% Glutaraldehyde		✓	0.85 ± 0.55
25% Glutaraldehyde w/ Phosphate	✓		0.62 ± 0.11
25% Glutaraldehyde w/ Phosphate		✓	0.74 ± 0.09
40% Glutaraldehyde	✓		0.54 ± 0.42
40% Glutaraldehyde		✓	0.29 ± 0.17
40% Glutaraldehyde w/ Phosphate	✓		0.69 ± 0.31
40% Glutaraldehyde w/ Phosphate		✓	1.21 ± 1.21

Though there was no appreciable phosphate uptake in the genipin samples guanylated using heat, results indicate that gelatin spheres guanylated at room temperature show successful phosphate binding.

There was minimal phosphate uptake in the glyceraldehyde samples guanylated using heat. The gelatin spheres guanylated at room temperature show phosphate binding, but there is not much of a difference between microspheres that contain the template ion in comparison to those

that do not. Phosphate uptake is below the minimum established value if significance, but may be more selective, although this hypothesis was not tested.

CHAPTER 8
DISCUSSION

Synopsis

Functionalized gelatin microspheres were designed to address the need for a cost effective alternative for phosphate removal in aqueous systems, specifically for patients with ESRD, where hyperphosphatemia is a common physiological encumbrance.

To the best of this authors' knowledge, previous work has not been reported in literature concerning the development of these novel polymers.

Various synthetic mechanisms were proposed and evaluated in order to derive a method to develop a robust material that could effectively bind phosphate. At the conclusion of each synthetic scheme, the attributes of the polymers that had the highest binding capacity were incorporated into the next design, as to develop a rigorous procedure for the development of tailored gelatin microspheres that utilized the best processing parameters.

There were two hypothesis that were tested: Could a surface functionalized gelatin polymer for phosphate removal in aqueous systems be developed and characterized, and could a molecularly imprinted polymer be developed and characterized for phosphate removal in aqueous systems. Each synthetic route investigated is illustrated in Figures 8-1 and 8-2.

The efficacy of phosphate uptake with these functionalized polymers was determined *in-vitro*, and three samples were identified as a synthetic success due to their statistical significance verified at $p \leq 0.05$. These polymeric microspheres did not degrade in an artificial environment created to simulate the physiological conditions of the gastrointestinal tract, which indicated their possible success for *in-vivo* applications.

Initial trials employed the use of genipin as a crosslinking agent. While crosslinking was easily accomplished, phosphate uptake was minimal. In an effort to establish the feasibility of

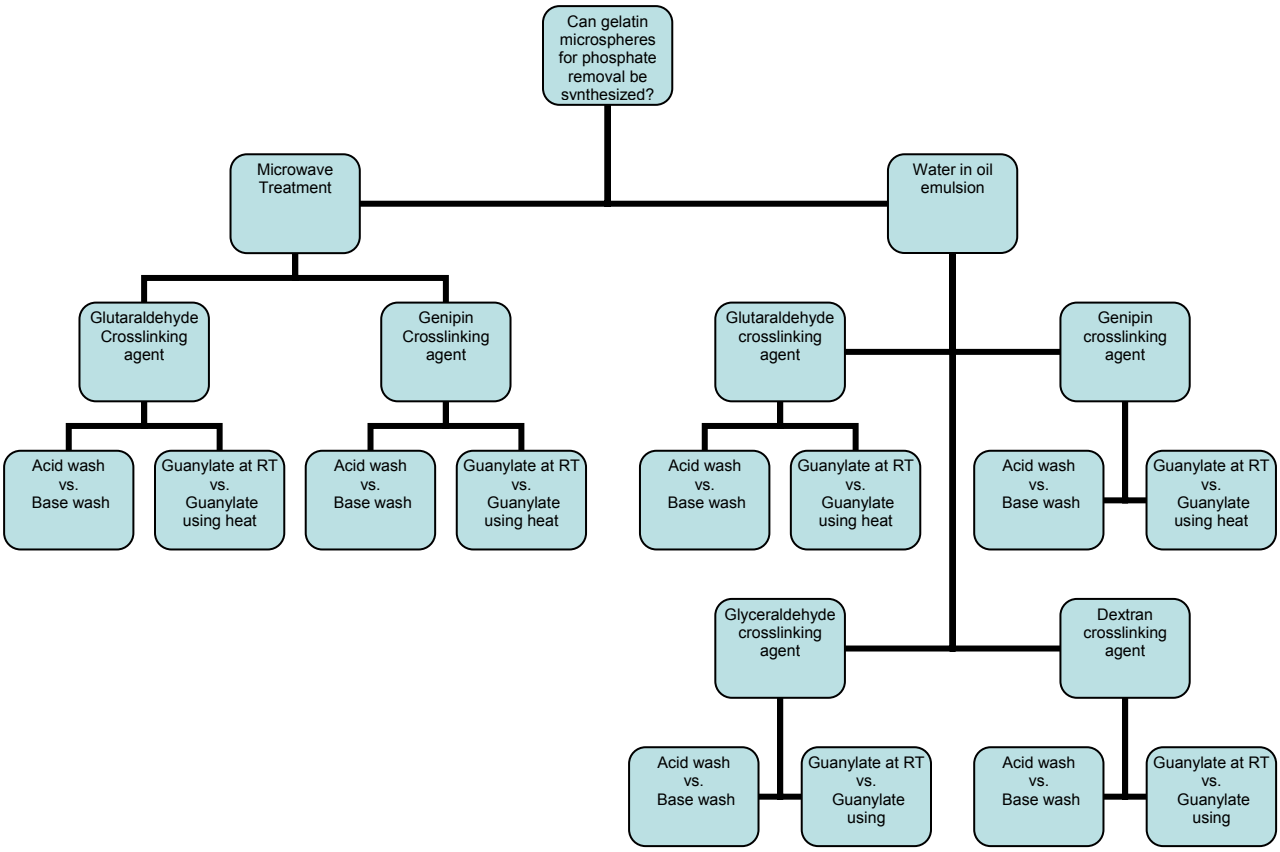

Figure 8-1. The synthetic pathway followed for the development of the gelatin microspheres.

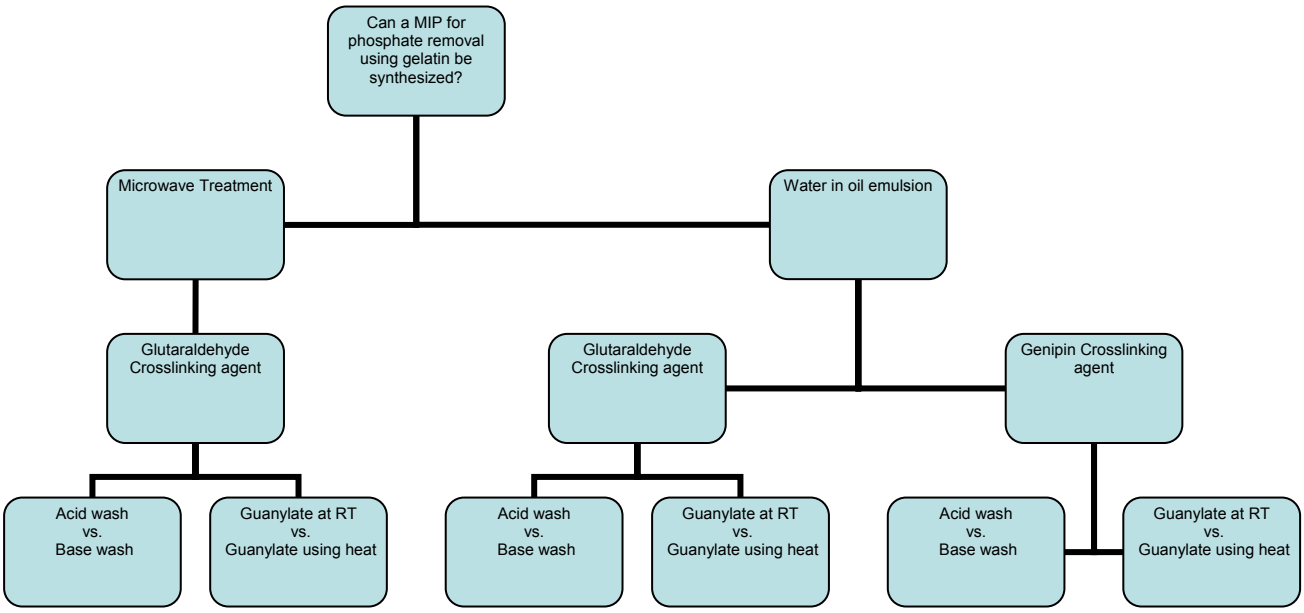

Figure 8-2. The synthetic pathway followed for the development of the molecularly imprinted gelatin microspheres.

using gelatin polymers as phosphate binders, additional crosslinker were investigated. These crosslinking agents chosen were glutaraldehyde, glyceraldehyde, and dextran, due to their biocompatibility and various applications in crosslinking gelatin.

From these results, samples were selected for complete evaluation that represented the best of the acid washed, base washed, room temperature guanylated, and heat assisted guanylated trials. The samples assessed were as follows:

1. Acid Washed:
   - 25% glutaraldehyde crosslinked gelatin, microwave treated, with and without phosphate
   - 15% genipin crosslinked gelatin, with and without phosphate
2. Base Washed:
   - 25% glutaraldehyde crosslinked gelatin, microwave treated, with and without phosphate
   - 15% genipin crosslinked gelatin, with and without phosphate
3. Room Temperature Guanylation:
   - 25% glutaraldehyde crosslinked gelatin, microwave treated, with and without phosphate
   - 15% genipin crosslinked gelatin, with and without phosphate
4. Heat Assisted Guanylation:
   - 25% glutaraldehyde crosslinked gelatin, microwave treated, with and without phosphate
   - 15% genipin crosslinked gelatin, with and without phosphate

Each polymer set included a control, which was the crosslinked polymer, and a sample of the crosslinked polymer with phosphate as an initial reactant. Samples were tested in triplicate, and the average and standard deviation values were calculated using a $p = 0.05$ statistical significance limit obtained from a statistical two tailed T-test.

The following figures summarize the body of data collected from all of the conducted experiments.

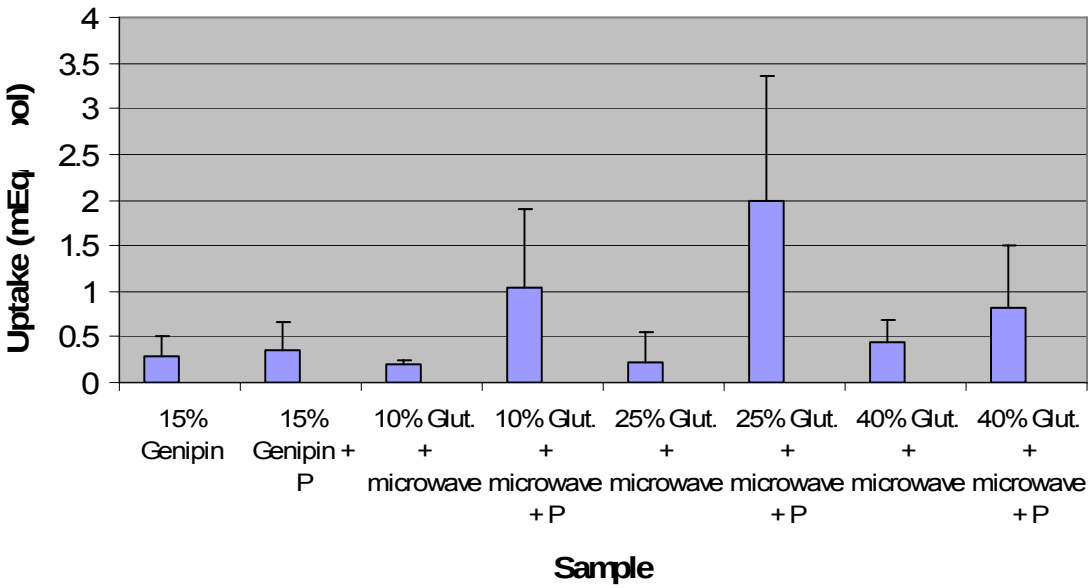

Figure 8-3. Phosphate uptake results for acid washed polymeric samples synthesized without and with the phosphate template ion.

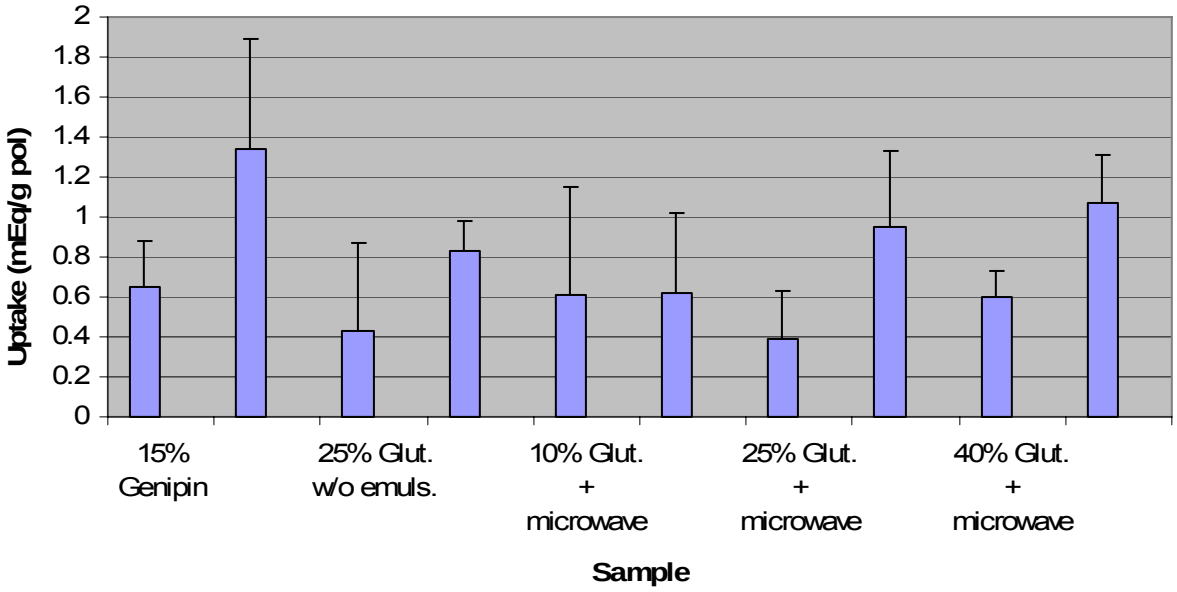

Figure 8-4. Phosphate uptake results for base washed polymeric samples synthesized without (left) and with (right) the phosphate template ion.

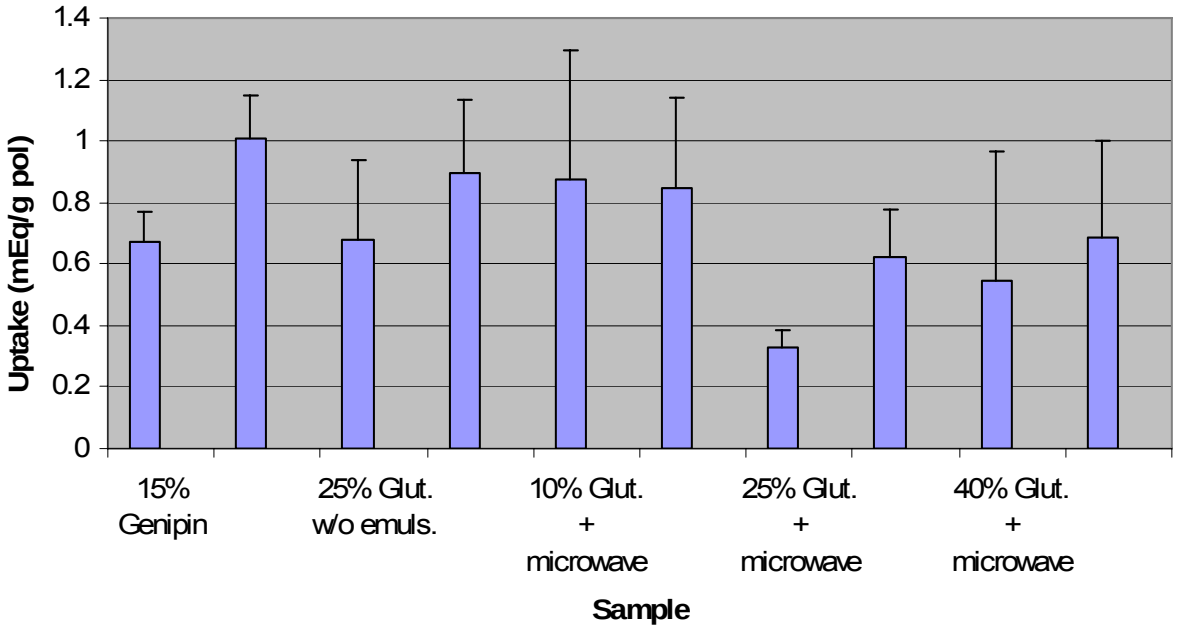

Figure 8-5. Phosphate uptake results for room temperature guanylated polymeric samples synthesized without (left) and with (right) the phosphate template ion.

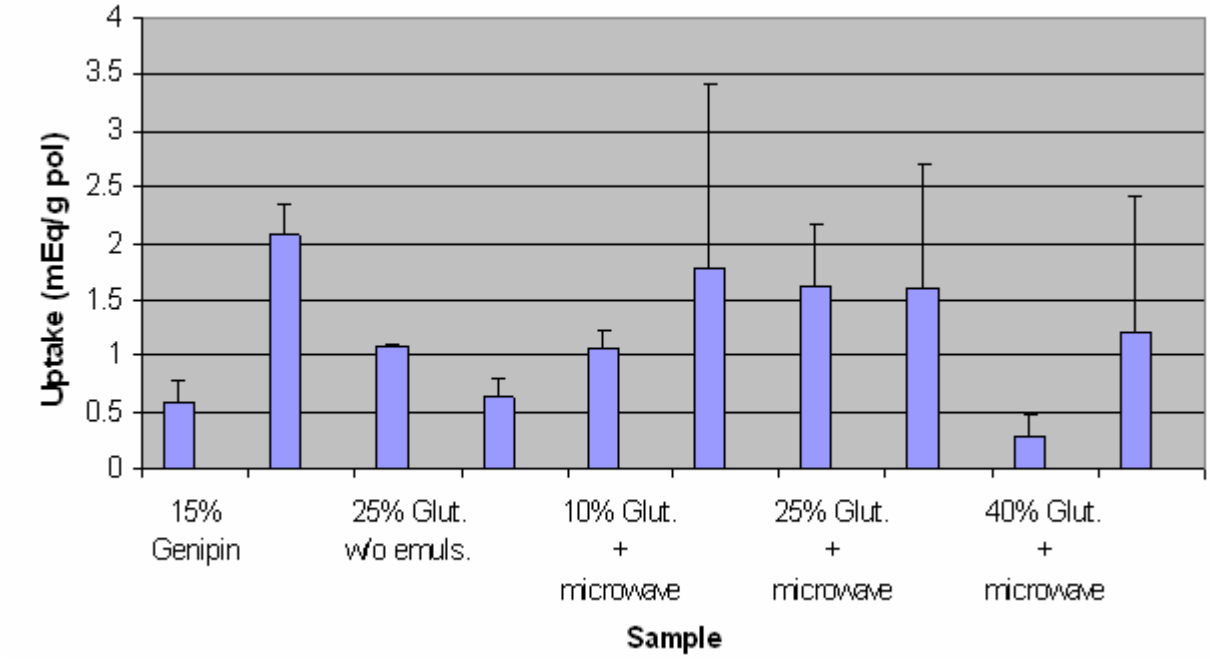

Figure 8-6. Phosphate uptake results for acid washed polymeric samples synthesized without (left) and with (right) the phosphate template ion.

Conclusions

The 15% genipin crosslinked polymers showed minimal phosphate uptake in most samples, except for those guanylated at room temperature. The room temperature guanylated polymeric microspheres reported values that were statistically significant, which indicate the successful guanylation of the arginine groups in the crosslinked polymer.

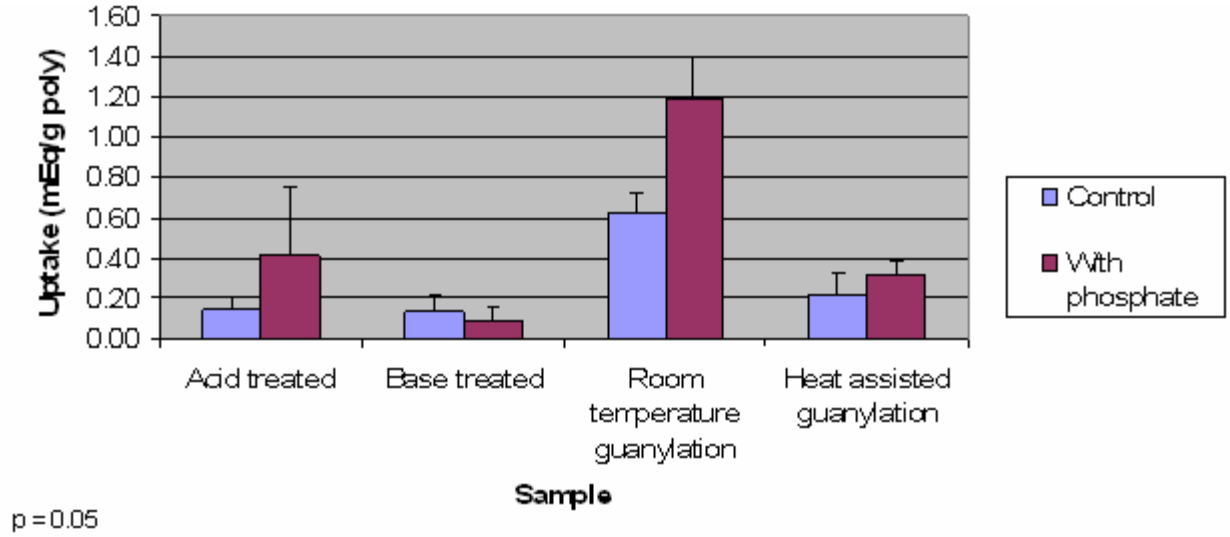

Figure 8-7. Phosphate uptake in surface functionalized polymers using genipin as a crosslinking agent.

These microspheres prepared by a simple water-in-oil type emulsion process and surface functionalized with guanine groups if desired. However, this did not account for the fact that, on average, the particles synthesized with phosphate as an initial component had a slightly higher phosphate ion concentration in comparison to their counterpart control particles. Thus, this feature must be attributed to the fact that the phosphate in the sphere is extracted in a manner in which cavities are created in which phosphate can be subsequently bound. The room temperature guanylated microspheres report significantly significant data.

The samples crosslinked with glutaraldehyde via microwave irradiation are believed to be molecularly imprinted polymer microspheres, which would explain the average difference in phosphate uptake between the samples containing phosphate, and those without.

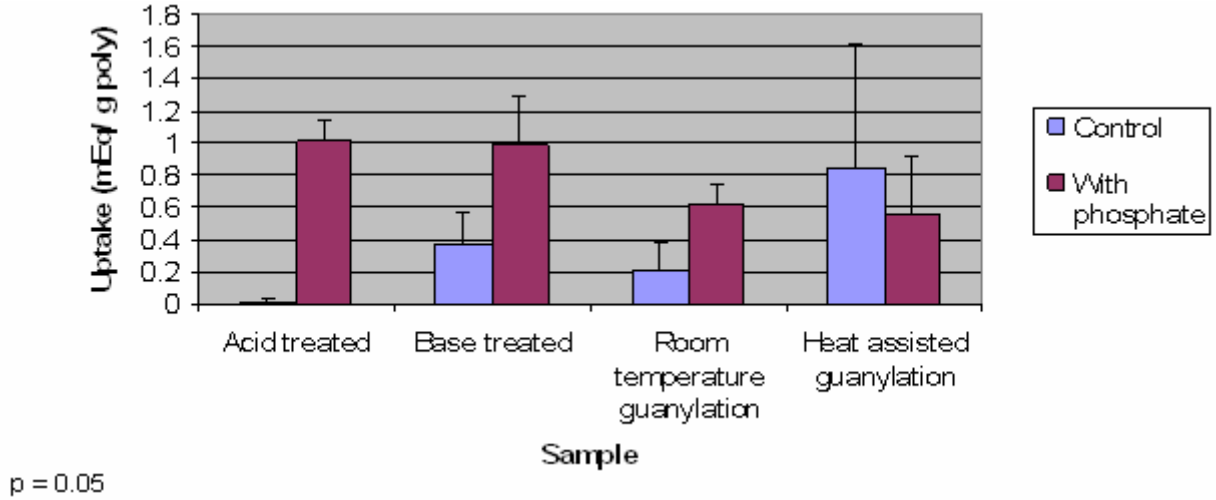

Figure 8-8. Phosphate uptake in surface functionalized polymers using glutaraldehyde as a crosslinking agent.

Crosslinking may have created rigid pores that are amenable to binding phosphate in solution after an acid or base extraction of the initial phosphate molecule. It is possible that the microwave treatment initiates crosslinking in a way in which many of the arginine groups on the gelatin structure are polymer bound, thus are not as available for subsequent guanylation at room temperature in comparison to the heat assisted process.

Statistically significant results were calculated for both room temperature and heat processed guanylated polymers.

The majority of the reported phosphate uptake success results evaluated were centered about the genipin and glutaraldehyde processed gelatin microspheres. The different chemical crosslinking mechanisms with gelatin could explain the increased stability and capacity to structurally manipulate the samples within this subset.

The entire body of data collected indicated that, in most cases, an overall phosphate binding increase in samples that contained phosphate in comparison to their control counterparts. One possible explanation may be that the phosphate present during synthesis creates additional cavities that, once extracted, are available for phosphate binding. Another reason may be that the phosphate acts as a "spacer" per se, which promotes polymer crosslinking to a greater extent than the control samples.

Genipin typically sells for $20 USD/ g. Using the microspheres prepared in these studies, it would require 250 mg of genipin to produce a product that would bind phosphate *in-vivo* as efficiently as Renagel®. Including the price of gelatin and oil, the microspheres prepared during these trials were approximately $5.50 USD/ g. Though the genipin particles were the most biocompatible polymer synthesized during these studies, the potential cost of production may preclude them as cost effective alternatives for use by those with acute renal failure.

Glutaraldehyde typically sells for $0.035 USD/ g. Using the microspheres prepared in these studies, it would require 3.0 g of glutaraldehyde to produce a product that would bind phosphate *in-vivo* as efficiently as Renagel®. Including the price of gelatin and oil, the microspheres prepared during these trials were approximately $0.25 USD/ g. Although the glutaraldehyde particles had cytotoxic concerns, they could be surpassed through aggressive washing procedures. Thus, the cost of production makes them viable candidates as cost effective alternatives for use by those with acute renal failure.

Comparative analysis of the two systems results in an overall recommendation of the genipin crosslinked microspheres as the more favorable system. Though the glutaraldehyde

produced can be prepared at a cost that is significantly lower than their genipin alternative, the inherent biocompatibility of genipin make them far more appealing as a pharmaceutical alternative, and is in accord with engineering aspect.

The potential cost analysis of the polymeric materials prepared during this research can not be directly compared to that of Renagel® because they do not include factors such as patent development, production facilities, etc. However, the cost summary does provide preliminary information about which MIT can possibly lead to the more low-cost technology.

One very important aspect to consider is that, even though the cost of producing a polymer that binds phosphate in solution may be greater than that of Renagel®, the selective template binding may not disqualify their usefulness as potential therapeutic agents.

Future Work

Crosslinking Agent

There are several suggestions for the future incorporation of different crosslinking agents for these studies. Glyceraldehyde and dextran should be further examined in greater compositional concentrations to establish their overall suitability for this application.

EDC, which is a zero length crosslinker that is extensively used with gelatin and collagens, may be investigated as a chemically efficient alternative.

Free amino/carboxylic acid determination studies should be performed to identify the extent of crosslinking achieved with each different agent, and the effects that changing the amount of crosslinker used affects the overall gelatinous microsphere. The maximum amount of each crosslinker required to provide the best gelatin microstructure for phosphate uptake can be identified.

Substrate Imprinting

This scheme is used to imprint phosphate molecules via a surface grafted thin polymer layer strategy.[36] The phosphate molecules are on a substrate, and a polymer film would be grafted from this surface. Once the substrate is removed, the guest molecule could be extracted from the host site, leaving behind a surface imprinted polymer, capable of recognition upon guest reintroduction. This may ultimately increase the number of imprint cavities available for phosphate uptake. The polymer could be ground and sintered to produce the desired particle size.

Instrumentation

Structural elucidation studies for these novel polymers should be performed using NMR.

The selectivity of the gelatin microspheres can be investigated using HPLC, which will show by peak separation, height, width, and tailing, whether or not phosphate has been favorably bound to the gelatin microsphere in comparison to other ions that may be in the solution.

Polymer Binding

Kinetic studies should be performed that establish the rate of phosphate binding to the gelatin microspheres.

Binding selectivity of phosphate should also be examined by incorporating ions that are competitive in nature to phosphate into the solution to be tested for phosphate uptake.

Swelling studies, as reported in Chapter 3 on Renagel, should be undertaken. The pH of the uptake solutions should be varied, and polymer swelling and phosphate uptake evaluated at each level. In particular, the pH of the testing solution should be lowered, as to mimic the acidic environment of the gastrointestinal system. This information would be instrumental in the development of an ideal set of polymer processing parameters, and should lend itself to the results obtained from the kinetic assays.

Enzyme Studies

Prior to actual *in-vivo* trials, which can be expensive, various enzymes which are known to exist in the gastrointestinal surroundings should be incorporated into the phosphate uptake test solution. Features such as polymer degradation and biocompatibility can be further investigated.

APPENDIX A
CALIBRATION OF A PHOSPHATE MEASURING APPARATUS

The process of determining phosphate (PO_4^{3-}) ion uptake in polymer samples has been well established and can be can be performed by methods such as ICP, UV/Vis, and other spectrophotometric techniques.

We have chosen to use the Hannah HI 93717 High Range ISM phosphate meter for measuring phosphate ion concentration largely because it is cost effective in relation to the previously mentioned instruments and the mobile nature of this handheld meter allows it to take real time, in field measurements with minimal sample preparation. The Hannah HI 93717 is a small, portable photometer that measures phosphate uptake in aqueous solutions upon exposure to an amino acid based developing reagent kit.

Figure A-1. Hannah HI 93717 handheld photometer.

However, limited information was available concerning the robustness of using data obtained using the HI 93717 in comparison to that from traditional, well established analytical devices. In an effort to address this, several calibration processes were tested in order to determine the efficiency, accuracy, and precision of the Hannah phosphate meter readings.

Experimental Methods

Initially, the Hannah HI 93717 meter was calibrated against a phosphate solution sample set of known concentrations (Table A-1).

Table A-1. Phosphate calibration values using the Hannah HI 93717 meter.

Sample	Conc. at 0 ppm (mg/ L)	Conc. at 5 ppm (mg/ L)	Conc. at 10 ppm (mg/ L)	Conc. at 20 ppm (mg/ L)
Trial 1	0.00	4.70	9.90	19.90
Trial 2	0.00	5.20	10.10	19.80
Trial 3	0.00	4.90	10.10	19.20
Trial 4	0.00	5.00	9.70	19.80
Trial 5	0.00	4.80	9.80	19.80
Average	0.00	4.92	9.92	19.63
Standard Deviation	0.00	0.19	0.18	0.28

Great care was taken in determining a sound set of testing parameters that would provide repeatable data values. Factors such as glassware treatment, reagent amounts used, and time elapsed to reading were standardized until reproducible numbers were consistently obtained. The data was graphically examined (Figure A-2), and the R^2 analysis obtained from the calibration curve (Figure A-3) showed very good agreement within the numbers.

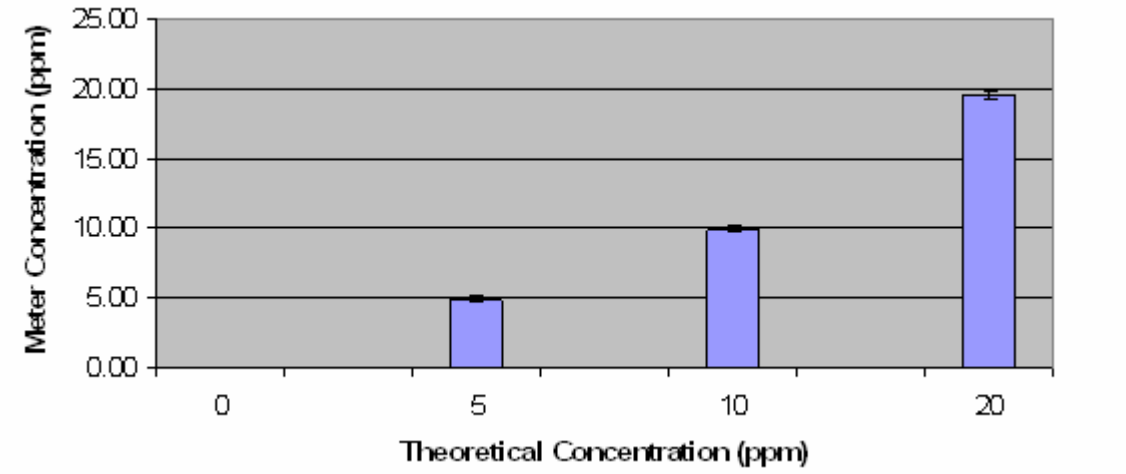

Figure A-2. Actual vs. Theoretical concentrations for phosphate ion using the Hannah HI 93717 phosphate meter.

Next, standard solution sets were tested on Shimadzu UV-2401PC UV-Vis spectrophotometer. The tested phosphate solutions were developed using a traditional ascorbic acid method. The data obtained is presented in Table A-2.

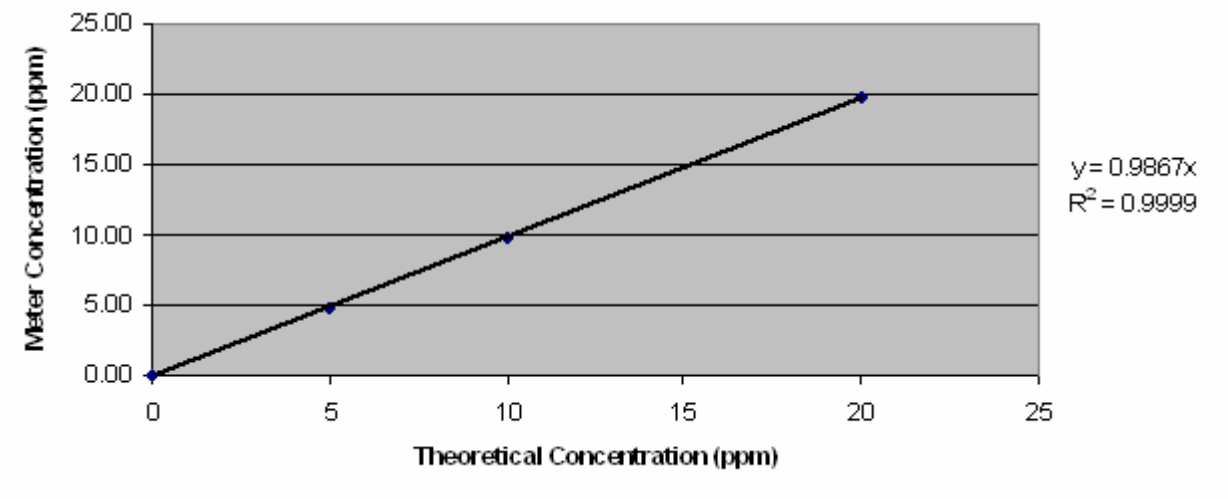

Figure A-3. Calibration curve for the Hannah HI 93717 phosphate meter.

Table A-2. Phosphate readings from the Hannah HI 93717 meter compared to those obtained from the Shimadzu UV/Vis.

Phosphate meter vs. UV/Vis		
Sample	meter (ppm)	UV/VIS (ppm)
2.5 ppm	2.6	-
5.0 ppm	5.5	5.8
10.0 ppm	10.4	10.4
20 ppm	20.6	20.2
20 ppm (different phosphate source)	19.9	19.7

The data indicated reasonable, acceptable deviation between the techniques. The use of the Hannah meter appeared to be an acceptable apparatus for phosphate determination.

Finally, industry standard Renagel® samples were measured for phosphate uptake. A set of 10 different 800 mg pills were dissolved in 300 mL of deionized water at a pH of 6.98. The slurry obtained was filtered, dried, and stored under vacuum to obtain a white, powder product. 10 different 100 mg samples of the powder were measured and placed in 50 mL centrifuge tubes, to each of which was added 30 mL of a phosphate standard solution at a pH of 7.37. The tubes were placed in a rotating incubator at 37 ^{o}C for 3 hours, removed, and phosphate uptake was

measured using the HI 93717 meter and determined using equation A-1. The results are found in Figure A-4.

$$PO_4^{3-} \text{ uptake} = [PO_4^{3-}]_{\text{standard solution}} - [PO_4^{3-}]_{\text{sample after 3 hours}} \quad \text{(A-1)}$$

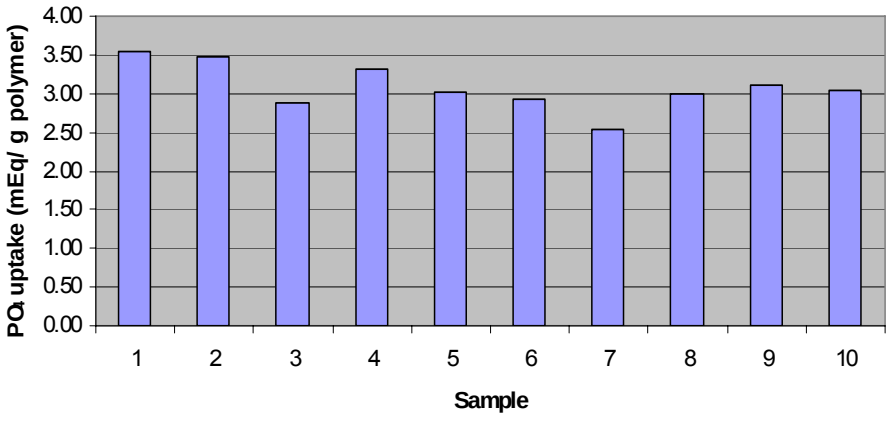

Uptake (mEq/ g polymer)	
3.54	
3.48	
2.88	
3.32	
3.03	
2.92	
2.54	
3.00	
3.11	
3.03	
Average	**STD**
3.08	0.30

Figure A-4. Phosphate uptake in Renagel® samples as measured by the Hannah HI 93717 phosphate meter.

Conclusions

Overall, the minimal relative deviation in the results obtained using the HI 93717 meter and UV/Vis allowed us to establish the use of the meter for analysis as a sound technique capable of providing accurate results for phosphate analysis for our studies. The Hannah meter will continue to be used as the initial, primary instrument for measuring phosphate in our experiments.

LIST OF REFERENCES

1. Pichot, C., Current Opinion in Colloid & Interface Science 2004, 9, (3-4), 213.

2. Mosbach, K., Molecular Imprinting. Trends in Biochemical Science 1994, 19, 9.

3. Zhang, H., Song, T., Zong, F., Chen, T., Pan, C., Int. J. Mol. Sci. 2008, 9, 98.

4. Wulff, G., Angew. Chem. Int. Ed. Engl. 1995, 34, 1812.

5. Hsu, C. Y., Lin, H. Y., Thomas, J. L., Chou, T. C., Nanotechnology 2006, 17, S77.

6. Sneshkoff, N., Crabb, K., BelBruno, J. J., Journal of Applied Polymer Science 2002, 86, 3611.

7. Wu, C., Science News 2000, 157, (12), 186.

8. Ramstrom, O., Molecular Imprinting Technology. http://www.molecular-imprinting.org/story/MIT.htm (Accessed May 25, 2008).

9. Marchand-Brynaert, J., Deldime, M., Dupont, I., Dewez, J., Schneider, Y., J. Colliod and Interface Science 1995, 173, 236.

10. Bolisay, L., D., V., March, J., Bentley, W., E., Kofinas, P., Mat. Res. Soc. Symp. Proc. 2004, 787, G3.1.1.

11. Huang, X., Wirth, M., Macromolecules 1999, 32, 1694.

12. Caro, E., Masque, N., Marce, R., M., Borrull, F., Cormack, P., A., G., Sherrington, D., C., Journal of Chromatography A 2002, 963, (1), 169.

13. Ghada El-Hajj Fuleihan, MD, MPH, Patient information: Primary hyperparathyroidism http://www.uptodate.com/patients/content/topic.do?topicKey=~hDJ1zL2gtaBL/J/ (Accessed May 25, 2008).

14. Bushinsky, D., Annu. Rev. Med. 1997, 48, 167.

15. Komiyama, M., Takeuchi, T., Mukawa, T., Asanuma, H., Molecular Imprinting. Weinhein, Germany: Wiley, John & Sons VCH, Inc.: 2003.

16. McClements, D., J., Decker, E., A., Weiss, J., Journal of Food Science 2007, 72, (8), R109.

17. Molpeceres, J., Guzman, M., Aberturas, M., R., Chacon, M., Berges, L., J. Pharmaceutical Sciences 1996, 85, 206.

18. Allemann, E., Leroux, C., Gurny, R., Doelker, E., Pharm. Res. 1993, 10, 1732.

19. Ye, L., Cormack, A., G., Mosbach, K., Analytica Chimica Acta 2001, 435, 187.

20. Booker, K., Bowyer, M., C., Holdsworth, C., I., McCluskey, A., Chem. Commun. 2006, 1730.

21. Rosenbaum, D. P., Holmes-Farley, S., R., Mandeville, W., H., Pitruzzello, M., Goldberg, D., I., Nephrol. Dial. Transplant 1997, 12, 961.

22. Fujiwara, I., Maeda, M., Takagi, M., Analytical Sciences 2000, 16, (4), 407.

23. Sambrook, P., The Musculoskeletal System, Elsevier Health Sciences, London, UK: Harcourt Publishers, Inc.: 2001; p 67.

24. Baker, S., B., Worthley, L., I., G., Critical Care and Resuscitation 2002, 4, 301.

25. Zivkovic, B., Lecture Notes - Physiology: Coordinated Response. http://coturnix.wordpress.com/(Accessed May 25, 2008).

26. Pauling, L., J. American Chemical Society 1940, 62, 2643.

27. Murray, G., Jenkins, A., Bzhelyansky, A., Manuel Uy, O., Johns Hopkins Apl Technical Digest 1997, 18, (4), 464.

28. Shea, K., Molecular Imprinting. http://www.chem.uci.edu/faculty/kjshea/ (Accessed May 25, 2008).

29. Remcho, V., Tan, Z. J., Analytical Chemistry News & Features 1999, 248A.

30. Arshady, R., Mosbach, K., Macromol. Chem. Phys. 1981, 182, (2), 687.

31. Vlatakis, G., Andersson, L., Muller, R., Mosbach, K., Nature 1993, 361, 645.

32. Weiss, R., Mizaikoff, B., Patent PCT/EP2003/005688, 2003.

33. Sreenivasan, K., Journal of Polymer Research 2001, 8, (3), 197.

34. Ulbricht, M., Belter, M., Langenhangen, U., Schneider, F., Weigel, W., Desalination 2002, 149, 293.

35. Alexander, C., Andersson, L., I., Ansell, R., J., Kirsch, N., Nicholls, I., A., O'Mahony, J., O., Whitcombe, M., J., Journal of Molecular Recognition 2006, 19, 106.

36. Simon, R., Collins, M., E., Spivak, D. A., Analytica Chimica Acta 2007, 591, (1), 7.

37. Shimelis, O., Trinh, A., Brandes, H., The Reporter 2007.

38. Van Hoof, N., Courthyen, D., Antignac, J., P., Van de Wiele, M., Poelmans, S., Noppe, H., De Brabander, H.,, Rapid Communications in Mass Spectrometry 2005, 19, 2801.

39. D'Souza, S., Alexander, C., Carr, S.W., Waller. A.M., Whitcombe. M.J., Vulfson, E.N., Nature 1999, 398, 312.

40. Parmpi, P., Kofinas, P., Biomaterials 2004, 25, 1969.

41. Ross, E. A., Scott III, W., Odukale, A. A., Alba, N., Batich, C., J. Pharmaceutical Sciences 2007, 96, (8), 2154.

42. Holmes-Farley, S., Mandeville, III, W. H., Whitesides, G., US Patent 6,083,495, 2000.

43. Gallieni, M., Cozzolino, M., Brancaccio, D., Kidney International 2000, 57, 1776.

44. RxList online. Renagel. http://www.rxlist.com/cgi/generic/sevel.htm (Accessed May 25, 2008).

45. Slatopolsky, E., A., Burke, S., K., Dillon, M., A., Kidney International 1999, 55, 299.

46. Leach, A., Molecular Modelling: Principles and Applications. Pearson Education, Upper Saddel River, New Jersey: Prentice-Hall: 2001.

47. Berendsen, H. J. C., Treatment of long-range forces in Molecular Dynamics and Protein Structure, Hermans, J., ed., Western Springs, IL: Polycrystal Book Service: 1985.

48. Olaj, O. F., Petrik, T., Zifferer, G., J. Chem. Phys 1998, 108, 8226.

49. Parker, R., Odukale, A., A., Fisher, D., Batich, C., Ross, E., A., Edwards, J., Int. J. Environ. Res. Public Health 2006, 3, (2), 202.

50. Tripos Inc., SYBYL 6.9 computer modeling program: St. Louis, Missouri., 2006.

51. Tripos, Inc., The Tripos Bookshelf Version 7.3. Yale University. http://graphics.med.yale.edu:5080/TriposBookshelf/index.html (Accessed May 25, 2008).

52. Gasteiger, J., Marsili, J., Marsili, M., Tetrahedron Letters 1978, 34, 3181.

53. Burke, S., Goldberg, D., Bonventere, J., Slatopolsky, E., Nephrol. Dial. Transplant 1996, 11, A41.

54. Ramstrom, O., Yu, C., Mosbach, K., Journal of Molecular Recognition 1996, 9, 691.

55. Mayes, A. G., Andersson, L. I., Mosbach, K, Analytical Biochemistry 1994, 222, (2), 483.

56. Andersson, L. I., Muller, R., Vlatakis, G, Mosbach, K., Proceedings of the National Academy of Sciences, USA 1995, 92, 4788.

57. Lodish, H., Berk, A., Zipursky, L., Matsudaira, P., Baltimore, D., Darnell, J., Molecular Cell Biology. W. H. Freeman and Company: New York, Houndsmills, Basingstoke, 2000.

58. Bialkowski, S., Triprotic Acid Titration with Strong Base. http://www.chem.usu.edu/~sbialkow/Classes/3600/Overheads/H3A/H3A.html (Accessed May 25, 2008).

59. Sellergren, B., In Molecularly Imprinted Polymers: Man made mimics of antibodies and their application in analytical chemistry, Elsevier publishers: 2001; Vol. 23, p 113.

60. Bigi, A., Cojazzi, G., Panzavolta, S., Roveri, N., Rubini, K., Biomterials 2001, 22, 763.

61. Stevens, P. V., Food Australia 1992, 44, (7), 320.

62. Talebian, A., Kordestani, S., S., Rashidi, A., Kem. Ind. 2007, 56, (11), 537.

63. Bourne, P., DNA & Protein Sequence Comparison. www.sdsc.edu/pb/edu/pharm207/2/lec2.html (Accessed May 25, 2008).

64. Babin, H., Dickinson, E. , Food Hydrocolloids 2001, 15, 271.

65. Prucker, O., Ruhe, J., Macromolecules 1998, 31, (3), 592.

66. Haginaka, J., Takehira, H., Hosoya, K., Tanaka, N., Journal of Chromatography A 1998, 816, (2), 113.

67. Dinarvand, R., Mahmoodi, S., Farboud, E., Salehi, M., Atyabi, F., Acta. Pharm. 2005, 55, 57.

68. Kriz, D., Ramstrom, O., Svensson, A., Mosbach, K., Analytical Chemistry 1995, 67, 2142.

69. Wulff, G., Kemmerer, R., Vietmeier, J., Poll, H.G., Nouveau Journal De Chimie - New Journal of Chemistry 1982, 6, 681.

70. Asanuma, H., Kakazu, M., Shibata, M., Hishiya, T., Komiyama, M, Chemical Communications 1997 (1971), 20, 197.

71. Challenge Bio Producst Company, Genipin. http://www.genipin.org/ (Accessed May 25, 2008).

72. Vaandering, B., Genipin. http://www.wou.edu/las/physci/ch350/Projects_2006/Vaandering/Genipin.htm (Accessed May 25, 2008).

73. National Institute for Occupational Safety and Health: Glutaraldehyde: Occupational Hazards in Hospitals. Cincinnati, OH.: NIOSH-Publications Dissemination: 2001.

74. Ted Pella, I. MSDS: Glutaraldehyde, 50%. http://www.tedpella.com/msds_html/18411msd.htm (Accessed May 25, 2008),

75. Bigi, A., Cojazzi, G., Panzavolta, S., Roveri, N., Rubini, K., Biomterials 2002, 23, 4827.

76. Liang, H. C., Chang, W. H., Lin, K. J., Sung, H. W., Journal of Biomedical Materials Research Part A 65A, (2), 271.

77. Encyclopedia Britannica online, Carbohydrates Homopolysaccharides. http://www.britannica.com/EBchecked/topic/160516/dextran, Encyclopedia Britannica, Inc.: Chicago, IL (Accessed May 2008).

78. Lindberg, B. a. S., S. , Acta. Chem. Scand. 1968, 22, 1907.

79. Wales, M., J. Polym. Sci. 1979, 55, 66.

80. Granath, K. A., J. Colloid Sci. 1958, 13, 308.

81. Gekko, K., American Chemical Society Symposium Series 1981, 150, 415.

82. Draye, J., P., Delaey, B., Voorde, A., Bulcke, A., V., D., Bogdan, B., Schacht, E., Biomterials 1998, 19, 99.

83. Oliveira, B., F., Santana, M., H., A., Re, M., I. , Brazilian Journal of Cemical Engineering 2005, 22, (3), 353.

84. Vandelli, M., A., Pifferi, G., Seghizzi, R., Cameroni, R., Pharmacy and Pharmacology Letters 5, 116.

85. Schacht, E., H., Journal of Physics: Conference Series 2004, 3, 22.

86. Sellergren, B., Shea, K., Journal of Chromatography 1993, 635, 39.

87. Reinholdsson, P., Hargitai, T., Isaksson, R., Tornell, B., Angewandte Makromolekulare Chemie 1991, 192, (1), 113.

88. Mosbach, K., Haupt, K., Liu, X. C., Cormack, P. A. G., Ramstrom, O. In ACS Symposium Series, 1998; American Chemical Society: 1998; p 29.

89. Holmes-Farley, S. M., III, W. H.; Whitesides, G. 6,509,013, 2003.

90. Yildirim, H., Vinyl Acetate Emulsion Polymerization and Copolymerization with Acrylic Monomers. Boca Raton, London, New York, Washington, D.C., 2000.

91. Salager, J.-L., Anderez, J. M., Briceno, M. I., de Sanchez, M. P., de Gouveia, M. R., Revista Técnica de la Facultad de Ingeniería Universidad del Zulia 2002, 25, (3), 129-139.

92. Laughling, R., The Aqueous Behavior of Surfactants. Academic Press: London, 1994.

93. Shah D. O., S. R. S., Improved Oil Recovery by Surfactant and Polymer Flooding. Academic Press: New York, 1977.

94. Bourrel M., G. A., Schechter R. S., Wade W. H. , J. Colloid Interface Sci. 1979, 72, 161.

95. Salager J. L., L. I., Miñana M., Silva F., J. Dispersion Sci. Technol. 1982, 3, 279.

96. Tanaka, N., Takino, S., Utsumi, I., J. Pharmaceutical Sciences 1963, 52, 664.

97. Sung H.W., H. D. M., Chang W.H, Huang L.L.H., Tsai C.C., Liang I.L., J. Biomater. Sci. Polymer Edn. 1999, 10, 751.

98. Yao C.H., L. B. S., Chang C.J., Hsu S.H., Chen Y.S., Materials Chemistry and Physics 2004, 83, 204.

99. Cortesi, R., Esposito, E., Osti, M., Menegatti, E., Squarzoni, G., Davis, S., Nastruzzi, C., European Journal of Pharmaceutics and Biopharmaceutics 1999, 47, (2), 153.

100. Centeno, S., A., Guzman, M., Yamazakikleps, A., Della Vedova, C., O., Journal of the American Institute for Conservation 2004, 43, (2), 139.

101. Bajpai, A., K., Choubey, J., J. Mater. Sci. Mater. Med. 2006, 17, 345.

102. Welz, M. M., Ofner III, C. M., , J. Pharmaceutical Sciences 1992, 81, 85.

103. Yannas, I. V., Tobolsky, A. V., Nature 1996, 215, 509.

104. Vandelli, M., A., Romagnoli, M., Monti, A., Gozzi, M., Guerra, P., Rivasi, F., Forni, F., J. Controlled Release 2004, 96, 67.

105. Yan, W., Wei, Z., Ding, S., Wan, M., Advanced Nanomaterials and Nanodevices 2002, 83.

106. Katritzky, A., R., Khashab, N., Bobrov, S., Helvetica Chimica Acta 2005, 88, 1664.

107. Sharma, S., Sharma, A., Samuelson, L., Kumar, J., Watterson, A., Parmar, V., Journal of Macromolecular Science 2004, 41, (12), 1459.

108. Schmidt, O., Schmidt, A., Toptchiev, D., US Patent 7,001,606 B2, 2006.

109. Dhal, P., K., Holmes-Farley, S., Petersen, J., US Patent 6,294,163 B1, 2001.

110. Nopper, D., Lammershop, O., Wulff, G., Gauglitz, G., Aanal. Bioanal. Chem. 2003, 377, 608.

111. Emgenbroich, M., Wulff, G., Chem. Eur. J. 2003, 9, 4106.

112. Vaidya, A., A., Lele, B., S., Kulkarni, M., G., Mashelkar, R., A., Journal of Applied Polymer Science 2000, 81, 1075.

113. Lui, J., Wulff, G., Angew. Chem. Int. Ed. 2004, 43, 1287.

114. Bernatowicz, M., S., Wu, Y., Matsueda, G., R., Journal of Organic Chemistry 1992, 57, 2497.

115. Huval, C., C., Holmes-Farley, S., R., Mandeville, W., H., Petersen, J., S., Sacchiero, R., J., Maloney, C., Dhal, P., K., Journal of Macromolecular Science 2004, A41, (3), 231.

116. Tadao, F., Takeichi, S., Journal of the Pharmaceutical Society of Japan 1997, 10, 1107.

117. Sivakova, S., Rowan, S., Chem. Soc. Rev. 2005, 34, 9.

118. Williamson, J., R. , Annu Rev Biophys Biomol Structure 1994, 23, 703.

119. Gilber, D., E., Feigon, J. , Current Opinion Structura Biol 1999, 9, 305.

BIOGRAPHICAL SKETCH

Anika Odukale is a native of Minnesota, where she graduated from the Summatech program at Minneapolis North Community High School. She then attended North Carolina State University, where she received a B.S. degree in chemistry, with a minor in African-American studies. To address the noticeable trend of an alarmingly low number of African-Americans, specifically women, involved in the sciences, Anika tutored students in math and chemistry, and taught for a pilot program that introduced African-American children aged 8-15 to accelerated math and science areas. She also was the president of the first NOBCChE chapter at the university.

While enrolled as an undergraduate, Anika consistently held Summer research Internship positions at the 3M Company, Burroughs Wellcome (currently Glaxo-Smith-Kline), and Interpoll Laboratory, as a means to further her research experiences and supplement herself financially for College.

Through her combined instructional and research experiences, Anika first realized her passion for teaching and scientific exploration. She became dedicated to learning how to inspire "Critical Thought" in students through non-traditional educational and scientific methods

Anika obtained a Masters' degree in Analytical Chemistry from Michigan State University. During her tenure there she successfully completed required courses, taught chemistry recitation courses and labs, and started a free tutorial program for first semester chemistry classes. She also served as an Instructor for the Charles Drew Tutorial Assistance in Chemistry program, which provided intensive supplemental instruction for gifted and talented students from underrepresented groups in science and engineering. This program was highly successful, attracting the attention and funding from the National Science Foundation.

Upon degree completion at Michigan State University, Anika attended the University of Florida and enrolled in the Doctoral degree program in the department of Materials Science and Engineering. She received a certificate in Forensic Science in the Drug Chemistry concentration, and a Master's Degree in Materials Science and Engineering while matriculating through the Doctoral degree program.

Anika has obtained a postdoctoral research position at the University of California at Santa Barbara. She is working under the direction of Professor Craig T. Hawker at the Materials Research Laboratory (MRL), where she is the program coordinator for the NSF funded Materials Research Facilities Network (www.mrfn.org), and work on polymeric encapsulants for organic light emitting devices (OLEDs) for the Mitsubishi Chemical Corporation.

Anika will continue to serve the community through mentoring and tutoring university students, specifically women and minorities, in the STEM areas.

Anika is married to Dr. Jesse Edwards III, an Associate Professor in Chemistry at Florida A&M University, who share a 1 year old son, Akil, and 12 year old stepson, Tyler Edwards.

.